PHD

Controlling Industrial and Commercial Electric Vehicles and Their Retired Batteries to Provide Grid Services and Backup Power

(Alternative Format Thesis)

Wei, Renjie

Award date:
2022

Awarding institution:
University of Bath

Controlling Industrial and Commercial Electric Vehicles and Their Retired Batteries to Provide Grid Services and Backup Power

By

Renjie Wei

BEng

The thesis submitted for the degree of

Doctor of Philosophy

in

The Department of
Electronic and Electrical Engineering
University of Bath

July 2022

Signature:……Renjie Wei………… Date:…26/07/2022…………

Contents

Abstract .... **V**

Publications .... **VII**

Acknowledgement .... **VIII**

List of Figures .... **IX**

List of Tables .... **XII**

List of Abbreviations .... **XIII**

List of Symbols .... **XIV**

Chapter 1. Introduction **1**

1.1. Background and motivation 2

1.1.1. The importance of EV development 2

1.1.2. Challenges existing in the development of EVs 3

1.1.3. Research gaps 4

1.2. Research aims 6

1.3. Research objectives and contributions 6

1.4. Thesis layout 9

Chapter 2. Review of EV optimal control and second life EV batteries **11**

2.1. Introduction 12

2.2. Optimal control of EV charging 12

2.2.1. The consequence of over penetration of EVs in networks 12

2.2.2. The different control strategies for EV charging 13

2.2.3. The optimal control of domestic EVs and industrial/ commercial EVs..16
2.3. Second life batteries 21
2.3.1. The economic analysis of SLBs 21
2.3.2. The buying price and the selling price for the SLBs 22
2.3.3. The prediction of the remaining life of the SLBs 23
2.3.4. The existing business model on SLBs. 24
2.4. Chapter summary 25

Chapter 3. Energy management of airport service electric vehicles to match renewable generation through rollout approach 27

3.1. Chapter overview.. 28
3.2. Abstract 31
3.3. Introduction... 31
3.4. Overview of methodology 35
3.5. Problem formulation: ASEV dynamics model 36
3.5.1. Modelling of Uncertain Ground Transport Workload 37
3.5.2. ASEV dynamics model 38
3.6. Near-optimal control of the ASEV dynamics model 45
3.7. Case study 49
3.7.1. Scenario 1): Comparison between the ‘greedy charging’ and the rollout algorithm for a typical sunny month in summer... 51
3.7.2. Scenario 2): Comparison between ‘greedy charging’ and the rollout algorithm for a typical month in winter 55
3.8. Conclusion... 57

Chapter 4. Monthly-payment-based business model for second-life batteries to provide flexibility services 59

4.1. Chapter overview.. 60

4.2. Abstract 63

4.3. Introduction 63

4.4. Overview of methodology 66

4.5. Methodology 67

4.5.1. SLB Pack Model 67

4.5.2. SLB Matrix Model 71

4.5.3. Flexibility Service Model 73

4.5.4. Heuristic Control and Business Model incorporated in Monte Carlo Simulation 76

4.6. Data environment and simulation results 81

4.6.1. Input Data 81

4.6.2. Numerical Results 83

4.7. Discussion 92

4.8. Conclusions 95

Chapter 5. Energy management for an electric bus charging station with facilitated second-life batteries 98

5.1. Chapter overview 99

5.2. Abstract 102

5.3. Introduction 102

5.4. Overview of methodology 106

5.5. System model 107

5.5.1. Electric bus model 107

5.5.2. EB charging model 107

5.5.3. SLB degradation model 108

5.5.4. Base load power consumption 110

5.5.5. Flexibility services for the network 110

5.6. Framework Formulation 111

5.6.1. Day-ahead scheduling 112
5.6.2. Sample average approximation based stochastic programming 118
5.7. Case studies.. 119
5.7.1. Scenario 1): the 'greedy charging' strategy for the EB charging station……………………………………………………………………………… 122
5.7.2. Scenario 2): the optimal control strategy for the EB charging station without SLB storage 124
5.7.3. Scenario 3): the optimal control strategy for the EB charging station with an SLB storage system 126
5.7.4. The comparison of the energy cost of the three control algorithms 128
5.7.5. Numerical results analysis 130
5.8. Conclusions... 131

Chapter 6. Conclusion 133

Chapter 7. Future work 140

References ……………………………………………………………………………….145

Abstract

The UK government has set a target to achieve net-zero carbon emissions by 2050. Major countries in the world have set similar targets to achieve net-zero carbon emissions. The electrification of transport is essential for achieving this target. According to a report published by the EU, transforming petrol or diesel vehicle into electric vehicles (EVs) will account for 80% of the carbon emission reductions until 2050. However, the increase of EVs bring about several challenges: 1) increasing EVs causes grid problems such as network overloads and low voltages. Uncoordinated EV charging, in particular, causes those acute problems, resulting in potentially significant network reinforcement costs for distribution network operators (DNOs) and the need for urgent solutions. 2) the handling of retired batteries from EVs will eventually become a mass-scale problem, which requires environmentally friendly, low-cost solutions. At present, retired batteries are directly broken down, with valuable materials recycled. However, considering the remaining potential of the retired batteries, direct recycling of retired EV batteries compromises the batteries' life-cycle economy and is not environmentally friendly.

This thesis aims to tackle the above two problems: network congestions caused by EVs and the handling of retired EV batteries. In light of this, this thesis makes the following original contributions:

1) For the use case of airport service electric vehicles (ASEVs), a new dynamic ASEV behaviour model is developed, alongside an optimal control method based on a customised rollout approach to optimally control the ASEVs, with the aim to minimise energy costs whilst meeting airport business needs (luggage transport).

2) A novel business model is developed that controls second-life batteries (SLBs) retired from EVs to both perform energy arbitrage and provide flexibility services, where any profit is shared among the battery processer and EV customers who sent in the SLBs.

The profit sharing is performed through monthly payments from the battery processer to the EV customers, thus circumventing the difficulty in forecasting SLB remaining life and performance at the beginning of their second life.

3) A novel electric bus charging station model with the SLB energy storage system is proposed. The SLB energy storage system can reduce the charge demand during the peak time, which reduces the energy purchased cost for EB charging station and help support the network during peak time. Furthermore, the SLB energy storage system will provide flexibility services for DNOs. It will significantly reduce the network congestions and the reinforcement investments of the network.

The above work facilitates the EV connections to the grid by making the EV charging behaviour friendly to the grid, improves the application of SLBs by proposing a potential beneficial business model, and increases both the energy and economic efficiency by adopting SLBs to support EV charging and the grid. Ultimately, these innovations will contribute to achieving the net zero carbon emissions target by 2050.

Publications

R. Wei, K. Ma, " Energy Management of Airport Service Electric Vehicles to Match Renewable Generation through Rollout Approach" in IEEE Transactions on Transportation Electrification (Submitted)

R. Wei, K. Ma, and L. Fang, " Monthly-Payment-based Business Model for Second-Life Batteries to Provide Flexibility Services" in Energy Power System Research (Submitted)

R. Wei, K. Ma, Z. Zhang and C. Gu, " Energy Management for Electric Bus Charging Station with Second-Life Batteries " in IEEE Transactions on Smart Grid (Submitted)

W. Kong, K. Ma, L. Fang, **R. Wei** and F. Li, "Cost-Benefit Analysis of Phase Balancing Solution for Data-Scarce LV Networks by Cluster-Wise Gaussian Process Regression," in IEEE Transactions on Power Systems, vol. 35, no. 4, pp. 3170-3180, July 2020, doi: 10.1109/TPWRS.2020.2966601

Acknowledgement

Firstly, I would particularly like to express my deepest gratitude to my esteemed supervisor team, Dr Kang Ma, Dr Chenghong Gu and Prof. Furong Li for their invaluable support and guidance throughout my studies. Your insightful feedback improved me to sharpen my thinking and brought my work to a high level.

I would like to thank all the tutors in our CSPD Group at the University of Bath, Dr Kang Ma, Dr Chenghong Gu, Prof. Furong Li, Dr Xiaoze Pei, Dr Yunjie Gu, whose expertise was helpful and provided me with useful resources. I would like to acknowledge my colleagues and group members, Dr Heng Shi, Dr Xiaohe Yan, Dr Ran Li, Dr Lurui Fang, Dr Yuankai Bian, Dr Minghao Xu, Dr Heng Shi, Dr Zhong Zhang, Dr Wangwei Kong, Dr Chi Zhang, Dr Qiuyang Ma, Dr Yichen Shen, Dr PengFei Zhao, Dr Yajun Zhang, Mr Peilin Liu, Mr Xin Gao, Mr Han Wang, Mr Haiwen Qin, Ms Yunting Liu, Ms Jianwei Li, , Mr Junlong Li, Mr Shuangqi Li, Mr Xinyuan He, Ms Lanqing Shan, Mr Yuanbin Zhu, Mr Can Tang and Ms Shuang Cheng, for their wonderful collaboration and patient support.

I would also like to express my heartfelt gratitude to Prof. Minxiao Han at North China Electric Power University, Prof. Guanjun Zhang at Xi’an Jiaotong University and Prof. Xinzhou Dong at Tsinghua University. I appreciate their guidance at the beginning of my PhD study.

Additionally, I could not have completed this research without the support of my friends, Mr Boyuan Yin, Mr Xuyang Wang, Ms Tian Gan, Mr Qiliang Xu and Mr Pengkun Yuan, who provided stimulating discussion as well as happy distractions to rest my mind outside of my research.

Finally, I would like to take this opportunity to express my greatest thanks to my family, especially to my parents who support me in every step of my study period. Thanks to their endless encouragement and support, I was able to touch on world-leading studies.

List of Figures

Fig. 3-1 Flowchart of the models and the optimal control approach 36

Fig. 3-2 Overview of the ASEV dynamics model. 39

Fig. 3-3 State transition graph for the ith ASEV. 44

Fig. 3-4 Pseudo-code for heuristic i), i.e. the “renewable matching” heuristic. 47

Fig. 3-5 Pseudo-code for heuristic ii), i.e. the “greedy charging” heuristic............. 48

Fig. 3-6 The time of use tariffs in the summer and winter month. 50

Fig. 3-7 The PV generation power of the summer and winter month. 51

Fig. 3-8 The SoC of the ASEVs in the summer month under rollout algorithm. 52

Fig. 3-9 The SoC of the ASEVs in the summer month under ‘greedy charging’ algorithm. 52

Fig. 3-10 The cost of Bristol Airport under ‘greedy charging’ and rollout algorithm in the summer month. 53

Fig. 3-11 The SoC of the ASEVs in the winter month under rollout algorithm. 55

Fig. 3-12 The SoC of the ASEVs in the winter month under ‘greedy charging’ algorithm. 56

Fig. 3-13 The cost of Bristol Airport under ‘greedy charging’ and rollout algorithm in the winter month. 56

Fig. 4-1 Procedure for battery processing 66

Fig. 4-2 Equivalent Circuit for Battery Pack 67

Fig. 4-3 Battery matrix structure 71

Fig. 4-4 Monte Carlo simulation incorporating heuristic control to assess profitability of the monthly-payment-based business model. 80

Fig. 4-5 The number of dying batteries each year in scenario 1. 84

Fig. 4-6 The ‘cumulative function’ of dying batteries in scenario 1. 85

Fig. 4-7 The revenue of the battery matrix for the three services. 85

Fig. 4-8 The total revenue and the net benefit of the battery matrix. 86

Fig. 4-9 The SLB energy throughput per year in scenario 1. 86

Fig. 4-10 The number of dying batteries each year in scenario 2. 87

Fig. 4-11 The ‘cumulative function’ of the dying batteries 88

Fig. 4-12 The revenue of the battery matrix for the three services. 88

Fig. 4-13 The total revenue and the net benefit of the battery matrix. 89

Fig. 4-14 The SLB energy throughput per year. 89

Fig. 4-15 The degradation curve of SLB energy capacity. 90

Fig. 4-16 The degradation curve of SLB terminal voltage. 90

Fig. 4-17 The obtained profits for one example EV owner throughout the SLB’s second-life. 91

Fig. 5-1 The control system of the EB charging station with SLB energy storage………. 104

Fig. 5-2 The overview of the EB charging station control methodology. 106

Fig. 5-3 The equivalent circuit of the SLB. 108

Fig. 5-4 The different time intervals of one day. 119

Fig. 5-5 The base load power consumption of the charging station. 120

Fig. 5-6. The electricity price in one day. 121

Fig. 5-7 The power of the EB charging station for charging services under ‘greedy charging’ algorithm. 123

Fig. 5-8. The number of charging EBs on the day with ‘greedy charging’ algorith123

Fig. 5-9 The SoC of the EBs on the day under ‘greedy charging’ algorithm. 123

Fig. 5-10. The EB charging power under ‘day-ahead scheduling’ without SLB energy storage 125

Fig. 5-11 The number of charging EBs under day-ahead scheduling without SLB energy storage. 125

Fig. 5-12 The SoC of the EBs under day-ahead scheduling without SLB energy storage 126

Fig. 5-13 The EB charging power from the network under ‘day-ahead scheduling’ with SLB energy storage. 127

Fig. 5-14. The number of charging EBs under day-ahead scheduling with SLB energy storage. 127

Fig. 5-15. The SoC of the EBs under day-ahead scheduling with SLB energy storage.. 128

Fig. 5-16. The EB charging power from the SLB energy storage under ‘day-ahead scheduling’. 128

Fig. 5-17. The comparison of the operational cost in the three scenarios of 5 continuous days. 129

List of Tables

Table 4-1 THE ELECTRICITY PRICE OF ONE DAY 82

Table 4-2 FIXED PRICE OF FLEXIBILITY SERVICES 82

Table 4-3 STATES OF SLBS AFTER 10-YEAR OPERATION IN SCENARIO 1.... 84

Table 4-4 STATES OF SLBS AFTER 10-YEARS OPERATION 87

Table 4-5 FINAL PROFIT RESULTS OF SCENARIO 1) AND SCENARIO 2) 89

List of Abbreviations

ASEV	Airport Service Electric Vehicle
CBSMS	Centralized Battery Swapping Management System
CDF	Cumulative Density Function
DAS	Day-ahead Scheduling
DNO	Distribution Network Operator
DP	Dynamic Programming
EB	Electric Bus
EMS	Energy Management System
EV	Electric vehicle
ICTs	Information& control technologies
MCS	Monte-Carlo Simulation
NPV	Net Present Value
PEB	Plug-in Electric Bus
PF	Power Factor
PV	Photovoltaic
SAA	Sample Average Approximation
SHS	Stochastic Hybrid System
SLB	Second-Life Battery
SoC	State of Charge
SOH	State of Health
TOU	Time of Use
V2G	Vehicle-to-Grid
WPD	Western Power Distribution

List of Symbols

E_m^g	Transmission electricity consumption
$E_{n,m,t}^c$	Obtained electricity
C_{max}	Capacity of the EBs
q_t	Bus departure frequency in time slot *t*
$f_{t,(m,m+1)}$	Passenger flow between bus stations
V_{used}	Buying price of the SLB in the n^{th} year
V_{new}	Price of the new battery with the similar value in the n^{th} year
f_{health}	State of health of the battery
f_{reuse}	SLB re-proposing cost
$f_{discount}$	Discount factor to encourage the use of SLB
Q_m	Measured capacity
Q_n	Nominal capacity
$\widetilde{w}_{jt}$	Time required for an ASEV to serve flight *j* at time *t*
$\emptyset(\mu, \sigma^2;\ x)$	Probability density function
$\Phi(\mu, \sigma^2; x)$	Cumulative distribution function
ρ_u	Upper bounds of $\widetilde{w}_{jt}$
ρ_l	Lower bounds of $\widetilde{w}_{jt}$
w_{jt}	Discretized random workload
S_{it}	State of an *i*th ASEV at Stage *t*
q_{it}	Discrete state
SoC_{it}	State of charge (SoC) of the *i*th ASEV's battery at Stage *t*
f_{Rit}	Battery cycles to failure for the *i*th ASEV at Stage *t*
C_{it}	Energy cost for the *i*th ASEV at Stage *t*
C_R	Energy price per kWh from renewable generation
E_c	Energy consumption during each stage
C_{Gt}	Price per kWh of the grid-supplied energy at Stage *t*
E_{Rt}	Available energy generated by renewable generation at Stage *t*
B_{it}	Battery degradation cost for the *i*th ASEV at Stage *t*
g_t	Total cost for all ASEVs at Stage *t*
N_{EV}	Total number of ASEVs
g_N	Terminal stage cost for all ASEVs

C_{GN}	Price per kWh of the grid-supplied energy at Stage *N*
SoC_{max}	Upper bound of the SoC
SoC_{iN}	SoC of the *i*th ASEV at Stage *N*
N_{delay}	Total number of times of ASEV delay on the day
$T_{delay,i}$	Duration of the *i*th ASEV delay
$C_{punishment}$	Punishment cost per time slot
SoC_{min}	Lower bound of the SoC
u_{it}	Control decision for ASEV *i* at Stage *t*
d_j	Stages of delay
d_{thre}	Threshold of delay
U_t	Constraint set for u_t at Stage *t*
EC_{j0}	SLB starting energy capacity
EC_{min}	Lower bounds of EC_{j0}
EC_{max}	Upper bounds of EC_{j0}
EC_{dj}	Energy capacity decrease (kWh) per kWh of energy discharged
EC_{nom}	Nominal energy capacity
EC_{EoL}	End-of-second-life energy capacity
N_{LC}	Battery life cycles
ω	Parameter that is fitted with respect to the type of battery
k_r	Threshold percentage
ΔR	Resistance increase
V_{oc_r}	Rated open-circuit voltage
V_{EoL}	End-of-second-life terminal voltage
I_r	Rated discharge current
R_{EoL}	Internal resistance when a battery’s second life ends
V_{oc}	Open circuit voltage
V_{oc_r}	Rated open circuit voltage
γ	Maximum drop of the open-circuit voltage
P_c	SLB charging power
I_c	Rated charging current
V_c	Charging voltage
P_{tar}	Target discharge power
η_d	Converter efficiency
x_i	On-off status of row *i*

V_{ij}	Voltage of the SLB at row *i*, column *j*
I_i	Discharge current of row *i*
V_{oc_ij}	Open circuit voltage of SLB *ij*
R_{ij}	Internal resistance of SLB *ij*
I_{ij}	Rated discharge current of SLB *ij*
λ_Δ	Mean rate of flexibility calls
Δt_{fs}	Time interval between two consecutive flexibility calls
F	Performance factor of flexibility service
T_a	Actual duration for which the battery processer delivers flexibility
T_r	Duration required by the DNO for flexibility services
R_{fs}	Total revenue from providing both types of flexibility services within a month
ρ_{nf}	Unit price per kWh of flexible energy delivered for the non-critical flexibility service
N_{nfs}	Number of non-critical flexibility services within a month
C	Contracted flexibility capacity in kW
$T_{a,i}$	Actual duration of the *i*th time of the non-critical flexibility service
ρ_{cf}	Unit price per kWh of flexible energy delivered for critical flexibility service
N_{cf}	Number of critical flexibility services within a month
$P_{b,i}$	Delivered power of critical flexibility service in kW
$T_{b,i}$	Actual time interval of the *i*th time of the critical flexibility service
$E_{s,t}$	Energy surplus at time *t*
$P_{j,dmax}$	Maximum discharge power of SLB *j*
R_{ea}	Revenue from energy arbitrage within a day or a month
P_t	Discharge power of the SLB matrix
ρ_t	Electricity price at time *t*
Δt	Time interval
η_d	SLB discharging efficiency
η_c	SLB charging efficiency
R_j	The income customer *j* will receive from the battery processer
C_{cost}	Operation and management cost of the battery processer
P_{profit}	Profit reserved for the battery processer
π	Percentage of revenue that the battery processer shares with all customers
$P_{i,t}^{char}$	Charging power for EB *i*

$P_{i,t}^{grid}$	Charging power from the grid
$P_{i,t}^{SLB}$	Charging power from the SLB
$EC_{SLB}^{nominal}$	Nominal energy capacity of SLB
EC_{SLB}^{EoL}	Energy capacity when SLB reach its end of life
SoC_{SLB}^{max}	Maximum SoC at the time stage *t* of SLB
SoC_{t}^{SLB}	Current SoC at the time stage *t* of SLB
T_{i}^{flex}	Scheduled time interval of the flexibility service
$t_{i,start}^{flex}$	Start time of the flexibility service
$t_{i,end}^{flex}$	End time of the flexibility service
P_{i}^{flex}	Delivered power of the flexibility service
C_{t}^{EBgrid}	Energy cost of EBs purchased from the grid at time slot *t*
$C_{t}^{SLBgrid}$	Energy cost of SLB charging at time slot *t*
C_{t}^{SLBdeg}	SLB degradation cost at time slot *t*
B_{t}^{flex}	Benefits of providing flexibility service
EP_{t}^{grid}	Electricity price at time slot *t*
$P_{SLB,t}^{grid}$	SLB charging power at time slot *t*
P_{t}^{SLB}	SLB discharged power at time slot *t*
LC_{t}^{SLB}	Remaining life cycles until its end-of-life
EP_{t}^{flex}	Price of the flexibility power
A_j	Percentage of the power of the base load consumption for the distribution transformer at time slot *t*
S_T	Total capacity of the distribution transformer
N_{pot}	Total number of chargers in the EB charging station
T_{arrive}	EB arrival time
$T_{departure}$	EB scheduled departure time
$SoC_{j,t}^{EB}$	SoC of EB *j* at time slot *t*
SoC_{min}^{EB}	Minimum value of the EB

SoC_{max}^{EB}	Maximum value of the EB
$\Delta SoC_{exp,t}^{EB}$	Expected SoC reduction for a trip at time *t*
$P_{dischar,max}^{SLB}$	Maximum discharging power of the SLB
$P_{char,max}^{SLB}$	Maximum charging power of SLB
$P_{j,t}^{travel}$	Energy consumption per hour for EB *j* at time slot *t*
P_{j}^{max}	Maximum charging power for EB *j*

Chapter 1.
Introduction

Chapter contents:

1.1. Background and motivation 2
1.2. Research aims 6
1.3. Research objectives and contributions 6
1.4. Thesis layout 9

This chapter briefly presents the background, motivation, objectives, challenges and contributions. It also shows the overview of this thesis.

1.1. Background and motivation

1.1.1. The importance of EV development

The UK government has set the target to achieve net-zero carbon emissions by 2050 [1], in an effort to tackle the pressing climate change problem [2]. Major countries in the world have set similar targets to achieve net-zero carbon emissions [3], alongside the climate emergency declared by a number of countries [4]. Among the four sectors of transport, energy, retail and industry, transport accounts for 27% of CO_2 emissions [5]. Therefore, the electrification of transport is necessary for achieving the target of net-zero carbon emissions. In light of this, there is a rapid increase of electric vehicles (EVs) replacing fossil fuel vehicles, from under 9000 EVs in 2010 to 565,000 in 2021 [6]. The UK government has taken a historical step with a plan to end the sale of fossil fuel vehicles by 2035 [7]. This translates to the huge potential growth of EVs (including HEVs and PHEVs) to replace fossil fuel vehicles in the years to come.

The progress report in 2021 [9] shows that although the first and second carbon budget has been met, the fourth and fifth budget is difficult to be met. These budgets were set to achieve an 80% reduction in carbon emission, not the Net-Zero. To achieve the new target on time, the progress in reducing carbon emissions should be accelerated. One of the important parts of reducing carbon emissions is transportation electrification.

In recent decades, the gas emission pollution produced by transport is a major concern. The report from the Department for Transport in the UK [5] shows that in 2019, the carbon emission from domestic transport produced 27% of the UK's total emissions (122 $MtCO_2e$ of 455 $MtCO_2e$). Although it is a reduction of 1.8% compared with the emissions from 2018, transport is still the largest emitting sector of carbon emissions. The report from the government illustrates that it is important to push the step of transportation electrification and developing the EVs.

1.1.2. Challenges existing in the development of EVs

There are a number of challenges associated with EVs. These challenges can be categorised into two classes:

1. The challenges associated with EV performance: the limited mileage range; the time required to charge batteries; the inconvenience of finding EV charging facilities; the recycling of retired EV batteries in future. With the increase of EV battery capacities, the mileage range problem might be relieved. However, this would require either longer charging time, thus aggravating inconvenience, or higher charging power if the charging time is not increased. The higher charging power would aggravate serious network problems

In particular, the processing of retired EV batteries brings both challenges and opportunities. From existing references, it is a huge waste to directly dump the retired batteries in landfills considering the retired batteries' energy potential [10]. Further, this is not environmentally friendly [11]. There is the potential for retired EV batteries to be re-purposed for applications that are less demanding than powering EVs. In other words, these retired EV batteries can have a second life.

2. The challenges EVs bring to the power grid: Since the distribution networks were not designed to host EVs, the rapidly increasing of EVs can cause network overloads, significant voltage drops, and excessive network losses. To enhance the stability and reliability of the power system for the connection of increasing EVs, a huge investment in grid reinforcement is required and the complexity of computation is much more than before. Due to the uncertainties and scalability of EVs, the connection of EVs is difficult to predict and this will bring more problems to the network planning for distribution

network operators.

1.1.3. Research gaps

To address these challenges mentioned above, two research topics are proposed to reduce the adverse effects of EV penetration and concerns brought by the increasing retired batteries: the control optimisation of EV charging and the second-life of the retired batteries. Up to now, a few references has studied the EV charging strategies and the possible solutions for retired EV batteries from different aspects. However, there are still a massive number of limitations in practice.

- **The problems existing in EV controlled charging strategy**

For EV charging, some conventional control strategies designed for residential EV customers have been given from existing studies, e.g., charging at midnight to avoid peak time [12]. However, these control strategies cannot be applied directly to all types of EVs. For the industrial/ commercial EVs, these control strategies are not primary choices in practice because such EVs are characterized by a heavy-duty, high-usage-frequency nature. A customized control strategy is supposed to be proposed to control their working and charging states.

Existing research has studied the EV optimal control strategies from different perspectives. However, there are still outstanding problems and they are summarised as follows:

For the scheduling part, it is necessary to collect the historical and statistical data to simulate the environment in which EVs operate. The accuracy of the data clustering or forecasting will significantly influence the efficiency of the optimal control strategy. Even for some customers, such as a public parking lot, it is hard to make accurate predictions.

The development of EV control algorithms should take into account problem dimensionality, computation efficiency and uncertainties in the environment. These difficulties result in the fact that EV control algorithms can only achieve approximate optimality.

EV battery degradation costs should be considered but this is a difficult task. The degradation of the EV battery is a complicated chemical process and depends on many factors, including the battery type and the operating environment. It is difficult to collect the battery performance information and simulate the degradation of the battery accurately.

- **The problems caused by EV batteries**

Although the retired EV batteries have the potential to serve for less-demand applications, e.g. providing grid services, there are still challenges that need to be addressed:

1) The accurate remaining life of the SLB is difficult to predict. Given the uncertainties of the remaining life, it is hard to do life-cycle cost-benefit analyses involving SLBs.
2) The SLBs of different types may be connected in the same system and such a mixture would reduce the SLBs’ remaining life.
3) There are uncertainties in future laws and regulations regarding the recycling of retired EV batteries. For environmental reasons, it is expected that the laws and regulations would favour the second use of retired EV batteries.

To sum up, two challenges are raised as follows: 1) for EV optimal control, modelling the operation of EVs and optimally managing the operation of EVs considering the related uncertainties in operation environments and reflecting the effects of battery degradation; and 2) proposing a feasible business model of SLBs which should both reduce the effect of the accuracy of SLB remaining life prediction and the difference between their characteristics; and encourage the EV owners to send SLBs to battery processers instead of landfill.

1.2. Research aims

This thesis aims to tackle the following research questions: 1) the optimisation problem about the management of airport service electric vehicles; 2) the business model of the second-life batteries when utilized for less-demand applications; 3) the control management of the electric bus charging station with the connection of second-life battery energy storage system.

This thesis aims to meet EV charging needs whilst respecting grid constraints, and develop a techno-economic solution to efficiently handle retired EV batteries, for the benefits of EV owners, the battery operator and the grid.

1.3. Research objectives and contributions

Chapter 1.1.2 has introduced that there are several research challenges existing in the development of transportation electrification. These challenges are divided into two different types. The first type of problems is about the modelling of EVs and how to achieve the control optimisation. To solve these problems, this thesis makes the original contributions that for the EV charging optimal charging strategy, for the first time chose airport service electric vehicles (ASEVs) as research objects and design a dynamics model for them and build a customized optimal control approach for the optimal operation of ASEVs.

The second kind of challenges are mainly about how to deal with the SLBs, including the accurate estimation of the SLB's remaining life, the potential less-demand applications and how to encourage EV owners to send the retired batteries for their second life applications. To address these challenges, this thesis for the first time designs an SLB business model based on a monthly-payment mode and applies the SLBs to perform energy arbitrage and provide flexibility services for the DNOs.

1.3.1. ASEV dynamics model and optimal control strategy

The uncontrolled charging behaviour of EVs leads to severe network problems. For the industrial/commercial EVs, their owners will pay more for EV charging. According to these consequences, setting the ASEVs as research objects, this thesis developed a novel dynamic model to simulate the operation of ASEVs. To optimally control the model to both reduce the power demand during peak time and save the investment cost for the EV owner (airport), a customized optimal control strategy based on the rollout approach is designed.

Firstly, this thesis develops a dynamic model of ASEV to guide its real-time management considering the uncertainties. In real-time management, the control of ASEV should be faced with a few uncertainties. They include the flight schedule, the number of passengers and the luggage weight. Unlike the previous models, the dynamic model describes the ASEV states, their transition over time and the effect produced by the control decisions. The model includes both discrete dynamics and continuous dynamics. For example, the discrete dynamics involves the transition of the ASEV states, including 'work', 'charge' or 'idle', and the continuous dynamics involves the change of the battery state of charge (SoC) over time. Besides, the model simulates the stochastic nature of the ground transport workload to reflect the influence of the nature uncertainties.

Secondly, this thesis proposes a customized optimal control strategy for the dynamic system. The optimal control of dynamic systems is related to stochastic dynamic programming because of their stochastic and dynamic nature. A rollout algorithm is borrowed and adapted for ASEV optimal controlling. This control method is real-time management, with the objective of minimizing the total operation cost for the airport and encouraging to reduce peak demand compared with some heuristic algorithms. The rollout approach is designed based on two suboptimal control algorithms and iteratively improve them to a more optimal strategy. Moreover, the rollout significantly addresses the challenge of ‘the curse of dimensionality’.

1.3.2. SLB monthly-payment-business model to perform energy arbitrage and provide flexibility services

To address the SLB application problems, this thesis proposes a novel business model for SLB to perform energy arbitrage and provide flexibility services. Previous references pay much attention to the prediction of the SLB's remaining life. However, despite the development of prediction methods, the investment in applying these methods to real-life keeps increasing. To address the challenge and adopt the SLBs to suitable applications, this thesis proposes a monthly-payment business model for SLBs. The model features a profit-sharing between battery processers and customers through monthly payments from the former to the latter. If there is a profit produced by a certain SLB, the battery processer will monthly pay to the SLB provider until its SLB reaches the threshold that indicates the end of life. In case a loss occurs in the business, the sharing will stop, and the model reveals the battery processer the true cost of the SLBs. Through the monthly payment mode, the task of predicting SLB remaining life for the second life applications and performance at the beginning will be bypassed. Also, a specific heuristic algorithm is designed to guide the SLBs to perform energy arbitrage and provide a range of flexibility services for DNOs. To sum up, the SLB business model will address the difficulties of forecasting SLB remaining life, control SLBs to perform energy arbitrage and provide flexibility services, and encourage the EV owners to send SLBs to battery processers by profit sharing at the same time.

1.4. Thesis layout

The rest of the thesis is organised as follows:

Chapter 2 reviews the existing literature on EV development, including the different optimal methodologies adopted in different EV scenarios, the application of SLBs.

Chapter 3 proposes the dynamic model of ASEVs which can describe both the working state of ASEVs and the uncertainties during the management process. To control the ASEVs based on the dynamic model, a customized rollout approach is developed to get the optimisation results. The feasibility of the optimal algorithm is validated through simulations in a summer and a winter typical month.

Chapter 4 proposes the business model of SLBs based on a monthly-payment methodology. The business model applies SLBs to supply flexibility services to DNOs and perform energy arbitrage to make profits. By a 10 years' simulation, the energy potential and economic efficiency of the business model is proved.

Chapter 5 proposes an EB charging station model with an SLB energy storage system. In this scenario, the SLB storage system supports the EB charging if necessary and provides flexibility services for DNOs. To validate the feasibility, a comparison between three different control algorithms is shown in the case study.

Chapter 6 shows conclusions of the thesis, including the key findings of the research and the contributions from the work.

Chapter 7 proposes some potential future topics in EV optimal control and the SLB applications.

Chapter 2.

Review of EV optimal control and second life EV batteries

Chapter contents:

2.1. Introduction 12

2.2. Optimal control of EV charging 12

2.3. Second life batteries 21

2.4. Chapter summary 25

This chapter reviews the existing studies on the optimal control of EV charging and the utilization of second life EV batteries.

2.1. Introduction

In this chapter, a comprehensive literature review is conducted on the EV optimal control and how to deal with SLBs retired from EVs.

2.2. Optimal control of EV charging

2.2.1. The consequence of over penetration of EVs in networks

Nowadays, EV charging is classified into two categories: battery charging and battery swapping. Battery charging is further classified into slow charging (e.g., domestic charging outlet) and fast charging (e.g., charging stations or parking lots). However, regardless of the charging mode, EVs would bring severe problems to the grid if the EV charging behaviour is not controlled.

- **Network overloads**

Power grids that were built decades ago were not designed to host unlimited EVs. Today, rapidly increasing EVs increase the network loading to an unprecedented level. This is particularly a problem if the EVs are charged in an uncoordinated fashion, which can result in cable and transformer overloads, equipment damages and consequent power outages [13].

For example, reference [14] demonstrates that with the connection of a single EV, the energy consumption will be potentially doubled for a local household. With a large population of grid-connected EVs, the number of grid congestion problems will rapidly increase. Additionally, reference [15] shows that the unpredicted EV charging demand will affect the network reinforcement.

- **Power quality degradations**

With the EV charged from the network, a huge number of power electronic devices, which are regarded as nonlinear loads, are connected to the grid. The harmonics from the nonlinear loads would cause power quality problems [16] [17].

For example, in reference [18], it shows that with the EV charger connected to the power grid, the highly nonlinear systems, including the power electronic converters, switching power semiconductor components, will cause severe disruption on the source side. Reference [19] clarified that the fast-charging stations made large effects on power quality and distribution transformer due to the adoption of voltage source converter in the process of EV fast charging.

- **Reinforcement cost for DNOs**

The uncertainties of the EVs in their load behaviours increase the complexities of network planning and operation, potentially leading to high reinforcement costs for the DNOs.

2.2.2. The different control strategies for EV charging

There are many different control strategies for the charging of high penetration of EVs. The objective of these control strategies is also variable, such as reducing the impact of the charging behaviours for the distribution networks and reducing the cost for the EV owners. For example, reference [20] developed an algorithm that controls the EV charging behaviour to reduce the peak demand for distribution networks. The control strategies are classified into two classes: centralized scheduling and decentralized scheduling.

- **Centralized scheduling**

The centralized scheduling means that there is an EV aggregator or a central controller that optimises the EV charging process. A number of pieces of literature focus on centralised control of EV charging: reducing the power fluctuation for a network [21], reducing the cost for parking lots, especially those equipped with renewable energy systems [22], and increasing the security and the efficiency of the network [23]. A number of algorithms are employed to perform centralised optimal control, e.g. two-stage stochastic programming, genetic algorithm, and scenario tree.

Among all these control methodologies, two-stage stochastic programming is of particular importance. In this modelling process, the decisions are made under uncertainties. For example, in reference [24], two-stage programming is used to manage the EV charging in an office building. In the first stage, the objective of the model is to minimize the expected cost, including the operation cost for the building, the energy cost for the day-ahead power market, the cancellation cost and the real-time electricity transaction cost. The second stage is to control the real-time EV charging taking the power scheduling from the first stage. In the second stage, it is necessary to satisfy all the EV charging demands although the actual EV power is not the same as is assumed in the first stage.

Reference [25] adopts two-stage programming in the planning of charging stations. In this case, the first stage is to determine the location of the charging stations using historical and statistical data, while the second stage is to enhance the charging station placement with the actual EV charging demands. In reference [26], a two-stage programming model is proposed to guide EV battery swapping in a battery swapping station. The first stage is to determine the location of the battery swapping station and the number of batteries stored in each station. The second stage is to satisfy the PHEV battery swapping demand at each time slot and provide energy backup services for the grid. In reference [27], the first stage is to make a charging strategy to minimise the EV owner's charging cost, while the second stage is to maximize the aggregator's economic benefit without increasing the EV owner's charging cost. In stage two, the EV charging control strategy is treated as a constraint.

However, the drawbacks of centralized control are also significant. Firstly, the centralized control strategy requires advanced information & communication infrastructure to transmit the information of all EVs in a timely manner. The data quality through the communication significantly affects the accuracy of the final decisions. Secondly, in this process, EV aggregators or operators are required to control the EV charging power. This business model itself incurs a transaction cost. Thirdly, the communication and computation burdens increase with the number of EVs, potentially hindering the scalability of the solution [28].

- **Decentralized scheduling**

A decentralized control strategy is where individual EVs determine their charging schedules to minimise the costs, taking into account their own needs and external incentives. Different EVs may communicate with each other, but there is no aggregator. Decentralized control strategies employ a range of mathematical models such as non-cooperative games [29], neural networks [30] and the Markov decision process [31].

Compared to EV centralized control strategies that aim to achieve a common good or a social benefit, decentralized control strategies mainly focus on reducing individual costs, aiming to indirectly realise a social benefit through external incentives and possible interactions among individual EVs. Reference [32] shows that to achieve the valley-filling, the decentralized algorithm is used to optimally schedule the EV charging behaviours. In the process, the EV charging profile will be constantly updated through the control signal broadcast to increase the time efficiency of the scheduling. In reference [33], the decentralized strategy is to minimize the energy purchased cost for EV owners and ensure grid stability. A game theory is introduced in the EV charging control to make a balance between the 'individual best-response strategy' and the 'socially optimal charging profiles'. Reference [34] introduces a decentralized method, in which the objective function includes both the generation cost and the battery degradation cost. It proves that such a decentralized control strategy can be nearly socially optimal under certain mild conditions.

The decentralised control strategy also has limitations in real applications. Firstly, decentralized control means a lack of global information [35], resulting in the difficulty of finding globally optimal solutions. Besides, although the demand for computational resources required is lower than the centralized control, the decentralized control will possibly pose a high communication burden.

2.2.3. The optimal control of domestic EVs and industrial/ commercial EVs

There are a number of differences in the control of industrial/commercial EVs versus domestic EVs. This is because:

1) Firstly, the operation model of industrial/commercial EVs is different from that of domestic EVs. The domestic EVs serve people's casual and commute purposes,

meaning that most of the time they are free for charging. Compared to domestic EVs, industrial/commercial EVs serve business needs as a top priority and thus may be busy even the whole day. Therefore, the control of industrial/commercial EVs tends to be more challenging to fit the tight schedule as compared to domestic EVs.

2) Secondly, the charging mode is another gap between them. For domestic EVs, slow charging (typically with a charging power of 7 kW) is popular [36] [37]. Fast charging (with a power of more than 20 kW [38]) is available at some public parking lots for domestic EVs. In contrast, to reduce the charging time and meet business needs, industrial/commercial EVs are mostly charged under the fast-charging mode.
3) Thirdly, for an industrial/commercial EV fleet, the control decision is made by a common EV owner, for example, an airport controls its ASEVs centrally. Thus, the control strategy for industrial/commercial EV charging is designed as centralised control. But for domestic EVs, the control strategy can be both designed as centralised or distributed control.

- **Research on domestic EV charging**

There is a variety of EV charging control strategies for domestic EV charging, depending on charging locations. In reference [24], the EV charging strategy is a centralised control strategy for charging at a commercial building. The charging strategy not only satisfies the charging demand of each EV but also controls the EV to be part of an energy management system for a commercial building with PV generation. In reference [39], the charging location is households. The charging strategy is designed that integrate EVs as part of an energy management system to provide vehicle-to-home service. The charging strategy is based on model predictive control and it is a combination of stochastic modelling and prediction. Apart from the references mentioned above, reference [40] shows that a distributed charging strategy is proposed for community EV charging, without the need for a central control unit being unnecessary. Reference [41] studies EV charging at commercial parking lots. With a two-stage control strategy, the energy cost can be significantly decreased.

From the references, domestic EVs charging at different locations corresponds to different charging strategies. Domestic EVs play specific roles at different charging locations. For charging at a commercial building, EVs can consume renewable energy and provide vehicle-to-building services [24]. When charging at home, EVs can be part of an energy management system or an energy hub [42]. Moreover, both the centralised control strategy and the distributed control strategy can be applied for domestic EV charging.

- **Research on industrial/commercial EV charging**

Compared with the research on domestic EV charging, industrial/commercial EV charging is mainly decided by their nature of business, such as electric taxis and electric buses. Electric buses (EBs) are a major type of industrial/commercial EVs widely used nowadays. The research on EBs can be sorted into three different areas: long-term scheduling for investment in EV fleets and charging infrastructure, the improvement of charging infrastructure and optimal control scheduling. In this thesis, we primarily concentrate on the scheduling of the EBs. In reference [43], EBs are wirelessly charged, where the charging power can be much higher than that of traditional plug-in EBs. The objective is to minimise the operating electricity cost. The charging control model is formulated as follows:

$$minf = \sum_{t=1}^{T}\sum_{i=1}^{I} L_{i,t} \tag{2-1}$$

subject to

$$E_m^g = SoC_{n,m,t} + E_{n,m,t}^c - SoC_{n,m+1,t} \tag{2-2}$$

$$E_m^g = SoC_{n,m,t} + E_{n,m,t}^c - SoC_{n,m+1,t} \tag{2-3}$$

$$SoC_{n,m,t} + E_{n,m,t}^c \le E_{max}^c \tag{2-4}$$

$$SoC_{n,m,t} \ge E_{min}^c \tag{2-5}$$

$$C_{max} q_t \ge f_{t,(m,m+1)} \tag{2-6}$$

This first equation describes the minimum charging requirement for each EV, where E_m^g is the transmission electricity consumption, $E_{n,m,t}^c$ is the obtained electricity. This constraint means that the EB should be charged with enough energy to ensure that it can arrive at the next station *m*+1. The second equation shows that the energy consumption of the travel between two bus stations should not be over the battery capacity and the $max\{E_m^g\}$ means the maximal transmission electricity consumption between two bus stations. The third and the fourth equations are the SoC limits that protect the battery. Considering the characteristics of the EBs, the EBs are supposed to provide satisfactory services for the passengers. All passengers should be taken and the charging time at the station should not influence the departure time. Based on this, the fifth equation is the passenger satisfaction constraint, where C_{max} is the capacity of the EBs, q_t is the bus departure frequency in time slot t, $f_{t,(m,m+1)}$ is the passenger flow between bus stations.

Given the problem formulation, a two-stage control algorithm is proposed to solve it. In this first stage, the determination of the electricity from the day-ahead market will be made based on historical data and some reasonable assumptions. And then regarding the day-ahead electricity as an input for the second stage, the target of the second stage is to minimize the energy and operational cost with a centralized optimal algorithm.

Besides the reference mentioned above, reference [44] denotes an optimal control strategy considering not only the limited EV driving ranges but also the crew labour regulation. The strategy solves the EB and the crew scheduling problem at the same time. In reference [45], the authors focus on the EB optimal management and reducing the number of battery chargers. The proposed method can reduce both the operational cost of EB and the investment in the battery charging infrastructure. Differently, reference [46] pays attention to the scheduling of multiple types of EBs and the simulation results show that the proposed method can reduce 15.93% of the annual total scheduling cost compared with the existing method.

In addition to EBs, reference [47] focus on the optimisation of allocating the charging stations to support electric taxies in large urban areas. Reference [48] demonstrates the potential of applying battery swapping to electric taxi and propose a feasible validation. Reference [49] shows the control management of the electric refrigerated truck. However, industrial/commercial EVs have apparent differences based on their different application, and the control strategy designed for a certain type of industrial/commercial EV cannot be directly applied to another type. To achieve the ‘zero-emission’ target from transportation, transportation electrification will cover more areas in addition to public transport. The research on optimal control of the EV needs to work on different types of industrial/business EVs.

2.3. Second life batteries

Nowadays, the implementation of SLB still faces with several challenges. These challenges include: the uncertain economic benefits, lack of automation in battery dismantling, the difficulties on accurately identify the SLB’s state of health of remaining life and the absence of standards and policies [50]. The most two important challenges are the uncertain economic benefits and the accurate estimation of SLB’s state of health and remaining life.

Existing references have compared the differences between the new batteries and SLBs in some certain scenarios. Reference [51] presents a project of solar-plus-second-life energy storage in California. With a comparison between the new batteries and SLBs, it concluded that if the SLBs can be sold less than 60% of their original price, it might be profitable in this project. Reference [52] studied the effect of the disassembling costs on the application of SLBs. It shows that to increaser the economic benefits of the SLBs compared with new batteries, it is important to reduce disassembling costs and the repurposing of the whole battery would make sense compared with reusing at module level.

2.3.1. The economic analysis of SLBs

The battery cost is a major component of the EV cost. The re-use of the retired batteries from EVs can benefit both EV owners and the battery processers. For EV owners, selling retired EV batteries for second-life applications can maximize the battery value, compared to sending them directly to recycling or landfills. For the battery processer, the application of SLBs may reduce the investment and the operational cost. For the economic analysis, the most important part is to compare the utilisation of SLBs with the utilisation of new batteries in providing the same service.

For example, in reference [51], the SLBs are used as stationary energy storage coupled with a PV system. To make a data-driven analysis, the SLB storage system project is compared with another storage system with new batteries. The operating environment of the two storage systems is set the same. The degradation of the SLBs is simulated by a data-based model and it will predict the capacity fade of SLBs. The SoC range is set between 15% to 65% to protect the batteries and the capacity threshold is 60% of its original capacity. The simulation results of the two storage systems show that with these conditions, the SLB storage system can save the total cost by 40% compared to using new batteries. However, the economic analysis is made based on the assumption of the costs of the SLBs being 80% of the new one. The ‘80%’ comes from assuming that the state of health of the SLBs is 80%. In reality, SLBs have different remaining lives, the pricing of SLBs would significantly affect the business feasibility.

2.3.2. The buying price and the selling price for the SLBs

Before applying SLBs to further applications, the first problem is to determine suitable pricing for the battery processer to buy retired EV batteries. In reference [53], the authors introduced the following formula for calculating the price:

$$V_{used} = V_{new} \times f_{health}(1 - f_{reuse} - f_{discount}) \tag{2-7}$$

where V_{used} is the buying price of the SLB in the n^{th} year, V_{new} is the price of the new battery whose capacity is the similar value in the n^{th} year, f_{health} is the state of health (SOH) of the battery, f_{reuse} denotes the SLB re-proposing cost and $f_{discount}$ is a discount factor to encourage the use of SLB. The SOH is one of the most often used parameters to define the potential of the battery. It is a ratio of the measured energy capacity of a battery to its nominal capacity, shown in Equation (2-8):

$$SOH(\%) = \frac{Q_m}{Q_n} \times 100\% \tag{2-8}$$

where Q_m represents the measured capacity and Q_n is the nominal capacity. Although the energy capacity of the SLB is possible to be measured by modern facilities, the accuracy of the direct measurement is still limited by several components, such as the precision of the instruments. It is essential to develop the prediction of the remaining life of the SLB.

2.3.3. The prediction of the remaining life of the SLBs

Existing research has made a lot of efforts on improving the accuracy of the prediction of the SLB's state of health (SOH) and remaining life. Reference [54] models battery degradations as a Brownian motion. The longer distance a Brownian particle moves, the deeper the degradation will be for the battery. A particle filter is used in this model to estimate the drift parameter of the Brownian motion. Reference [55] shows a prediction model based on a relevance vector machine. To improve the efficiency and accuracy of the model, a wavelet denoising approach is used to reduce uncertainties and a mean entropy method is employed to choose the optimal embedding dimension. References [56] and [57] both advise that deep learning be employed to estimate the capacity and predict the SLB lifespan. The difference between the two research papers is that: the first one introduces a combination of the extreme learning machine and broad learning to make the prediction, and the second one proposes a full end-to-end deep learning to boost the forecast process and reduce the error rate.

The existing methods for predicting SLBs' health and remaining life have several limitations. The first limitation is about the challenges to achieve these predictions in real-time operation. It includes: 1) these prediction methods are designed based on modern complex intelligent algorithms, the cost of adopting these algorithms is a large burden for the battery processers; 2) the relationship between the time efficiency and the economy benefits is still uncertain and there is no existing study which has discussed about it. For the battery processers, it is difficult to find a balance between the time efficiency and the profits. Another kind of limitations are about the real-time SLB states: 1) each method is suitable for a specific type of battery, not mixed types of SLBs in a real-world setting. There is no single method suitable for all SLB types because of the different mechanisms of battery degradations; 2) experiments that underpin existing references are performed in laboratory conditions with constant environment parameters. However, in a real-world setting, environment parameters vary from time to time, challenging the validity of the regression models derived from the laboratory experiments. With these challenges, it is hard for the battery processer to choose an appropriate prediction method for the remaining life of SLBs.

2.3.4. The existing business model on SLBs.

There are existing business models for the SLBs. Reference [58] proposes that the EV owner can lease new batteries from the manufacturers instead of directly purchasing them. The EV owner needs to pay a monthly rent for the new batteries. After the retirement of the batteries, the SLBs will be leased to customers who need an energy storage system. With the proposed model, the EV batteries can work for about 15 years and the profit rate can reach 35%. Reference [59] shows three different business models for SLBs. The first one is that the original equipment manufacturers (OEMs) only sell the SLBs to an agent, who can design the SLB applications. The SLB agent helps the SLB customers to solve the SLB application problems. The second one is that instead of simply selling the SLBs, the OEMs participate in solving the SLB application problems with the SLB agent. For the third one, the OEM of the SLBs should take both sell the SLBs and deploy them for applications for the customers. Reference [60] introduces an SLB business model that is built on a power system equipped with a 'centralized battery swapping management system' (CBSMS), a smart battery rapid tester, a local load management system, a battery bank, and a solar photovoltaic grid integrated/standalone system or a mobile unit for battery charging and swapping. In this power system, the SLBs serve as an energy storage system that contributes to the EV control and peak demand reductions for the grids.

2.4. Chapter summary

This chapter performs a comprehensive review of the existing research on the optimal control of EVs and SLBs, from both technical and economic perspectives.

However, there are also gaps existing in solving these two problems. They are concluded as follows:

For the EV charging optimisation, the existing research mainly focuses on domestic EVs. There is an absence of studying kinds of industrial/commercial EVs while they are faced with the need for transportation electrification, like ASEVs. Furthermore, considering the uncertainties existing in the operation nature and the business demand, the scheduling of these EVs is difficult to be made.

For the SLBs, as mentioned above, the buying price depends on their SOH and remaining life. Although a massive number of references have studied the prediction methods, in reality, the high investment and operation complexity still block the application of these methods.

To increase the development of EVs, both the EV charging optimisation problems and the SLB application problems need to be solved. However, mostly the two problems are addressed separately. It might be feasible to apply SLBs to optimally control the operation of EVs so that the two problems can be solved at the same time.

To bridge the above challenges, this thesis, 1) proposes a dynamic model for the control of ASEV and designs a customized rollout approach as a near-optimal control method for this model in Chapter 3; 2) proposes a monthly-payment-based business model for SLBs and provide flexibility services for grids and perform energy arbitrage in Chapter 4; 3) combine the SLB storage system with EB charging station to enhance the optimisation efficiency of the charging station in Chapter 5.

Chapter 3.

Energy management of airport service electric vehicles to match renewable generation through rollout approach

Chapter contents:

3.1. Chapter overview 28
3.2. Abstract 31
3.3. Introduction 31
3.4. Overview of methodology 35
3.5. Problem formulation: ASEV dynamics model 36
3.6. Near-optimal control of ASEV dynamics model 45
3.7. Case study 49
3.8. Conclusion 57

This chapter develops a novel dynamic model for the ASEVs and designed a customized algorithm based on the rollout approach to solving the EV charging optimisation problems.

3.1. Chapter overview

With the target of ‘zero-emission’, transferring traditional diesel vehicles to EVs is essential for not only residential customers but also industrial/commercial users. However, unlike domestic EVs, industrial/commercial EVs should satisfy business demands based on their characteristics, which means a high-usage-frequency operation nature. For different types of industrial/commercial EVs, it is necessary to design specific control strategies to achieve optimal control considering the different working natures.

This chapter takes airport service EVs as the research object to achieve energy management and guide the charging strategy to reduce the energy generation cost. The ASEVs are different from other kinds of industrial/commercial EVs. For example, compared with EBs, its departure time depends on the arrival/departure time of flights, which are frequently faced with delay or even cancellation. But the EBs have to be departed on time according to its time schedule. Compared with electric taxis, the ASEVs are mostly adopted centralized control strategies but not distributed control strategies.

Firstly, this chapter proposes a novel ASEV dynamics model. This model involves both the discrete variables, e.g. the state of the ASEVs (charging, idle or work) and continuous variables, e.g. the SoC of each ASEV. Furthermore, considering the uncertainties in this model, including the number of passengers and the luggage weight, stochastic programming is used to model the uncertain ground transport workload. The model transfers the ground transport workload uncertainties to ASEV’s working time for each flight and adopt related distributions to describe it. To perform the optimal control of the ASEVs, a near-optimal control strategy based on the rollout approach is proposed to minimize the operational cost, including the energy purchase cost and the battery degradation cost, and match the renewable generation.

In the case studies, a medium-sized airport is chosen and the simulations are operated in a summer month and a winter month. To validate the feasibility of the proposed management strategy, a comparison between the benchmark model and the proposed dynamics model is shown in the case studies. In this chapter, the benchmark control strategy is assumed as the ‘greedy charging’ heuristic algorithm. The simulation results denote that on both summer days and winter days, the rollout approach results in a reduction of over 10% of the total cost compared with a ‘greedy charging’ strategy. It also reflects the related accuracy of the proposed dynamics model of the ASEV and the customized rollout approach.

The rest of the chapter is cited from the author’s submitted article in IEEE Transactions on Transportation Electrification. The structure of this chapter is organised in an alternative-based format, where the indices, equations, tables, figures and titles are numbered independently.

Statement of Authorship

This declaration concerns the article entitled:									
Energy Management of Airport Service Electric Vehicles to Match Renewable Generation through Rollout Approach									
Publication status (tick one)									
Draft manuscript		**Submitted**		**In review**	√	**Accepted**		**Published**	
Publication details (reference)	R. Wei, K. Ma, " Energy Management of Airport Service Electric Vehicles to Match Renewable Generation through Rollout Approach" in IEEE Transactions on Transportation Electrification								
Copyright status (tick the appropriate statement)									
I hold the copyright for this material	√	Copyright is retained by the publisher, but I have been given permission to replicate the material here							
Candidate's contribution to the paper (provide details, and also indicate as a percentage)	The candidate proposed the idea of the paper, he designed the methodology, and predominantly executed the coding to derive the experimental results. Other authors helped the candidate with the design of case studies, the format of the paper, and the improvement of academic writing. The percentage of the candidate did compared with the whole work is indicated as follows: Formulation of ideas: 80% Design of methodology: 100% Simulation work: 100% Presentation of data in journal format: 90%								
Statement from Candidate	This paper reports on original research I conducted during the period of my Higher Degree by Research candidature.								
Signed	Renjie Wei	**Date**	26/07/2022						

3.2. Abstract

Traditional diesel-based airport service vehicles are characterized by a heavy-duty, high-usage-frequency nature and a high carbon intensity per vehicle per hour. Transforming these vehicles into electric vehicles would reduce CO_2 emissions and potentially save energy costs in the context of rising fuel prices if proper energy management of airport service electric vehicles (ASEVs) is performed. To perform such energy management, this thesis proposes a new customized rollout approach, as a near-optimal control method for a new ASEV dynamics model, which models the ASEV states, their transitions over time, and how to control decisions affect them. The rollout approach yields a near-optimal control strategy for the ASEVs to transport luggage and charge batteries, with the objective to minimize the operation cost, which incentivizes the charging of the ASEVs to match renewable generation. Case studies demonstrate that the rollout approach effectively overcomes the “curse of dimensionality” challenge. On both typical summer and winter days, the rollout algorithm results in a total cost of approximately 10% less than that of the underlying “greedy charging” heuristic, which charges a battery whenever its state of charge is not the maximum. The rollout algorithm is proven to be adaptive to flight schedule changes at short notice.

3.3. Introduction

The transition to electric vehicles (EVs) is vital for fulfilling the target of reducing CO_2 emissions by 80% by 2050 in the UK, relative to the 1990’s level [61]. Much attention was devoted to electrifying tens of millions of consumer vehicles. Although they are vast in number, they have a relatively low carbon intensity in terms of emission per vehicle per hour, because an average consumer vehicle remains dormant in most hours of the day and it is of a light-duty nature. Unlike consumer vehicles, airport service vehicles are characterized by a heavy-duty, high-usage-frequency nature, a high carbon intensity per vehicle per hour, and a strong correlation with flight patterns. Transforming diesel-based airport service vehicle fleets into EVs would dramatically reduce CO_2 emissions for this carbon-intensive industry. In this context, airport service electric vehicles (ASEVs) specifically refer to electric trailers that transport checked luggage between the sorting facility in the terminal and departure/arrival flights. The aim of this paper is to develop an optimal energy management strategy for the ASEVs in terms of battery charging and task assignment.

Existing research work focuses on consumer EVs and taxis at different locations, e.g. households, office buildings, highway service stations, etc. References [24], [62] focus on consumer EV charging at commercial buildings. A number of references consider domestic EVs as a part of home energy management systems [62], [39], [63], an energy hub [42] or a community energy system [40]. A number of references investigate the operation of electric vehicle parking lots [64], [41], including airport parking lots [65]. References [66], [67] both develop stochastic optimization models for the joint operation of EV fleets and renewable generation. Reference [68] develops a balanced charging strategy to satisfy both the EV owners (saving costs) and the network operator (relieving loads). However, the electrification of heavy-duty, high-usage-frequency, carbon-intensive commercial/industrial transport is a seriously under-researched area. In particular, no research work focuses on the optimal management of ASEVs. Reference [69] develops an optimization model to schedule airport ground operations, including aircraft and shuttle bus scheduling. Although that reference does not focus on EVs, it acknowledges the importance of the optimization of airport ground operations.

Although existing research has provided many optimal strategies for electric vehicle charging, for ASEV, they are not suitable for solving the energy management problem. Due to the flights not always arriving on time, the optimal plan is supposed to adjust to the real situation.

Also, because consumer EVs are owned by many different individuals, their behaviour reflects human lifestyles as well as individual random behaviour. However, ASEVs demonstrate fundamentally different behaviour as compared to consumer EVs, because ASEVs are centrally controlled and their behaviour depends on the flight schedule, the number of passengers, and luggage weight. ASEVs constitute a dynamic system of a stochastic, dynamic, hybrid nature that is distinct from consumer EVs and not reported in the existing literature. The uncertainty in the ground transport workload renders the model of a stochastic nature. The existence of both discrete variables (the decision variables for individual ASEVs to undertake ground transport tasks, charge, or idle) and continuous variables (the battery state of charge) renders the model of a hybrid nature. Both types of variables change over time, rendering the model a dynamic nature. It should be noted that, although the ASEV dynamics shares a similar stochastic, hybrid, and dynamic nature with a stochastic hybrid system (SHS) [70], it is not an SHS, because the discrete variables of the ASEV dynamics system do not follow a controlled Markov chain.

There are ASEV suppliers [71], [72], [73], but the optimal control of the ASEVs was an unanswered question. For an airport with tens of ASEVs, the dynamic system has a prohibitively large number of states (i.e. the “curse of dimensionality”), too large to derive an accurate optimal solution to the ASEV control problem. Therefore, two research questions arise from the optimal scheduling of ASEVs: 1) the modelling of the ASEVs as a distinctive dynamic system of a stochastic dynamic, hybrid nature; and 2) the derivation of an optimal control strategy for the dynamic system.

The optimal control of a dynamic system is related to the stochastic dynamic programming [19] in terms of its stochastic and dynamic nature. The rollout algorithm for dynamic programming [74], [75] can be borrowed but it needs to be adapted for the optimal control of ASEVs: the underlying heuristic control strategies need to be defined and uncertainties need to be properly modelled.

In summary, the following challenges are identified from the literature survey:

1) The optimal management of ASEVs considering its uncertainties is still a problem not yet investigated.

2) There is an absence of an ASEV dynamics model, which describes the ASEV states, their transitions over time, and how to control decisions affect them. Compared with the existing dynamics model, the ASEV model should reflect the uncertainties of the ground transport workloads and the flights, which are never discussed before.

3) There is an absence of an energy management method, which controls the ASEVs to meet a low-cost, low-carbon objective, subject to the ASEV dynamics. The existing real-time control algorithm is mainly consisted of modern artificial intelligent algorithms. Considering that the investment and the computational complexity, a customized control algorithm needs to be designed for the ASEV dynamics model.

To bridge the above gaps, this paper makes the following original contributions:

1) This paper proposes a new ASEV dynamics model. The model involves: i) discrete dynamics, i.e. the changes of the ASEV discrete states to “work”, “charge”, or “idle” over time; ii) continuous dynamics, i.e. the changes of the battery state of charge (SoC) over time; and iii) a stochastic nature of the ground transport workload.

2) To perform energy management of the ASEVs, this paper proposes a new customized rollout approach, as a near-optimal control method for the ASEV dynamics model. The approach controls the ASEVs to transport luggage and charge batteries, with the objective to minimize the total operation cost. Two customized suboptimal heuristic

control strategies are proposed as the base strategies for the rollout approach, which then iteratively improves the heuristic control strategies into a near-optimal control strategy. The rollout approach effectively overcomes the “curse of dimensionality” challenge.

The energy management of ASEVs through the rollout approach will bring a number of benefits: 1) it will save costs for the airport; 2) by matching the ASEV battery charging load curve with renewable generation, the control method encourages the ASEVs to consume locally generated renewable energy, reduces CO_2 emissions, and makes the charging load curve friendly to the grid.

The rest of this paper is organized as follows: Chapter 3.4 gives an overview of the methodology; Chapter 3.5 presents the ASEV dynamics model; Chapter 3.6 presents the optimal control method for the ASEV dynamics model; Chapter 3.7 performs case studies, and Chapter 3.8 concludes the paper.

3.4. Overview of methodology

The optimal control of ASEVs aims to minimize the total operation cost, including the energy cost and battery degradation cost. Electrical energy comes from two sources: 1) energy from the grid under the time of use tariffs, and 2) energy purchased directly from local renewable generation. The 2nd energy source has a lower tariff than the 1st source. This encourages ASEVs to consume locally generated energy for local balancing.

The ground transport workload depends on the number of passengers and luggage weight for each flight. The uncertainties in the ground transport workload are incorporated into the ASEV dynamics model, which models the control decisions, the ASEV states and their transitions.

As a near-optimal control method for the ASEV dynamics model, the rollout approach starts from two suboptimal heuristic control strategies and iteratively improves the better one of the two heuristics toward reducing the total operation cost.

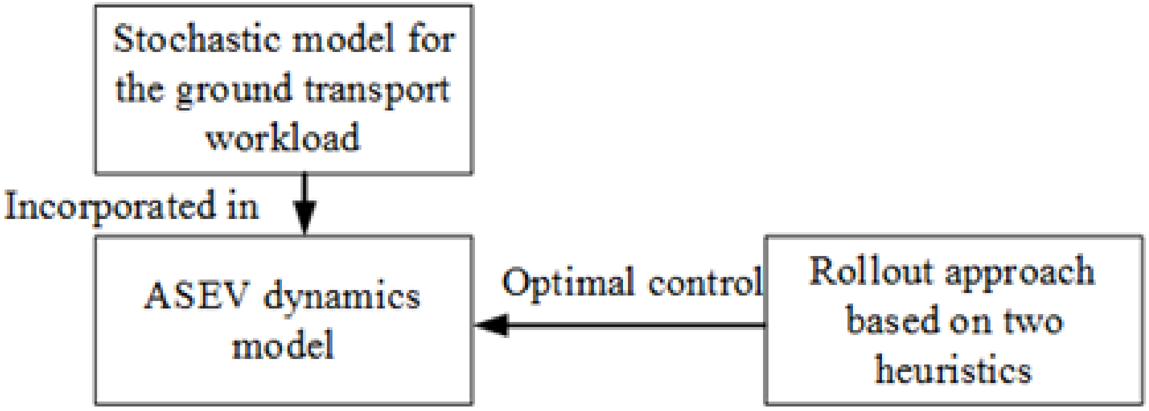

Fig. 3-1 Flowchart of the models and the optimal control approach

Fig. 3-1 shows a flowchart consisting of the three components: the stochastic model of the ground transport workload, the ASEV dynamics model, and the rollout approach.

3.5. Problem formulation: ASEV dynamics model

The ASEV uncertainties are divided into two different parts: the uncertainties of the ground transport workloads and the uncertainties of the flights. For the uncertain ground transport workloads, the proposed model adopted an appropriate model which is explained in Chapter 3.5.1. For the uncertainties of the flights, including the flights delaying or cancelling, a Guassian noise is added to the model to reflect the delaying time of each flight.

3.5.1. Modelling of Uncertain Ground Transport Workload

Before presenting the ASEV dynamics model, the ground transport workload model is presented. Suppose the *j*th flight is awaiting ground transport service at time *t* (called flight *j* at time *t*) because it has landed or is ready to depart. The time required for an ASEV to serve this flight is stochastic because: 1) although the airline company knows the number of passengers and luggage weight for the flight in question, the information may not be shared with the airport. 2) Even if the information were made available to the airport, there is random noise in the time required to service the flight. Denote the time required for an ASEV to serve flight *j* at time *t* as $\widetilde{w}_{jt}$, which follows a truncated normal distribution ψ [76].

$$\psi(\mu,\sigma,a,b,\widetilde{w}_{jt}) = \begin{cases} 0 & \text{if } \widetilde{w}_{jt} \le a \\ \dfrac{\emptyset(\mu,\sigma^2;\ \widetilde{w}_{jt})}{\Phi(\mu,\sigma^2;b)-\Phi(\mu,\sigma^2;a)} & \text{if } b \le \widetilde{w}_{jt} \le a \\ 0 & \text{if } \widetilde{w}_{jt} \ge b \end{cases} \tag{3-1}$$

where μ and σ are the mean and deviation of the “parent” normal distribution, respectively. a and b are the upper and lower bounds, respectively. $\emptyset(\mu,\sigma^2;\ x)$ and $\Phi(\mu,\sigma^2;x)$ are the probability density function and cumulative distribution function, respectively, of the “parent” normal distribution with mean μ and deviation σ. The truncated normal distribution model is justified because: 1) a normal distribution is a default choice when there is no detailed knowledge to support alternative complicated probability distributions, and 2) $\widetilde{w}_{jt}$ is bounded in reality.

Suppose that the 24 hours of a day are discretised into 144 stages, starting from Stage 0 to Stage 143 at an interval of 10 minutes. Let w_{jt} denote the discrete number of stages (essentially the amount of time) required for an ASEV to serve the *j*th flight that is awaiting service at Stage *t*. Therefore, w_{jt} is a random discrete variable.

Now the continuous random variable $\widetilde{w}_{jt}$ is discretized into w_{jt}: first, divide the time range of $[b, a]$ into m stages at an interval of $\Delta t = 10$ minutes (assuming that the length of $[b, a]$ is $m\Delta t$). These m stages are represented by m integers from $b/\Delta t$ to $a/\Delta t - 1$, therefore, $w_{jt} \in [b/\Delta t, a/\Delta t - 1]$ and w_{jt} is an integer. Secondly, the probability of w_{jt} taking value *k* out of the m values is given by

$$\text{Prob}\left(w_{jt} = k\right) = \Phi(\mu, \sigma^2; \rho_u) - \Phi(\mu, \sigma^2; \rho_l) \tag{3-2}$$

where Φ is the cumulative distribution function as defined in (3-1). ρ_u and ρ_l are the upper and lower bounds of $\widetilde{w}_{jt}$ within Stage *k*, respectively. w_{jt} is the discretized random workload, as explained above. For example, $w_{jt} \in \{1, 2, 3, 4\}$, meaning that the ground transport for the *j*th flight at Stage t requires 10 minutes ($w_{jt} =$ 1 stage) to 40 minutes ($w_{jt} =$ 4 stages) to complete. The probability of w_{jt} taking each discrete value is given by (2). w_{jt} is a critical input for the ASEV dynamics model introduced in Chapter 3.5.2.

3.5.2. ASEV dynamics model

In this chapter, an ASEV dynamics model is presented, which models the control decisions, the ASEV states and their transitions over time. The model considers the uncertain ground transport workload as modelled in Chapter 3.5.1.

At any Stage *t* (time is discretised into stages), the ASEV fleet state S_t consists of the states of all individual ASEVs. S_{it} denotes the state of an *i*th ASEV at Stage *t*, given by

$$S_{it} = [q_{it}, SoC_{it}, f_{Rit}] \tag{3-3}$$

where q_{it} is a discrete state: $q_{it} = 1$ means that the *i*th ASEV is charging at Stage *t*; $q_{it} = 0$ means that it is idling; $q_{it} < 0$ means that it is working (in this paper, “working” means undertaking ground transport) and it will take $|q_{it}|$ stages to complete the work. SoC_{it}, a continuous state, is the state of charge (SoC) of the *i*th ASEV’s battery at Stage *t*. f_{Rit} denotes the battery cycles to failure for the *i*th ASEV at Stage *t*.

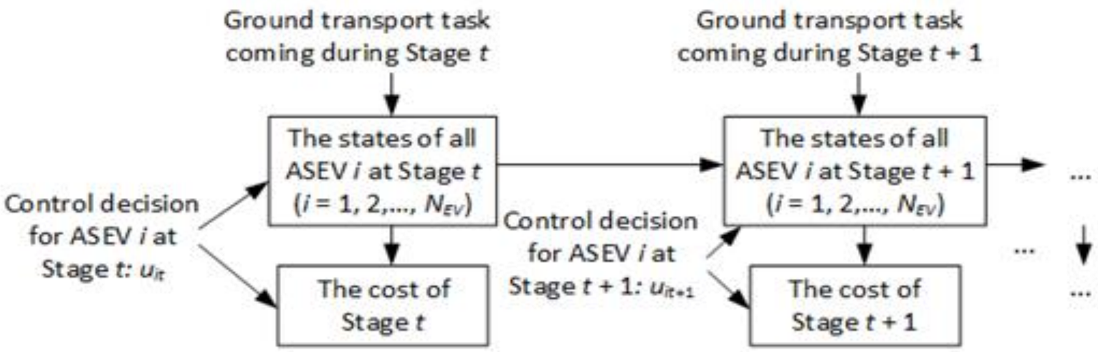

Fig. 3-2 Overview of the ASEV dynamics model.

According to Fig 3-2, the optimal control is performed online, i.e. the control decision for each Stage *t* is made when the state S_{it} at Stage *t* becomes known.

The energy cost for the *i*th ASEV at Stage *t* is given by:

$$C_{it} = \begin{cases} C_R \cdot max\{q_{it}, 0\} \cdot E_c & \text{if } max\{q_{it}, 0\} \cdot E_c \le E_{Rt} \\ C_R E_{Rt} + C_{Gt}(max\{q_{it}, 0\} \cdot E_c - E_{Rt}) & \text{otherwise} \end{cases} \tag{3-4}$$

where C_R denotes the energy price per kWh from renewable generation. E_c denotes the energy consumption (some of the energy is charged to the battery and the rest is lost) during each stage. E_c is a constant given the assumption of the constant battery charging power. C_{Gt} denotes the price per kWh of the grid-supplied energy at Stage *t*. E_{Rt} denotes the available energy generated by renewable generation at Stage *t*. q_{it} is given in (3-3). The “max” term in (3-4) ensures that the energy cost is incurred only when the ASEV is charging. Equation (3-4) is based on the principle that the ASEV fleet gives priority to consuming the cheap energy directly purchased from renewable generation over consuming the grid-supplied energy. For the E_{Rt}, it is assumed to be accurately predicted by a combination of historical data and prediction algorithms and for each time stage, it is known to the airport control system.

The battery degradation cost for the *i*th ASEV at Stage *t* is given by

$$B_{it} = f(SoC_{it}, E_w, f_{Rit}) \quad \text{if } q_{it} < 0 \tag{3-5}$$

where q_{it}, SoC_{it} and f_{Rit} are given in (3-3). E_w is the energy discharged during Stage *t*. Function *f* is the linear function for battery degradation cost during its normal charging-discharging cycles, with its coefficient derived from [77]. It is the function of the SoC, energy discharged during Stage *t*, and the cycles to failure. If the battery is over-charged or deep discharged, some parameters in this function will be changed and the degradation cost increases more with the same energy discharged.

The total cost (including energy and battery degradation costs) for all ASEVs at Stage *t* is given by:

$$g_t = \sum_{i=1}^{N_{EV}} (C_{it} + B_{it}) \quad t = 0,1,2 \dots, N-1 \tag{3-6}$$

where C_{it} and B_{it} are given in (3-4) and (3-5), respectively. N_{EV} is the total number of ASEVs.

Ideally, all ASEV batteries, except for those which is under work state or just finishing work, should be charged to full at the end of the day to prepare the ASEVs for ground transport the next day. If any battery is not charged to full at the last stage of the day

(Stage *N*), this incurs a terminal stage cost. Also, if a flight needs the ASEV but there is no ASEV available, a punishment for the delay is added. In this paper, it is included in the terminal stage cost because it is calculated at the end of each day. The terminal stage cost is given by

$$g_N = \sum_{i=1}^{N_{EV}} C_{GN} B(SoC_{max} - SoC_{iN}) + \sum_{i=1}^{N_{delay}} T_{delayi} C_{punishment} \tag{3-7}$$

where C_{GN} denotes the price per kWh of the grid-supplied energy at Stage *N*. B denotes the battery energy capacity. SoC_{max} is the upper bound of the SoC. N_{EV} is the total number of ASEVs. SoC_{iN} denotes the SoC of the *i*th ASEV at Stage *N*. N_{delay} is the total number of times of ASEV delay on the day and $T_{delay,i}$ is the duration of the *i*th ASEV delay. $C_{punishment}$ denotes the punishment cost per time slot.

The objective of the ASEV optimal control is to minimize the summation of g_t over all stages of the day.

$$\text{Min } J = g_N + \sum_{t=0}^{N-1} g_t \tag{3-8}$$

where g_t and g_N are given in (3-6) and (3-7), respectively.

When the SoC of the *i*th ASEV battery reaches either the upper bound or the lower bound, there are two state constraints:

Case 1: an ASEV *i* is prevented from switching to work because of a low SoC.

$$\text{If } q_{it} \geq 0 \text{ and } SoC_{it} \leq SoC_{min}, \text{ then } q_{it+1} = u_{it} \geq 0 \tag{3-9}$$

where q_{it}, q_{it+1}, and SoC_{it} are defined in (3-3). SoC_{min} denotes the lower bound of the

SoC. u_{it} is the control decision for ASEV *i* at Stage *t*: $u_{it} = 1$ means "to charge battery"; $u_{it} = 0$ means "to idle"; and $u_{it} = -1$ means "to work (i.e. undertake ground transport)".

Case 2: an ASEV *i* is prevented from battery charging because its SoC has reached the upper bound.

$$\text{If } q_{it} \geq 0 \text{ and } SoC_{it} = SoC_{max}, \text{ then } q_{it+1} = u_{it} \neq 1 \quad (3\text{-}10)$$

where q_{it}, q_{it+1}, and SoC_{it} are defined in (3-3). SoC_{max} is defined in (3-7); u_{it} is defined in (3-9).

When the SoC of the *i*th ASEV battery is above the lower bound and the ASEV is not currently working, a control-based state transition can occur. This is further divided into two cases:

Case 1: the ASEV *i* is controlled to work.

$$\text{If } SoC_{min} < SoC_{it} \text{ and } q_{it} \geq 0 \text{ and } u_{it} = -1, \text{ then } q_{it+1} = -w_{jt} \quad (3\text{-}11)$$

where SoC_{min} is defined in (3-9). q_{it}, q_{it+1}, and SoC_{it} are defined in (3-3). u_{it} is defined in (3-9). w_{jt} denotes the number of stages (the amount of time) required for an ASEV to serve the *j*th flight that is awaiting service at Stage *t*, as explained in Chapter 3.5.1.

When a flight *j* is awaiting ground transport service at Stage *t*, it should be served as soon as there is at least one free ASEV.

$$\text{If } w_{jt} > 0 \text{ and } \exists i{:}\, q_{it} \geq 0 \text{ and } SoC_{it} > SoC_{min} + E_{wf}, \quad (3\text{-}12)$$

then $\exists i$: $q_{it+1} = -w_{jt}$ and $u_{it} = -1$

where E_{wf} denotes the energy required for serving this flight and the other variables are defined the same as in (3-11).

If a flight *j* is awaiting service at Stage t but because no ASEV is available, the service for flight *j* is delayed to Stage *t* + 1. This translates to:

$$\text{if } w_{jt} > 0 \text{ and } \forall i: q_{it} < 0, \text{ then } w_{jt+1} = w_{jt} \text{ and } d_j \leftarrow d_j + 1$$
$$t = 0,1,2 \dots, N-1 \tag{3-13}$$

where w_{jt} is defined in Chapter 3.5.1. q_{it} is defined in (3-3). d_j denotes the stages of delay. It is initialized to zero.

A hard constraint exists that the stages of service delay for any flight should be no more than a threshold.

$$d_j \leq d_{thre} \tag{3-14}$$

where d_{thre} is the threshold of delay; d_j is defined in (3-13).

Case 2: the ASEV *i* is controlled to idle or charge.

$$\text{If } SoC_{it} < SoC_{max} \text{ and } q_{it} \geq 0 \text{ and } u_{it} \geq 0, \text{ then } q_{it+1} = u_{it} \tag{3-15}$$

where SoC_{max} is defined in (3-7). q_{it}, q_{it+1}, and SoC_{it} are defined in (3-3). u_{it} is defined in (3-9).

When the *i*th ASEV is working, its work cannot be interrupted by any control decision.

The ASEV will naturally complete the work. This is expressed as

$$\text{If } q_{it} \leq -2, \text{ then } q_{it+1} = q_{it} + 1 \text{ and } u_{it} = -1 \tag{3-16}$$

$$\text{If } q_{it} = -1, \text{ then } q_{it+1} = 0 \text{ and } u_{it} = 0 \tag{3-17}$$

where all variables are defined the same as in (3-12).

Fig. 3 presents a state transition graph describing the relation among q_{it}, w_{jt}, and u_{it}.

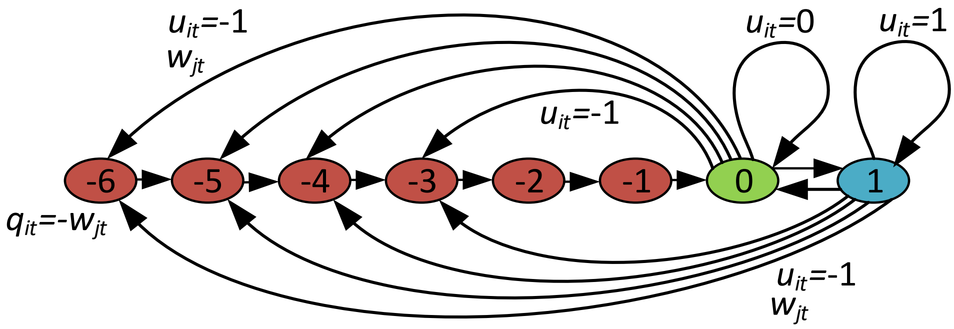

w_{jt} is a random discrete variable describing the number of stages required to serve flight j. In this example, w_{jt} belongs to the set {3, 4, 5, 6}, meaning that the ground transport requires at least 15 minutes (3 stages) and at most 30 minutes (6 stages) to complete.

Fig. 3-3 State transition graph for the *i*th ASEV.

In Fig. 3-3, each circle represents a state of the *i*th ASEV. The value in each circle is q_{it}, i.e. the discrete state of the *i*th ASEV at Stage *t*. Red circles mean that the *i*th ASEV is working. The green and blue circles mean that the *i*th ASEV is idling and charging, respectively. As mentioned above, work cannot be interrupted. Therefore, in Fig. 3-3, the state transits naturally from -6 to 0 over time, as described by (3-16) and (3-17).

For any ASEV *i* at stage *t*, the continuous dynamics of its battery SoC depends on its control decision u_{it}.

$$SoC_{it+1} = \begin{cases} SoC_{it} - E_w & \text{if } u_{it} = -1 \\ SoC_{it} + min\{\gamma E_c, SoC_{max} - SoC_{it}\} & \text{if } u_{it} = 1 \\ SoC_{it} & \text{if } u_{it} = 0 \end{cases} \quad (3\text{-}18)$$

where SoC_{it} and SoC_{it+1} are defined in (3-3). u_{it} is defined in (3-9). E_w is defined in (3-5). E_c is the energy consumption during each stage, as defined in (3-4). γ is the efficiency of the battery. γE_c is therefore the energy charged to the battery during each stage.

With the ASEV dynamics model established, the next step is to determine a sequence of control variables u_{it} (defined in (3-9)) for all *i* (all ASEVs) and for all *t* (all stages of a day), with the objective to minimize the total operation cost (defined in (3-8)).

3.6. Near-optimal control of the ASEV dynamics model

Based on the ASEV dynamics model detailed in the last chapter, a rollout approach is presented as a near-optimal control method to determine a sequence of control variables u_{it} for each ASEV at each stage *t*.

At each stage *t*, the optimal cost-to-go function J_t is defined as the minimum total cost from Stage t to Stage $N-1$ (the last stage of the day) plus the terminal stage cost g_N (as given by (3-7)). Because the prohibitively large number of states in the ASEV dynamics model cause a combinatorial explosion, it is impossible to calculate the accurate cost-to-go function J_t, thus being impossible to develop an accurate optimal control strategy for the ASEV dynamics model. A customized rollout approach is developed to yield a near-optimal control strategy through approximations. It consists of the following steps:

Two customized suboptimal heuristic control strategies are developed to approximate the cost-to-go function J_m as $\tilde{J}_m$, given the starting state S_m (the ASEV fleet state at Stage m). The two heuristics are elaborated as follows:

Heuristic i): the "renewable matching" heuristic. At each Stage *t* from Stage m to the last stage of the day, control the ASEVs to charge only when is available renewable energy as dictated by the renewable generation profile. When a flight is awaiting ground transport service, always assign the available ASEV with the greatest SoC to take the work. The pseudo-code for heuristic i) is presented in Fig. 3-4.

Heuristic ii): the "greedy charging" heuristic. Given the starting state S_m at Stage *m*, control the ASEVs to charge as early as possible until the maximum SoC is reached. When a flight is awaiting ground transport service, always let the available ASEV with the greatest SoC take the work. The pseudo-code for heuristic ii) is presented in Fig. 3-5.

Heuristic i) is not always feasible because, when renewable energy is seriously deficient throughout the day, the ASEV batteries all have too low SoC values to undertake the "peak" workload of ground transport. If heuristic i) is not feasible from Stage *t*, then heuristic ii) is selected. If both heuristics are feasible from Stage *t*, the better one (the one that leads to a lower $\tilde{J}_t$) of the two heuristics is selected. The approximate cost-to-go $\tilde{J}_t$ for the selected heuristic is recorded for use in Step 2).

0. Initialize the approximate cost-to-go (starting from Stage m) as zero, i.e. $\tilde{J}_m = 0$.
1. Loop over all stages t from Stage m to the last stage of the day {
    2. Order all available (not currently working) ASEVs by increasing SoC values at Stage t.
    3. If a flight j is awaiting ground transport at Stage t, control the available ASEV i with the highest SoC value to serve this flight. Set this ASEV i as unavailable.
    4. Initialize the total energy consumption (the energy taken from the grid and renewable source by the ASEV fleet batteries) at Stage t to zero, i.e. $E_t = 0$.
    5. If the available renewable energy at Stage t is positive, i.e. $E_{Rt} > 0${
        6. Loop over all available ASEVs i from the one with the lowest SoC value to the one with the highest SoC value {
            7. Control ASEV i to charge if it is not currently working and that it is not controlled to work.
            8. The total energy consumption by the ASEV fleet $E_t \leftarrow E_t + E_c$, where E_c is the energy charged to ASEV i at Stage t.
            9. If $E_t \geq E_{Rt}$ then exit the inner loop (E_{Rt} is the available renewable energy at Stage t).
        }
    }
    10. Calculate g_t, the cost of Stage t, according to (6). Update the approximate cost-to-go: $\tilde{J}_m \leftarrow \tilde{J}_m + g_t$
}
11. Calculate g_N, the terminal stage cost, according to (7). Update the approximate cost-to-go: $\tilde{J}_m \leftarrow \tilde{J}_m + g_N$. Output the approximate cost-to-go $\tilde{J}_m$.

Fig. 3-4 Pseudo-code for heuristic i), i.e. the “renewable matching” heuristic.

0. Initialize the approximate cost-to-go (starting from Stage m) as zero, i.e. $\tilde{J}_m = 0$.
1. Loop over all stages t from the current Stage m to the last stage of the day{
    2. Order all available ASEVs by increasing SoC values at Stage t.
    3. If a flight j is awaiting ground transport at Stage t, control the available ASEV i with the highest SoC value to serve this flight. Set this ASEV i as unavailable.
    4. Initialize the total energy consumption (the energy taken from the grid and renewable source by the ASEV fleet batteries) at Stage t to zero, i.e. $E_t = 0$.
    5. Loop over all available ASEVs i {
        6. Control ASEV i to charge if it is not currently working and that it is not controlled to work.
        7. The total energy consumption by the ASEV fleet $E_t \leftarrow E_t + E_c$, where E_c is the energy charged to ASEV i at Stage t.
    }
    8. Calculate g_t, the cost of Stage t, according to (6). Update the approximate cost-to-go: $\tilde{J}_m \leftarrow \tilde{J}_m + g_t$
}
9. Calculate g_N, the terminal stage cost, according to (7). Update the approximate cost-to-go: $\tilde{J}_m \leftarrow \tilde{J}_m + g_N$. Output the approximate cost-to-go $\tilde{J}_m$.

Fig. 3-5 Pseudo-code for heuristic ii), i.e. the “greedy charging” heuristic.

2) Given S_t (the ASEV fleet state at Stage *t*) which consists of S_{it} for all ASEVs *i*, the rollout approach generates the set of all possible S_{t+1} by enumerating all feasible control decisions u_{it} (defined in (3-9)) for Stage *t*, considering the workload w_{jt} (defined in (3-11)). The approach then selects the “best” S_{t+1} that produces the minimum approximate cost-to-go among all S_{t+1} in the set [74]. The mathematical expression is

$$S_{t+1} = \mathrm{argmin}_{S \in N(S_t)} J(S) \tag{3-19}$$

where S_t is the state at Stage *t*. $N(S_t)$ is the set of all possible states at Stage *t* + 1. $J(S)$ is the approximate cost-to-go $\tilde{J}_{t+1}$ of the better one of the two heuristics, expressed as the function of state S. The rollout control u_{it} for all ASEVs *i* is the control that corresponds to the transition from S_t to S_{t+1}.

An alternative expression with the same meaning is given by

$$u_t = \mathrm{argmin}_{u_t \in U_t \text{ and } S \in N(S_t)} [g_t + J(S)] \tag{3-20}$$

where u_t is the set of control decisions for all ASEVs i at Stage *t*, i.e. $u_t = \{u_{it}$ for all $i\}$. U_t is the constraint set for u_t at Stage *t*. S_t, $N(S_t)$, and $J(S)$ is defined in (3-19). g_t is defined in (3-6).

This process iterates until S_t, S_{it}, and u_{it} for all stages *t* are determined. The sequence of u_{it} for all ASEVs *i* and all stages *t* constitute a near-optimal control strategy, which controls each ASEV to charge, idle, and work at each stage.

3.7. Case study

In this chapter, case studies are performed to validate the ASEV dynamics model and the customized rollout approach. The case studies are based on Bristol Airport, a medium-sized airport in the UK. The flight information, including its scheduled time and real-time, is obtained from the Bristol Airport website [78]. Considering the scale of the airport, the number of ASEVs is set as 35. The renewable power output profiles for summer and winter are obtained from [79] and [80], respectively. The battery charging type is fast charging at a constant power of 22 kW [81]. The battery cycle efficiency is

90% [82]. To prevent overcharge and deep discharge, the upper and lower threshold of SoC of each battery is 20% and 80%. If the SoC of the battery is over 80% or lower than 20%, the degradation cost will increase significantly. The battery capacity is 50 kWh [83]. The case studies consider photovoltaic (PV) generation. The price for PV energy is £0.04/kWh. The tariffs of the grid-supplied energy follow a time of use (TOU) tariff system, which is shown in Fig. 3-6.

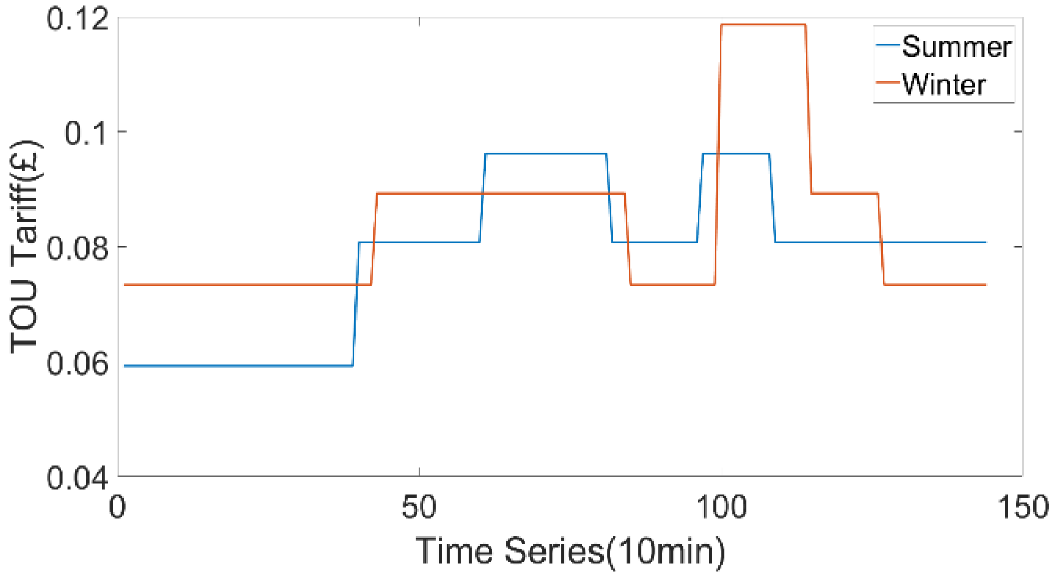

Fig. 3-6 The time of use tariffs in the summer and winter month.

To validate the algorithm, this chapter performs two sets of simulations. The first set is a comparison of the 'greedy charging' algorithm and the rollout algorithm in a typical summer month. The second set is a comparison between the 'greedy charging' algorithm and the rollout algorithm in a typical winter month, which corresponds to a substantially different PV output profile and TOU tariff from those in the summer month.

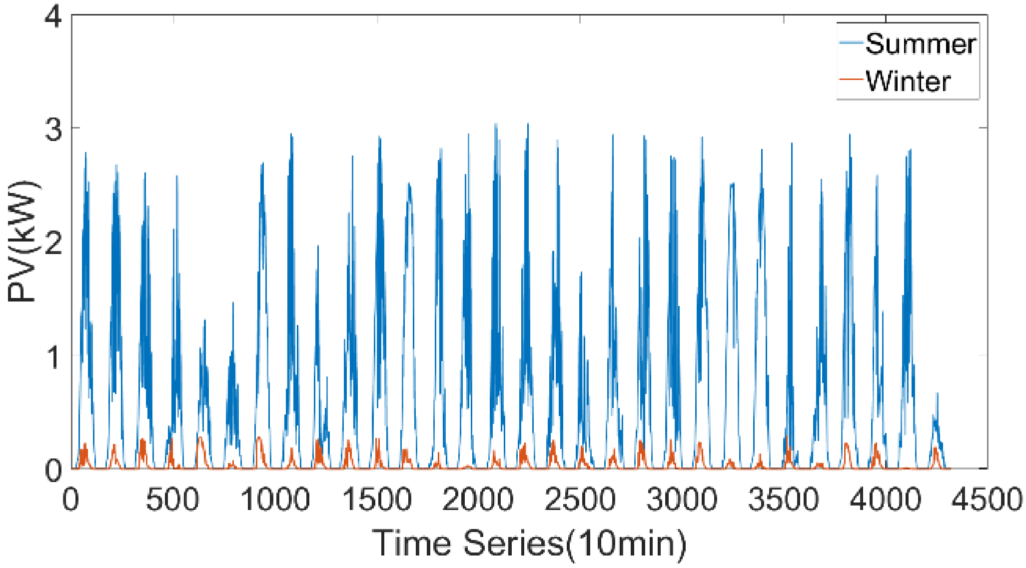

Fig. 3-7 The PV generation power of the summer and winter month.

3.7.1. Scenario 1): Comparison between the 'greedy charging' and the rollout algorithm for a typical sunny month in summer

One typical month in summer is chosen for the case study. The blue curve in Fig. 3-7 shows the PV output profile for the month. The workload of serving any given flight is a random variable. The random workload model is explained in Chapter 3.4.1. Each flight is served by one ASEV.

The SoC of the ASEVs under the 'greedy charging' algorithm is shown in Fig. 3-8 Compared with the control algorithm, the 'greedy charging' algorithm is set as the benchmark. The SoC of the ASEVs under the 'greedy charging' strategy is shown in Fig. 3-9. Each colour in the two figures represents an ASEV.

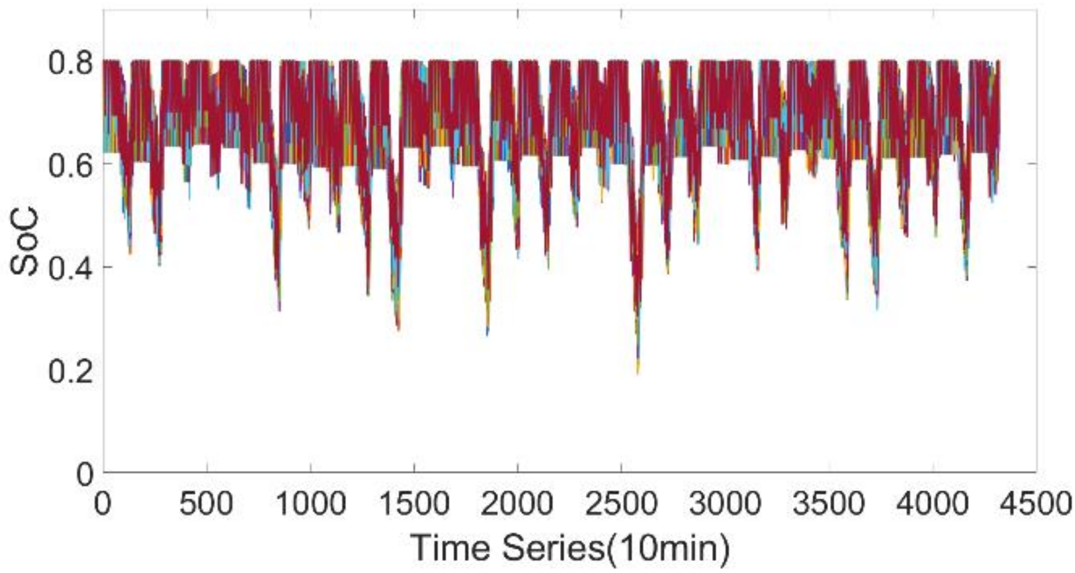

Fig. 3-8 The SoC of the ASEVs in the summer month under rollout algorithm.

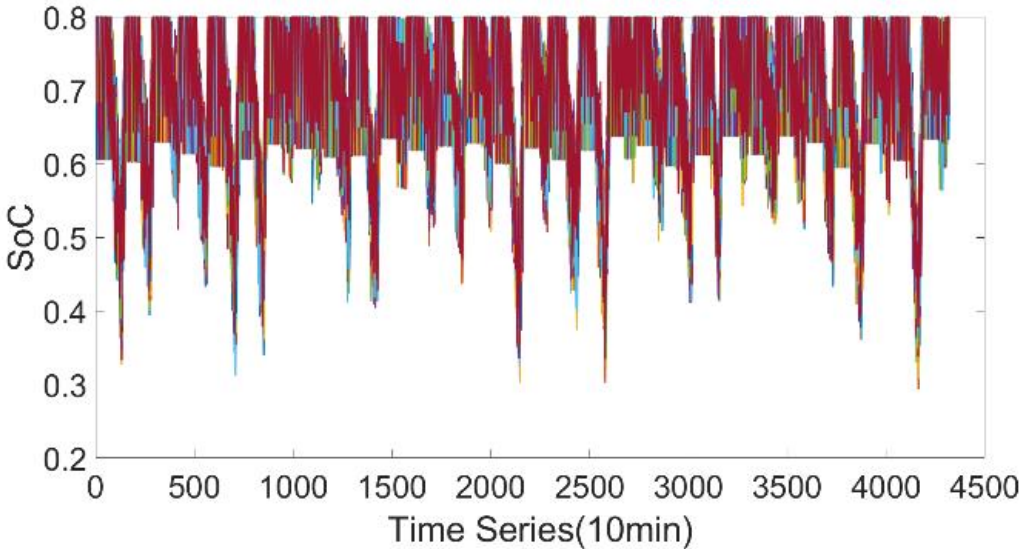

Fig. 3-9 The SoC of the ASEVs in the summer month under 'greedy charging' algorithm.

The operation costs of ASEVs under the two different algorithms are shown in Fig. 3-10.

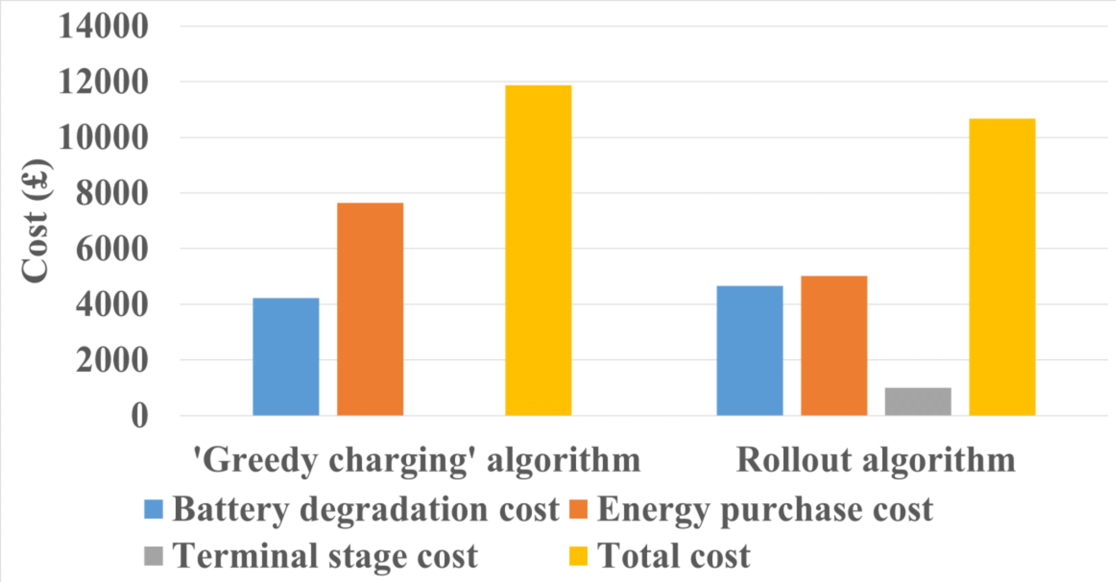

Fig. 3-10 The cost of Bristol Airport under 'greedy charging' and rollout algorithm in the summer month.

When the 'greedy charging' algorithm is applied, in the summer month, for every time slot, there is no ASEV working beyond the upper bound or under the lower bound of its SoC range. It is assumed that there is no punishment for the ASEV's late departure. The total cost is £11,871.3 for the airport in the month. The battery degradation cost, energy purchase cost and terminal stage cost are about £4,221.3, £7,649.7 and £0 respectively.

If the rollout algorithm is applied, the total cost in the summer month is £10,673.2 for the airport. This is broken down into the battery degradation cost, energy purchase cost, and terminal stage cost of £4,668.6, £5,012.1, and £922.4, respectively.

From the comparison of the 'greedy charging' algorithm and the rollout algorithm, it is clear that the rollout algorithm incurs a total cost of 10.5% less than that of the 'greedy charging' algorithm. The battery degradation cost and energy purchase cost of the rollout algorithm is 11.1% more than and 51.3% less than those of the 'greedy charging' algorithm, respectively. In Fig. 3-8, it is shown that using the rollout algorithm, the ASEV battery may have an SoC below the lower bound. This is because the ASEV would be charged without considering possible flight delays. However, the rollout algorithm achieves a significant saving in the energy purchase cost, compared to the 'greedy charging' algorithm, because: the 'greedy charging' algorithm does not care about the electricity price at all but charges the battery whenever the SoC is not at the maximum. In contrast, the rollout algorithm takes advantage of both the cheap PV energy and the low tariff period of the grid-supplied energy.

In Fig. 3-8 and Fig. 3-9, the charging-discharging frequency of 'greedy charging' is greater than that of the rollout algorithm. However, the battery degradation cost under the 'greedy charging' algorithm is less than that under the rollout algorithm. This is because under the 'greedy charging' according to Heuristic ii), the average SoC at the start of charging is greater than that under the rollout algorithm. In other words, the rollout algorithm leads to deeper discharges and thus a greater battery degradation cost than the 'greedy charging' algorithm. Secondly, as mentioned above, occasionally, the SoC of the ASEV under the rollout algorithm drops below the lower threshold, resulting in a higher-than-usual degradation cost. The terminal stage cost of 'greedy charging' is £0 because it charges an ASEV battery whenever it is not full and the ASEV is not working, regardless of the electricity price. This ensures that the ASEV batteries all have the maximum SoC value at the end of the day, resulting in a zero terminal stage cost. In contrast, the rollout algorithm only charges the ASEV batteries when the electricity price is low. As a result, at the end of the day, not all ASEV batteries are fully charged, causing a positive terminal stage cost.

3.7.2. Scenario 2): Comparison between 'greedy charging' and the rollout algorithm for a typical month in winter

Scenario 1) is a typical month in summer in the UK. Scenario 2) considers a typical month in winter in the UK. The flight information is collected from the airport website same as the Scenario 1). However, the daytime is significantly different, resulting in a different PV generation profile. The red curve in Fig. 3-7 shows the output profile of the PV generation in the winter month [80]. The price curve of grid-supplied energy is also different from the summer one, which is shown as the blue curve shown in Fig. 3-6.

The simulation results of SoC of the ASEVs under two different algorithms are shown in Fig. 3-11 and Fig. 3-12. The operation costs of ASEVs under the two different algorithms are shown in Fig. 13. As same as above, each colour in the two figures represents an ASEV.

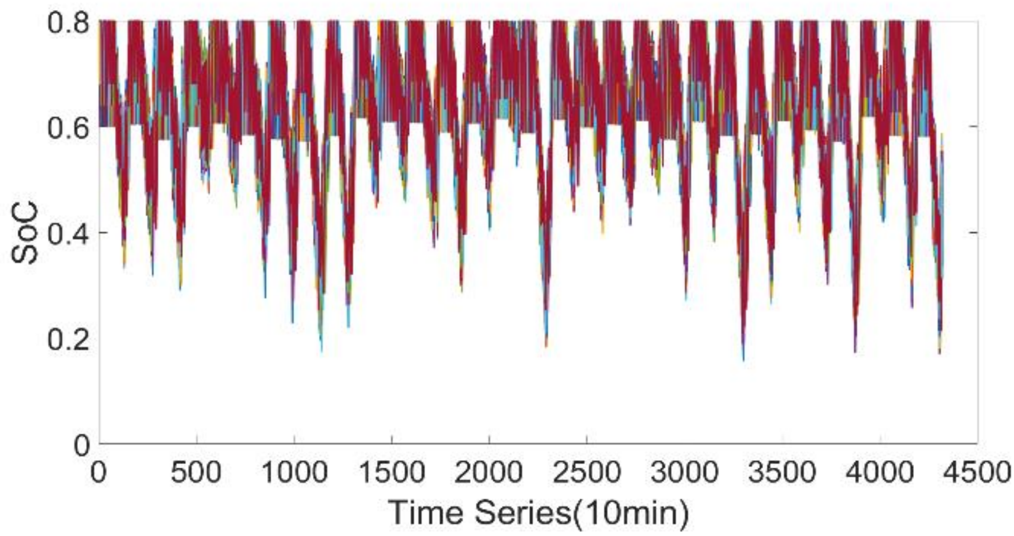

Fig. 3-11 The SoC of the ASEVs in the winter month under rollout algorithm.

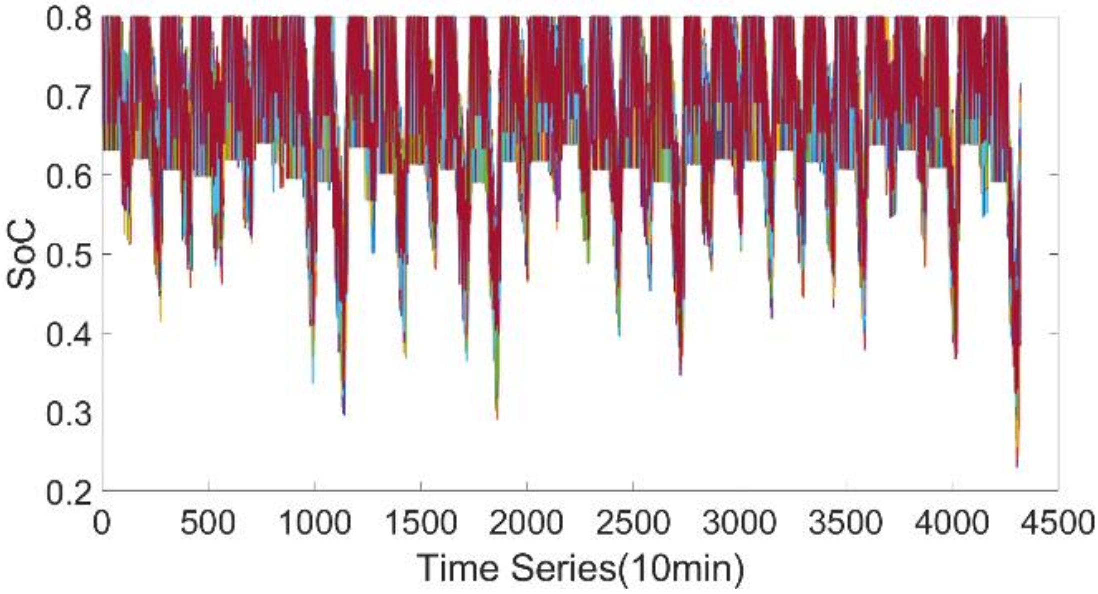

Fig. 3-12 The SoC of the ASEVs in the winter month under ‘greedy charging’ algorithm.

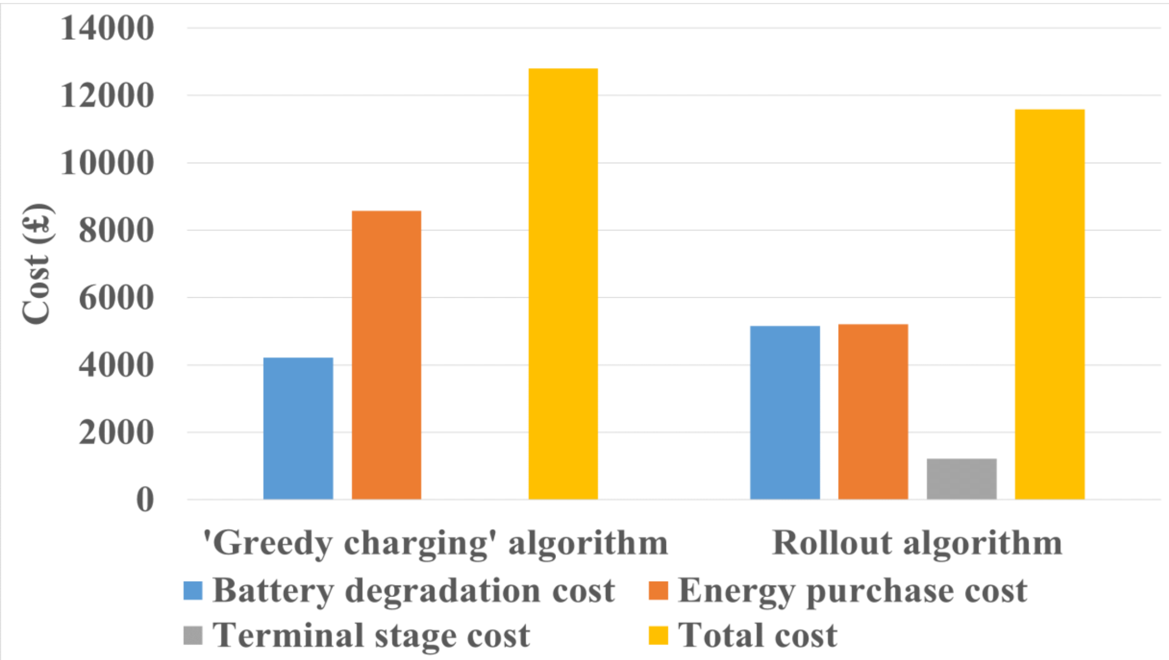

Fig. 3-13 The cost of Bristol Airport under ‘greedy charging’ and rollout algorithm in the winter month.

The case study proves that both the rollout algorithm and the ‘greedy charging’ algorithm are adaptive towards differing flight schedules. But the total cost under the rollout algorithm is 10.6% less than that under the ‘greedy charging’ algorithm. The comparisons of the three cost components (i.e. the battery degradation cost, the energy purchase cost and the terminal stage cost) show a similar trend to that in Scenario 1). The rollout algorithm yields a battery degradation cost 11.1% greater than that under the ‘greedy charging’ algorithm, and an energy purchase cost 51.7% less than that under ‘greedy charging’. The ‘greedy charging’ algorithm leads to a zero terminal stage cost, whereas the rollout algorithm leads to a terminal stage cost of £992.4. The reason for having such a trend is the same as that explained in Scenario 1).

From the simulation results, considering the total cost, the rollout algorithm may be better than the ‘greedy charging’ algorithm. But in future, if the degradation cost increases, the ‘greedy charging’ algorithm can be set as a possible protection control strategy for the ASEVs.

3.8. Conclusion

This paper proposes a new dynamics model for airport service electric vehicles (ASEVs) and a new customized rollout approach as a near-optimal control method for the ASEV dynamics model. Case studies compare the rollout algorithm and the ‘greedy charging’ algorithm (it charges the battery whenever its SoC is not the maximum) for a typical summer month and a typical winter month. The two months have very different PV output profiles and TOU tariffs. In both cases, the rollout algorithm achieves a lower total cost than the ‘greedy charging’ algorithm. This is because the rollout algorithm takes advantage of the cheap PV energy as well as the off-peak price of the grid-supplied energy. However, the ‘greedy charging’ algorithm can help reduce the degradation cost. The battery of the ASEV under the ‘greedy charging’ algorithm may work for a longer time than the rollout algorithm. The research outcome will guide the airport to control the

ASEV based on the transportation electrification in the airport. It helps the airport better save costs and reduce carbon emissions in the context of transport electrification, facilitate local consumption as well as the penetration of distributed generation, and make the battery-charging load friendly to the grid.

Chapter 4.
Monthly-payment-based business model for second-life batteries to provide flexibility services

Chapter contents:

4.1. Chapter overview 60
4.2. Abstract 63
4.3. Introduction 63
4.4. Overview of methodology 66
4.5. Methodology 67
4.6. Data environment and simulation results 81
4.7. Discussion 92
4.8. Conclusions 95

This chapter develops a novel business model for SLBs with a monthly payment-based strategy. In this business model, the SLBs are utilized to perform energy arbitrage and provide flexibility services. The case studies validate its feasibility with a 10-year simulation

4.1. Chapter overview

The UK government has confirmed that the purchase of new petrol and diesel cars will be moved in 2030. With the increasing number of EVs, their retired batteries will be on a mass scale. When the capacity of the battery is reduced to approximate 70%~80%, it has to be retired from the EVs. However, these batteries still have potential in other fewer demand applications. These applications are known as second-life applications and these retired batteries are called second-life batteries.

This chapter proposes a monthly payment-based business model for the SLBs. In this model, without direct payment to the SLB providers, profits sharing is introduced in this model between the battery processer and the SLB providers. If the SLB makes profits, the monthly payments to the SLB providers will cease until the SLB reaches its end of life. In case the SLB does not make profits, there is no sharing for the providers. With the monthly payment strategy, the business model reflects the true value of the SLBs and it is not necessary to increase the additional investment in predicting the lifespan of the SLBs at the beginning of the second-life applications. In this chapter, the SLB is utilized to perform energy arbitrage and provide flexibility services for a DNO to make profits.

To validate the feasibility of the SLB business model, the case studies perform a 10-year horizon simulation, considering two different scenarios. The two scenarios represent two possible SLB pack replacement modes for the SLB matrix. In the first scenario, the SLB packs cannot be replaced but will be removed from the battery matrix when it reaches its end of life. In the second scenario, those 'retired' SLBs will be replaced by the new SLBs with similar parameters. The case study shows the degradation results of the SLBs and the profits of the business model in 10 years. In the first scenario, the net present value of the profit in 10 years is £2,648,782 and in the second scenario, the net present value of the profit is £3,433,247. The case studies indicate the feasibility of the business model from the technical and economic aspects. The proposed monthly-payment business model improves the economic and energy efficiency of the EV batteries and thus it will increase the development of EVs.

The rest of the chapter is cited from the author's submitted article in Energy Power System Research. The structure of this chapter is organised in an alternative-based format, where the indices, equations, tables, figures and titles are numbered independently.

Statement of Authorship

This declaration concerns the article entitled:			
Monthly-payment-based business model for second-life batteries to provide flexibility services			
Publication status (tick one) **Draft manuscript** [ ] **Submitted** [ ] **In review** [√] **Accepted** [ ] **Published** [ ]			
Publication details (reference)	R. Wei, K. Ma, L. Fang " Monthly-payment-based business model for second-life batteries to provide flexibility services " in Energy Power System Research		
Copyright status (tick the appropriate statement) I hold the copyright for this material [√] Copyright is retained by the publisher, but I have been given permission to replicate the material here [ ]			
Candidate's contribution to the paper (provide details, and also indicate as a percentage)	The candidate proposed the idea of the paper, he designed the methodology, and predominantly executed the coding to derive the experimental results. Other authors helped the candidate with the design of case studies, the format of the paper, and the improvement of academic writing. The percentage of the candidate did compared with the whole work is indicated as follows: Formulation of ideas: 80% Design of methodology: 100% Simulation work: 100% Presentation of data in journal format: 90%		
Statement from Candidate	This paper reports on original research I conducted during the period of my Higher Degree by Research candidature.		
Signed	Renjie Wei	**Date**	26/07/2022

4.2. Abstract

With the rapid increase of electric vehicles (EVs), they will eventually retire on a mass scale. However, the pricing of retired EVs depends on the pricing of their batteries. Such pricing depends on how the batteries are used in their second lives. The pricing cannot be appropriately determined at the beginning of their second lives as a one-off price because it is difficult to forecast the lifetime and performance of the second-life batteries (SLBs). To reflect the true value of SLBs, this paper develops a new monthly-payment-based business model, where the SLBs are controlled to both perform energy arbitrage and provide flexibility services for the grid. Any profit is shared between the battery processer and EV owners on a 'monthly basis'. The monthly payment to any EV owner ceases when its SLB reaches the technical threshold of the end of life – a "wait and see" strategy to eliminate the need for forecasting. Numerical simulations reveal the scenarios in which this model would make profits, considering stochastic changes in the energy arbitrage prices along with a conservative estimation of the long-term income from providing flexibility services.

4.3. Introduction

With the rapid growth of electric vehicles (EVs), the handling of their retired batteries is gaining increasing attention. When customers send their retired gasoline vehicles for disposal, they receive a payment (in the UK, this can be a few hundred British Pounds) and there is a pricing methodology underlying this. Likewise, when customers send their retired EV batteries for disposal, they should receive payments, which depend on the true value of the batteries.

Re-purposing the retired EV batteries for second-life applications is an area that i) attracts growing research attention and industrial trials, supported by increasing government funding from the UK and European Union (EU) [84], [85]; ii) minimizes environmental impact, promotes circular economy and is part of the long-term decarbonization agenda [86]. A proposed EU regulation defines a framework that will facilitate second-life batteries (SLBs) as either standalone or grid-connected energy storage systems [87]. In light of these, the true value and pricing of retired EV batteries that are re-purposed for second life applications depend on the second use process. It is difficult to determine a one-off price at the beginning of the second life because it is difficult to forecast the remaining life and performance of various types of batteries under a time-varying environment. This calls for a methodology to properly price the batteries, using an appropriate payment mode, based on the modelling of the second use process.

A number of references explored a range of second-life battery (SLB) applications. Unlike the new batteries, the degradation of SLBs is more rapid and the available energy capacity is significantly lower. Thus, the SLBs will only take less-demand applications. Reference [88] shows that it is feasible to use SLBs as a stationary energy storage system and reference [89] shows the economic potential of adopting SLBs compared with new batteries. Reference [90] illustrates that SLB systems can be introduced to the electric bus charging station to charge the buses. SLB systems are also deployed to provide ancillary services, such as frequency regulation [91], spinning reserve [92], demand side response including energy arbitrage [93] [94] [95], rural energy access [96], energy management with renewables [97] [98], (including renewable smoothing [99] and microgrid energy management [98] [100]), backup power for telecommunication facilities [101], etc.

A number of references focus on estimating the remaining life of SLBs. Reference [102] estimates the effective capacity of second-life lithium-ion batteries. References [57], [56] predict the remaining life of SLBs through deep learning. However, existing literature has two limitations: 1) those references perform experiments under controlled lab environments that have a constant temperature, but a real operation environment varies from time to time. 2) Those references focus on specific types of batteries, not applicable to SLBs of mixed types that are different from each other. The two limitations prevent the extrapolation of those forecast methods to the real case of this paper.

This paper makes an original contribution by developing a novel business model for SLBs. The model is characterized by profit sharing between the battery processer and customers through monthly payments from the former to the latter. If there is a profit, the monthly payments to any customer cease if its SLB reaches the threshold that indicates the end of life. In case the business incurs a loss, there is no sharing, and the model reveals the true cost of the SLBs to the battery processer. In this way, the model reflects the true value of SLBs, bypassing the difficult task to forecast the SLB lifetime and performance at the beginning of the second life. On the technical side, a customized heuristic algorithm is developed to control the SLB matrix to both provide a range of flexibility services for a distribution network operator (DNO) and perform energy arbitrage. In this process, both the energy capacity and terminal voltage degradations are modelled to limit the SLB lifetime in a realistic way.

The rest of this paper is organized as follows: Chapter 4.4 presents an overview of the SLB business model; Chapter 4.5 presents the business and technical models for SLBs and a method for the calculation of stochastic revenues; Chapter 4.6 performs case studies; Chapter 4.7 performs the discussion of the case studies and Chapter 4.8 concludes the paper.

4.4. Overview of methodology

An overview of the SLB business is presented in Fig. 4-1.

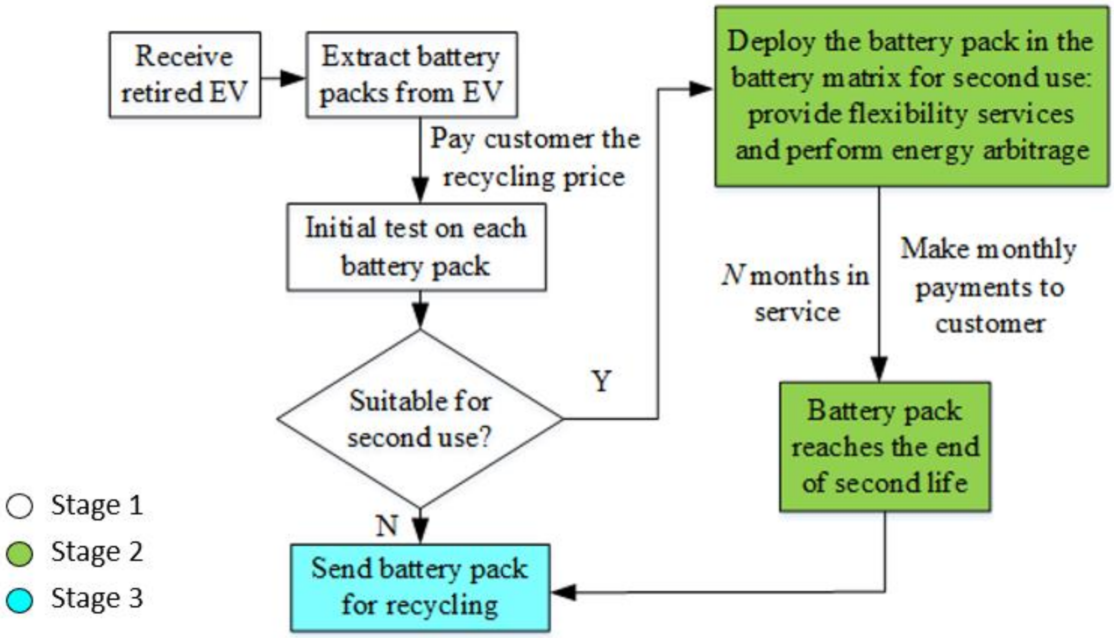

Fig. 4-1 Procedure for battery processing

In stage 1, when the battery processer receives a retired battery, it does an initial test to determine whether the retired battery is suitable for a second use or not. If not, then the battery is sent for recycling. At this time, the SLB processer makes an initial payment to the EV owner (also the customer) for purchasing the retired battery. The initial payment reflects the value of useful materials within the SLB. In stage 2, the processer deploys the received SLB pack in the SLB matrix for second use if the initial test gives a positive result. Then, the battery processer controls the SLB matrix to both provide flexibility services and perform energy arbitrage and shares any profit with the customers every month. More specifically, if there is a profit, the battery processer makes monthly payments to each customer's account proportional to the nominal capacity of the customer's SLB pack in service during that month. Stage 2 ends if the SLB pack reaches the end of its second life. In stage 3, the SLBs that reach the end of their second life is disassembled for recycling.

4.5. Methodology

4.5.1. SLB Pack Model

SLBs will be repurposed at the pack level to save re-manufacturing costs. For any SLB pack j that is suitable for second-life applications, its starting energy capacity, EC_{j0}, is modelled by a truncated Gaussian distribution, where subscript 0 denotes the start of the second life. The probability density function of EC_{j0} is given by

$$\psi(\mu, \sigma, EC_{min}, EC_{max}; EC_{j0}) = \begin{cases} 0 & \text{if } EC_{j0} \leq EC_{min} \\ 0 & \text{if } EC_{j0} \geq EC_{max} \\ \dfrac{\emptyset(\mu, \sigma^2;\, EC_{j0})}{\Phi(\mu, \sigma^2; EC_{max}) - \Phi(\mu, \sigma^2; a)} & \text{otherwise} \end{cases} \quad (4\text{-}1)$$

where μ and σ denote the mean and the standard deviation; EC_{min} and EC_{max} denote the lower and upper bounds of EC_{j0}, respectively. $\emptyset(\mu, \sigma^2;\, EC_{j0})$ and $\Phi(\mu, \sigma^2; x)$ are the probability density function and cumulative distribution function, respectively, of the “parent” normal distribution with mean μ and deviation σ^2.

The equivalent circuit of an SLB pack is referenced from [103]:

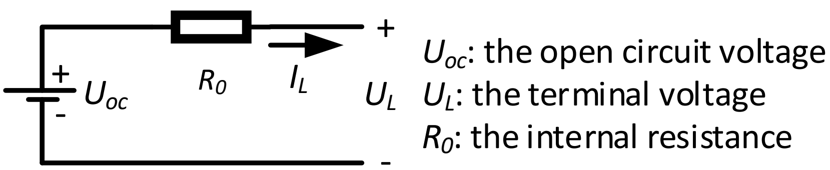

Fig. 4-2 Equivalent Circuit for Battery Pack [103]

An SLB pack suffers from two degradations [104]: 1) energy capacity degradation and 2) terminal voltage degradation (equivalent to an increase of the internal resistance R_0). In this chapter, the battery degradation is simplified as a physics model based on the battery pack model shown in Fig. 4-2.

For any SLB j, the 1st degradation is modelled as an energy capacity decrease (kWh) per kWh of energy discharged. Such a decrease is denoted as EC_{dj}, modelled by a Gaussian distribution. The mean energy capacity decrease per kWh of energy discharged is given by

$$\overline{EC}_{dj} = \frac{EC_{nom} - EC_{EoL}}{N_{LC} \cdot EC_{nom} \cdot SoC_{max}(\omega + SoC)} \tag{4-2}$$

where EC_{nom} and EC_{EoL} denote the nominal energy capacity and the end-of-second-life energy capacity, respectively. N_{LC} denotes the life cycles. SoC_{max} and SoC denotes the maximum SoC and the current SoC, respectively. ω is a parameter that is fitted with respect to the type of battery. The standard deviation of the Gaussian distribution of EC_{dj} is set as $0.1\overline{EC}_{dj}$.

A battery's second life ends when its energy capacity deteriorates to a predefined threshold EC_{EoL}. This battery is then sent for recycling. EC_{EoL} is the end-of-life capacity:

$$EC_{EoL} = k_r \cdot EC_{nom} \tag{4-3}$$

where k_r is the predefined threshold percentage. EC_{nom} is the nominal capacity of the j^{th} battery pack.

For any SLB j, the 2nd degradation is modelled as an internal resistance increase (Ω) per kWh of energy discharged, resulting in a terminal voltage decrease. The resistance increase is denoted as ΔR, modelled by a Gaussian Distribution. The mean internal resistance increases per kWh of energy discharged are given by

$$\overline{\Delta R} = \frac{V_{oc_r} - V_{EoL}}{I_r \cdot N_{LC} \cdot EC_{nom} \cdot SOC_{max}(\omega_2 + SOC)} \tag{4-4}$$

where V_{oc_r} and V_{EoL} denote the rated open-circuit voltage and the end-of-second-life terminal voltage, respectively. I_r is the rated discharge current. ω_2 is a parameter that is fitted with respect to the type of battery. N_{LC}, EC_{nom}, SOC_{max} and SOC are defined in (4-2).

A battery's second life ends when its internal resistance increases to a predefined threshold R_{EoL}, which is given by

$$R_{EoL} = \frac{V_{oc_r} - V_{EoL}}{I_r} \tag{4-5}$$

where V_{oc_r}, V_{EoL}, and I_r are defined in (4-4).

Both degradations occur simultaneously with the day-to-day operation of the SLB pack. The SLB lifetime is determined by whichever degradation first reaches the end-of-life threshold.

Battery calendar ageing is embedded into the degradation models (energy capacity and terminal voltage degradations) for simulations. The reason for this integration is that the SLBs are not deployed for idling (i.e., not merely suffering calendar ageing) but are under constant operations to generate profits. This makes it difficult to single out calendar ageing from the overall ageing caused by the energy capacity and terminal voltage degradations. In similar situations, existing references do not single out calendar ageing from the overall ageing but embed the former into the latter [105], [99].

In Fig. 4-2, the open circuit voltage V_{oc} is a function of the SoC:

$$V_{oc} = V_{oc_r}\left(1 - \gamma \frac{SOC_{max} - SOC}{SOC_{max} - SOC_{min}}\right) \tag{4-6}$$

where V_{oc_r} is the rated open-circuit voltage. γ is the maximum drop of the open-circuit voltage as a percentage of V_{oc_r}. SoC_{max}, SoC_{min}, and SoC denote the maximum SoC, minimum SoC, and the current SoC, respectively.

SLB packs are operated within a predefined SoC band: $SoC \in [SoC_{min}, SoC_{max}]$. Two-stage charging applies to battery packs. The first stage is constant current charging and the second stage is constant voltage charging [106]. In the first stage, the charger for a battery pack is equivalent to a current source, of which the current is equal to the rated charging current. The charging power is given by

$$P_c = V_{oc} I_c + I_c^2 R_0 \tag{4-7}$$

where V_{oc} is the open-circuit voltage given by (4-6). I_c is the rated charging current. R_0 is the internal resistance as shown in Fig. 4-2.

In the second stage, i.e. the constant voltage charging, the charging power is given by

$$P_c = V_c \frac{V_c - V_{oc}}{R_0} \tag{4-8}$$

where V_c is the charging voltage. Other variables are defined in (4-7).

4.5.2. SLB Matrix Model

The battery processer has N_{batt} SLBs that are of different characteristics (energy capacities, power capabilities, etc.). These batteries are arranged into an SLB matrix, where SLBs in the same row are connected in series and different rows are connected in parallel to each other. SLBs with similar discharge currents are clustered into the same row, whereas those with different discharge currents are clustered into different rows. This is achieved through k-means clustering. Parameter *k* is determined through the knowledge of the types of SLBs. For example, *k* = 5 if a battery processer can take five types of SLBs in terms of the discharge current ratings. Each row of the SLB matrix has a switch that controls its on and off status.

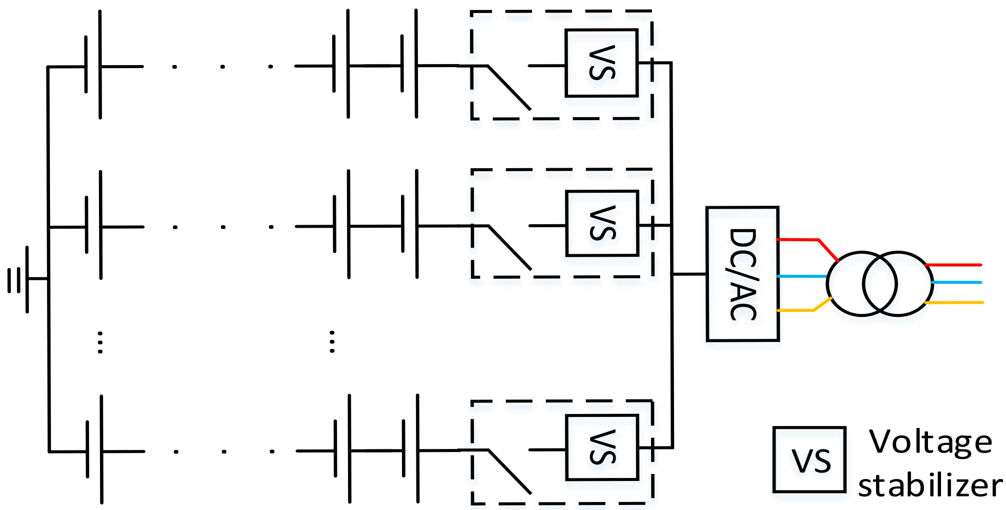

Fig. 4-3 Battery matrix structure

Fig. 4-3 shows the structure of the SLB matrix. In the matrix, voltage stabilizers step down high DC voltages (thousands of volts) from the rows to the same low DC voltage, which is fed into an inverter (DC/AC) connected to a transformer. The SLB matrix system outputs a three-phase AC power to the 11 kV distribution grid.

The SLB system can be connected to 11 kV or even 33 kV distribution networks which have larger capacities than 415 V networks. Currently, there are mature methodologies to determine the network connection fees for pure loads, but not for batteries which sometimes act as loads and sometimes as a generation. Therefore, the connection fee for batteries is uncertain and is regarded as part of the initial investment.

The lifetime of the SLB matrix depends on the lifetime of the SLBs. An SLB is removed from the matrix for recycling when it reaches the end of its second life. A row of the matrix where SLBs are connected in series is out of service when too many SLBs in the row have reached the end of second life that the voltage of the row drops below a lower threshold. The SLB matrix reaches its end of life when all rows are out of service. However, if there are incoming EVs that bring SLBs to replace the dead ones, the SLB matrix would be able to run for the long term.

At any time *t*, the SLB matrix can be controlled to follow a target discharge power by solving the following mixed-integer quadratic optimization model. To keep the expressions concise, time *t* is dropped in the optimization model.

$$\min\left(P_{tar} - \eta_d \sum_i x_i \sum_j V_{ij} I_i\right)^2 \tag{4-9}$$

$$x_i \in \{0,1\}$$

where P_{tar} is the target discharge power; η_d is the converter efficiency; x_i is the on-off status of row *i*, also the control variable; V_{ij} is the voltage of the SLB at row *i*, column *j* (i.e. SLB *ij*); I_i is the discharge current of row *i*.

The voltage of SLB *ij* is given by

$$V_{ij} = \begin{cases} V_{oc_{ij}} - I_i R_{ij} & \text{if } SOC_{ij} > SOC_{min} \\ 0 & \text{if } SOC_{ij} \le SOC_{min} \end{cases} \tag{4-10}$$

where V_{oc_ij} is the open circuit voltage of SLB *ij*; R_{ij} is the internal resistance of SLB *ij*. Other variables are defined in (4-9) and (4-6).

At any time *t*, the discharge current of row *i* and the total discharge power of the battery matrix are given by

$$I_i = \min_j \{I_{ij}\} \tag{4-11}$$

$$P = \sum_i \sum_j V_{ij} \, I_i \tag{4-12}$$

where I_{ij} is the rated discharge current of SLB *ij*. V_{ij} is defined in (4-9).

With respect to charging, each SLB is charged individually. If there is a limit on the total charging power for the battery matrix, the battery packs with lower SoC have priority in charging. Each SLB is charged using the two-stage charging as explained in Chapter 4.5.1.

4.5.3. Flexibility Service Model

SLBs are controlled to both provide flexibility services and perform energy arbitrage. This chapter introduces two types of flexibility services: non-critical flexibility service and critical flexibility service.

The non-critical flexibility service is the provision of demand reduction or generation increase (the SLBs serve as a generation) when the network is congested but is not suffering any fault. This is based on the model published by Western Power Distribution (WPD), a UK distribution network operator (DNO) [107], whose purpose is to relieve overloads for highly loaded distribution substations. For the non-critical flexibility service, the battery processer (as the flexibility provider) submits its availability period and flexible kW value (i.e. the demand that can be reduced or the generation that can be injected into the grid during peak time) to the DNO. Each time when flexibility is required, the DNO would notify the battery processer to deliver its flexible kW by specifying the start time [107]. The DNO does not specify the end time but will give the battery processer an instruction to cease the flexibility service [107].

The critical flexibility service is the provision of demand reduction or generation increase (the SLBs serve as a generation) when the network is suffering a fault. This represents an urgent unpredictable need, and hence the DNO does not inform the battery processer in advance. When the battery processer receives the notification from the DNO, it needs to discharge power to the grid as much as it can throughout the full duration (normally less than 30 minutes) in order to support this urgent need of the grid.

Both types of flexibility service calls are assumed to occur continuously and independently at a constant average rate, i.e. following a Poisson point process [108]. Therefore, the time interval between two consecutive flexibility calls follows an exponential distribution:

$$f_{\Delta}(\Delta t_{fs}) = \begin{cases} \lambda_{\Delta} e^{-\lambda_{\Delta} \cdot \Delta t_{fs}} & if\ \Delta t_{fs} > 0 \\ 0 & \text{otherwise} \end{cases} \tag{4-13}$$

where λ_{Δ} denotes the mean rate of flexibility calls. Δt_{fs} denotes the time interval between two consecutive flexibility calls.

When the DNO calls the battery processer for a flexibility service, both the start time of the flexibility service and its required duration are modelled by truncated Gaussian Distributions, which take the same form as (4-1).

When the battery processer is providing non-critical flexibility service, it discharges power at the contracted flexibility capacity (in kW). Suppose that the contracted flexibility capacity is *C*. A performance factor is defined by the DNO to measure the performance of the battery processer, i.e. to what extent the battery processer fulfils the flexibility contract [106] [107]. The performance factor is given by

$$F = g\left(\frac{T_a}{T_r}\right) = \begin{cases} 1 & \text{if } T_a/T_r \geq 0.9 \\ 0.8 & \text{if } 0.8 \leq T_a/T_r < 0.9 \\ 0.7 & \text{if } 0.7 \leq T_a/T_r < 0.8 \\ 0.6 & \text{if } 0.6 \leq T_a/T_r < 0.7 \\ 0 & \text{if } T_a/T_r < 0.6 \end{cases} \tag{4-14}$$

where T_a is the actual duration for which the battery processer delivers flexibility. T_r is the duration required by the DNO for flexibility services. For the non-critical flexibility service, the SLB packs are not always able to deliver the contracted flexibility capacity *C* for the required duration T_r, because the flexibility service is called at short notice when the total energy available in the SLBs may not be sufficient. Such an underperformance compromises the revenue. For the critical flexibility service, the SLB matrix discharges the maximum possible power, subject to the transformer capacity limit and the available energy, whichever is more constraining.

The total revenue from providing both types of flexibility services within a month is given by

$$R_{fs} = \rho_{nf} \sum_{i=1}^{N_{nfs}} C \cdot T_{a,i} \cdot PF_i + \rho_{cf} \sum_{i=1}^{N_{cf}} P_{b,i} \cdot T_{b,i} \tag{4-15}$$

where ρ_{nf} is the unit price per kWh of flexible energy delivered for the non-critical flexibility service. N_{nfs} is the number of non-critical flexibility services within a month. *C* is the contracted flexibility capacity in kW. $T_{a,i}$ is the actual duration of the *i*th time of the non-critical flexibility service. PF_i is the performance factor of the ith time of the flexibility service. ρ_{cf} is the unit price per kWh of flexible energy delivered for critical flexibility service. N_{cf} is the number of critical flexibility services within a month. $P_{b,i}$ is the delivered power of critical flexibility service in kW. $T_{b,i}$ is the actual time interval of the *i*th time of the critical flexibility service.

Considering the contract between the consumers and the DNO, the flexibility prices ρ_{nf} and ρ_{cf} (defined in (4-15)) are fixed within the contract period of one year. However, after the current contract expires, the prices are likely to change to new values which are fixed throughout the next contract period. The absolute flexibility prices over the long term are difficult to forecast. In this study, it is assumed that the flexibility prices increase each year (i.e. between two consecutive contracts) by an inflation rate of 2%. This corresponds to a conservative revenue calculation because future growth of electric vehicles and electric heat pumps will increase network congestion and thus possibly increase the flexibility prices beyond 2% per annum.

4.5.4. Heuristic Control and Business Model incorporated in Monte Carlo Simulation

A heuristic algorithm is developed that controls the SLB matrix (detailed in Chapter 4.5.2) to both provide flexibility services (detailed in Chapter 4.5.3) and perform energy arbitrage. The heuristic algorithm determines the charge, discharge and idling of the SLB matrix. The business model is that any profits from the above activities are shared among customers every month, in proportion to their nominal SLB capacity in service in that month. Both the heuristic control and the business model are incorporated into a Monte-Carlo simulation (MCS) framework, which simulates the day-to-day operation of the SLB matrix throughout its lifetime. Fig. 4-4 shows the MCS framework with the heuristic control and the business model.

Before performing the MCS, the days when non-critical flexibility services are called, the service start time (which is simulated but which the battery processer does not know until 30 minutes in advance), required durations are sampled by MCS, based on truncated Gaussian distributions as explained in called 4.5.3. The days when critical flexibility services are called and their start time are also simulated (the battery processer does not know them).

Suppose that the electricity buying and selling prices are known to the battery processer. The prices are classified as low, medium, and high prices. In Fig. 4-4, the grey block of “Calculate energy surplus” estimates the energy surplus at any time *t*. The energy surplus at time *t* is given by

$$\boldsymbol{E_{s,t} \approx \varphi \sum_{j} EC_{nom_j} \cdot \left(SoC_{j,t} - SoC_{min}\right) - \sum_{t} \sum_{j} P_{j,dmax} \cdot \Delta t \cdot \delta(\rho_t)} \tag{4-16}$$

$$\text{where } \delta(\rho_t) = \begin{cases} 1 & \text{if } \rho_t \geq \rho_H \\ 0 & \text{otherwise} \end{cases}$$

Although the degradation is simulated objectively, the actual degree of degradation at any time *t* is unknown to the battery processer. Therefore, an average degradation factor φ $(0 < \varphi < 1)$ is introduced for the battery processer to estimate the degradation. EC_{nom_j} is the nominal energy capacity of SLB *j*. $SoC_{j,t}$ is the SoC of SLB *j* at time *t*. ρ_H

is the threshold for a high electricity price. $P_{j,dmax}$ is the maximum discharge power of SLB *j*.

In Fig. 4-4, the blue block of "Charge batteries" first determines the total charging power that is limited by the transformer capacity. This block then calls the SLB matrix charging function as explained in Chapter 4.5.2. In Fig. 4-4, the green block of "Discharge batteries" first determines the SLB discharge power, subject to the transformer and converter capacities, whichever is lower. It then calls the SLB matrix discharging function as explained in Chapter 4.4.2. In Fig. 4-4, the yellow block is detailed in Chapter 4.5.1.

The revenue from energy arbitrage within a day or a month is given by

$$\boldsymbol{R_{ea}} = \sum_{\boldsymbol{t=1}}^{\boldsymbol{N}} \boldsymbol{\phi(P_t) \cdot P_t \cdot \Delta t \cdot \rho_t} \tag{4-17}$$

$$\text{where } \phi(P_t) = \begin{cases} \eta_d & \text{if } P_t \geq 0 \\ \frac{1}{\eta_c} & \text{if } P_t < 0 \end{cases}$$

In (4-17), *N* stands for the last time point of the day or month. P_t is the discharge power of the SLB matrix given by (4-12) (discharge is positive and the charge is negative). ρ_t is the electricity price at time *t*. Δt is the time interval. η_d and η_c are the discharge and charge efficiencies, respectively.

The costs of SLB degradations are implicitly considered: the degradations lead to a limited lifetime of the SLB matrix, thus limiting the total revenue throughout the lifetime. The total monthly revenue for the battery processer is given by

$$R = R_{fs} + R_{ea} \tag{4-18}$$

where R_{fs} is given by (4-15) and R_{ea} is given by (4-17).

It should be noted that according to Fig. 4-4, the control algorithm prevents gaming between energy arbitrage and flexibility services. In other words, for any flexibility call, from when its advance notice is released until the whole process ends, the SLB matrix does not charge to avoid aggravating grid congestions.

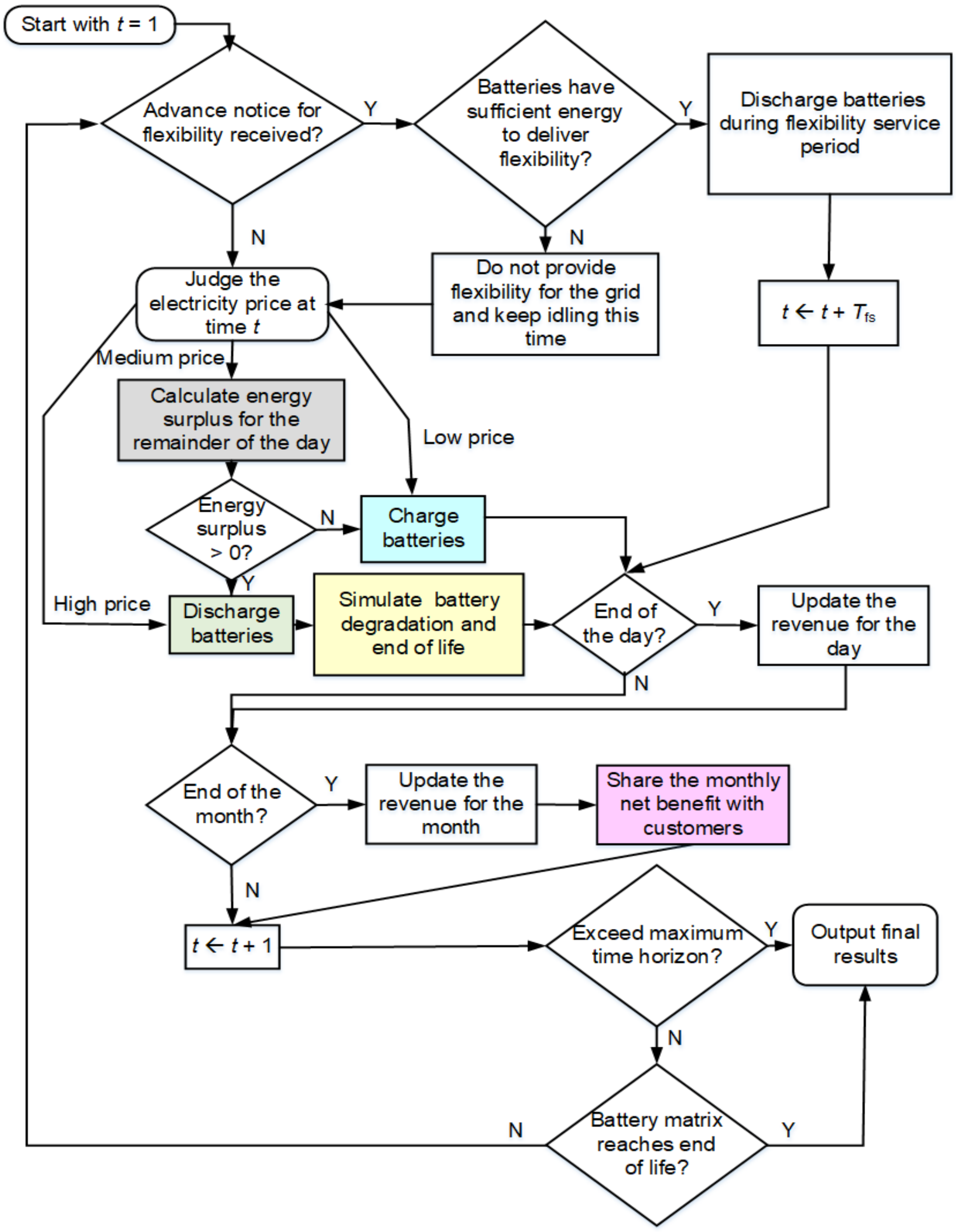

Fig. 4-4 Monte Carlo simulation incorporating heuristic control to assess profitability of the monthly-payment-based business model.

- **The monthly-payment-based business model**

The pink block in Fig. 4-4 represents the monthly payment-based business model: the battery processer shares part of the revenue with customers in proportion to each customer's SLB energy contribution by the end of each month. Each customer *j* receives an income R_j from the battery processer in the month concerned.

$$R_j = \frac{EC_{bj}}{EC_{b_{sum}}}\left(R - C_{cost} - P_{profit}\right) = \frac{EC_{bj}}{EC_{b_{sum}}} R \cdot \pi \tag{4-19}$$

where EC_{bj} is the energy contribution of customer *j*'s battery packs that are in service at the end of the month. $EC_{b_{sum}}$ denotes the total energy contribution of battery packs in service. R is given by (18). C_{cost} denotes the operation and management cost of the battery processer. P_{profit} denotes the profit reserved for the battery processer. $R_j = 0$ when customer *j*'s SLB reaches the end of second life. π denotes the percentage of revenue that the battery processer shares with all customers. π is set to meet two requirements: 1) ensure a profitable business for the battery processer; 2) offer competitive rewards to customers in competition with other battery processers.

In this paper, the business model entails a monthly payment to EV owners.

4.6. Data environment and simulation results

Case studies are performed on the monthly-payment-based business model alongside the heuristic control.

4.6.1. Input Data

This chapter presents the input data for case studies. The battery processer has an SLB matrix consisting of 2,000 SLBs in 5 rows, with 400 SLBs in each row. The rated open-circuit voltages of SLBs are 300 V. However, their actual open-circuit voltages are different, depending on their degradation and SoC. The charge current of the SLBs is about 0.8C. The range of discharge current ranges from 0.5C to 1C. The efficiency of battery charging and discharging is 90%. The internal resistance ranges from 0.9 Ω to 1.8 Ω and the nominal energy capacity ranges from 15 kWh to 30 kWh. To avoid over-charging and over-discharging, the SoC of each SLB is controlled between 20% and 80% under all circumstances except for when providing critical flexibility services through deep discharges. In the latter circumstance, the SoC lower limit is 10%. The electricity price provided by the local distribution network is given in Table 4-1. The prices of the flexibility services are shown in Table 4-2 [109].

Table 4-1 THE ELECTRICITY PRICE OF ONE DAY

0.00-7.00	7.00-17.00	17.00-22.00	22.00-0.00
£0.07/kWh	£0.11/kWh	£0.18/kWh	£0.11/kWh

Table 4-2 FIXED PRICE OF FLEXIBILITY SERVICES

Non-critical flexibility*	Non-critical flexibility	Critical flexibility
£300/MWh	£305/MWh	£600/MWh

*The non-critical flexibility corresponds to the “secure” type of flexibility service in [110]. The critical flexibility corresponds to the “restore” type of flexibility service in [110].

The average interval between two non-critical flexibility calls is 3 days. The average interval between two critical flexibility calls is 21 days.

In this paper, the price series of the energy arbitrage is shown in Table III. The maximum price is £0.18/kWh and the minimum price is £0.07/kWh. The mean value of the price series is about £0.11/kWh and the standard deviation is about £0.04/kWh.

4.6.2. Numerical Results

This chapter presents the revenues from the SLB businesses, including energy arbitrage, critical flexibility service and non-critical flexibility service. The simulation is performed over a 10-year horizon, considering two scenarios. The simulation is performed on MATLAB 2020.

- **Scenario 1): SLB matrix replaced by whole**

Scenario 1) is defined as when any SLB reaches its end of life, it will be removed from the SLB matrix without replacement. After the 10-year horizon, the revenues from the three services are plotted in Fig. 4-7. The average revenues of the three services (energy arbitrage, critical flexibility, and non-critical flexibility) are £5,483.04, £20,459.23 and £19,253.28 per month, respectively. The total revenue and the net benefit per month are shown in Fig. 4-8. In Fig. 4-7, it is shown that all these revenues decrease over time. This is because the capacity of the SLB matrix decreases as increasing SLBs reach the end of life. SLBs will reach the end of life because of two reasons: 1) the energy capacity drops below the lower threshold; 2) and the terminal voltage drops below the lower threshold. The number of the SLBs that die from each of the two reasons is shown in Table 4-3. Fig. 4-5 and Fig. 4-6 show the number of SLBs reaching the end of life at a constant rate. The maximum rate appears in the 64th month. Fig. 4-9 shows the second life energy throughput each year.

In summary, without replacing dead SLBs, the maximum life of the SLB matrix is 115 months. In the implementation, considering the operation cost of the business, the SLB matrix should be replaced before 115 months.

Table 4-3 STATES OF SLBS AFTER 10-YEAR OPERATION IN SCENARIO 1

Number of dead SLBs because of low energy capacity	Number of dead SLBs because of low terminal voltage	Remaining SLBs in service
235	1586	179

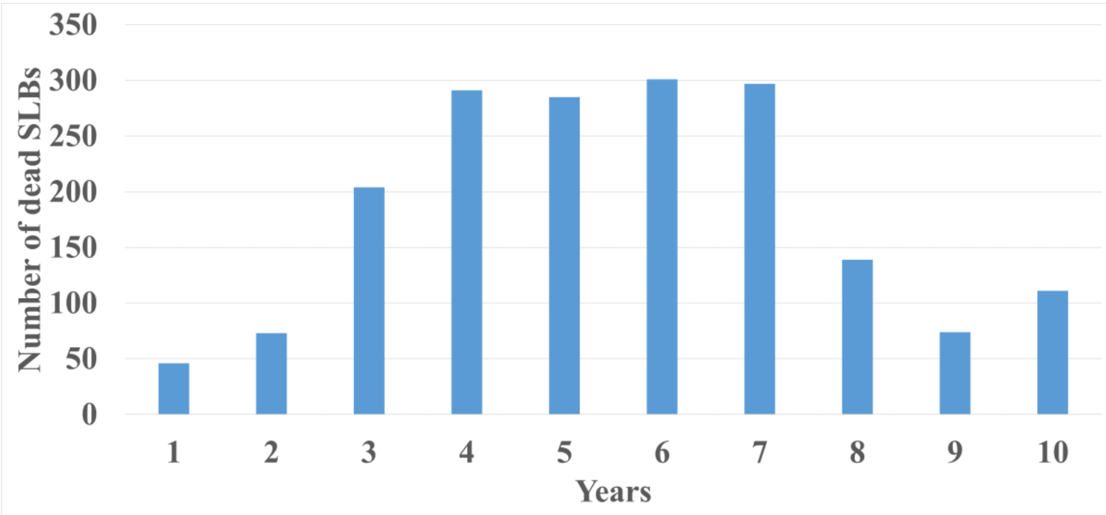

Fig. 4-5 The number of dying batteries each year in scenario 1.

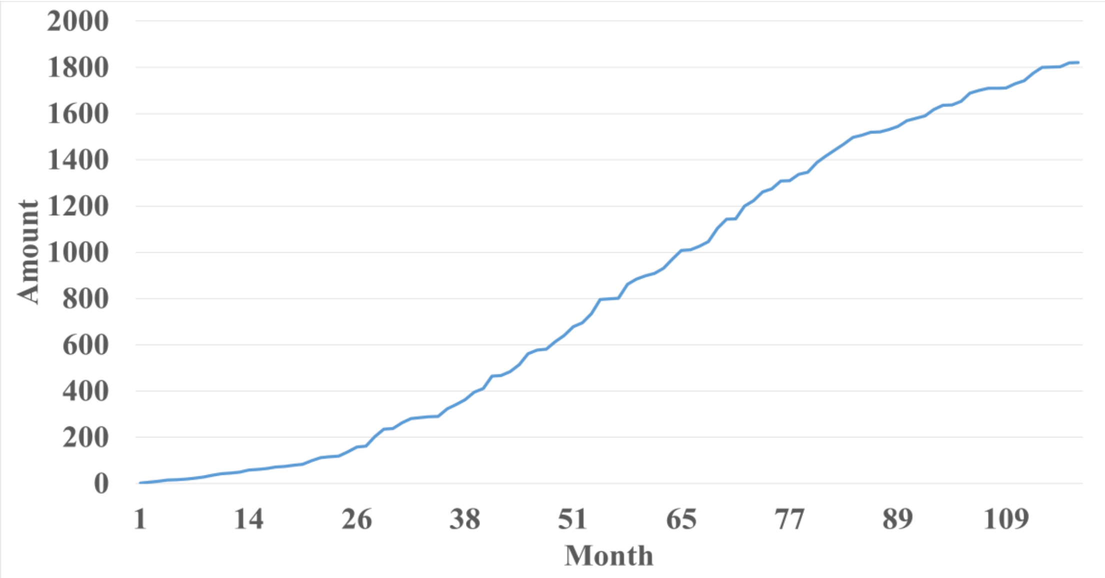

Fig. 4-6 The 'cumulative function' of dying batteries in scenario 1.

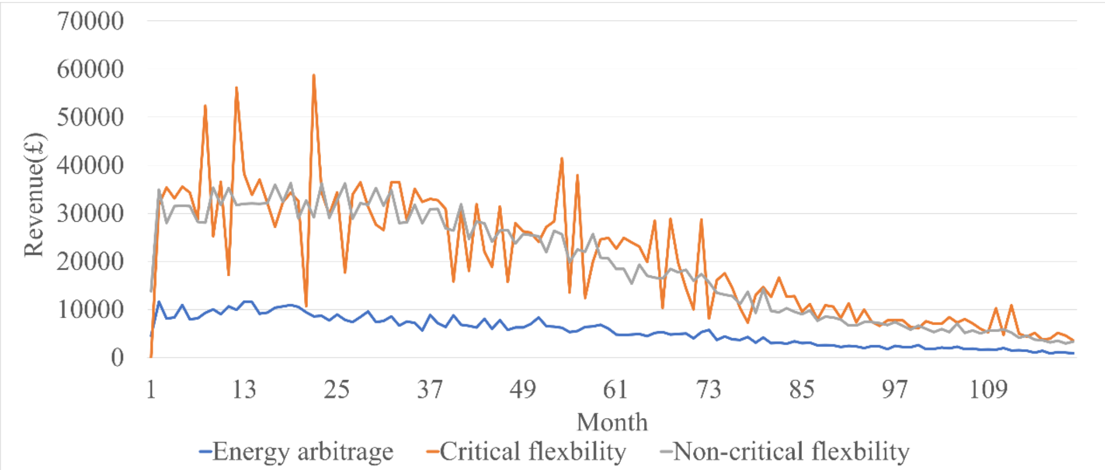

Fig. 4-7 The revenue of the battery matrix for the three services.

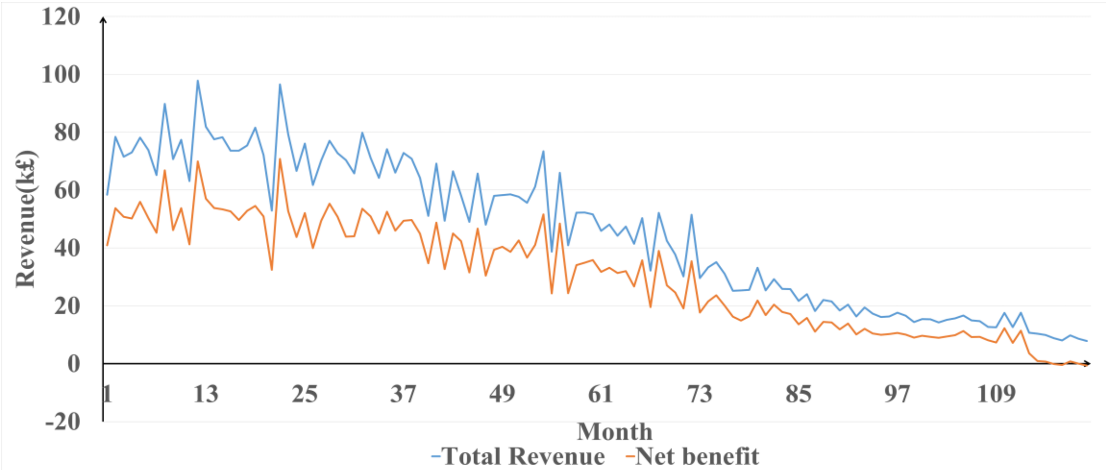

Fig. 4-8 The total revenue and the net benefit of the battery matrix.

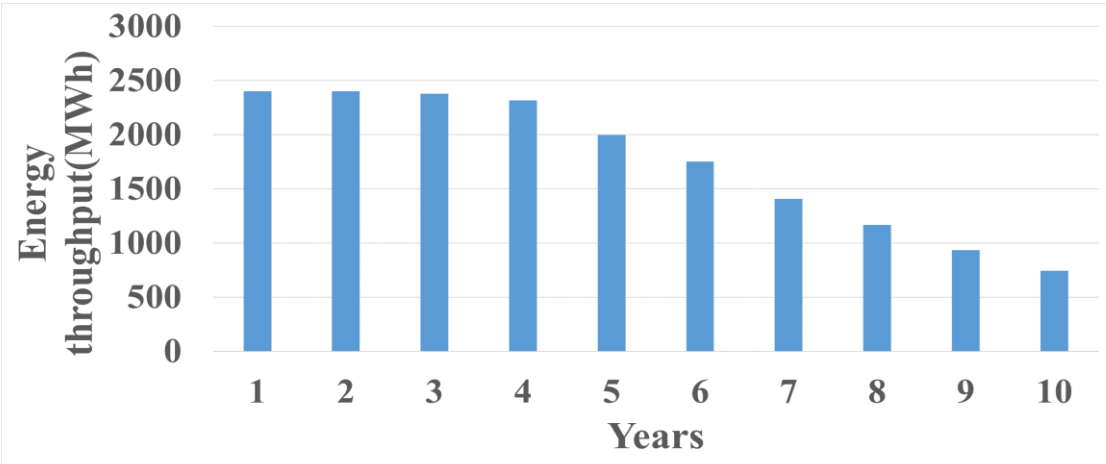

Fig. 4-9 The SLB energy throughput per year in scenario 1.

- **Scenario 2): SLB matrix replaced by SLB packs**

For Scenario 2), the dying SLBs are replaced by new SLBs on a real-time basis. This is to ensure that the SLB matrix can continue with its operation indefinitely. The new SLBs are of the same type and have the same nominal parameters as the dying ones.

The business is also simulated over a 10-year period. The input data, including the electricity price curve and the flexibility prices, are as same as in Scenario 1. Fig. 4-10 and Fig. 4-11 indicate the distribution of SLB end of life, and Table 4-4 shows the number of SLBs dying from insufficient terminal voltage and energy capacity. Fig. 4-14 shows the second life total energy throughput each year. Fig. 4-12 shows the revenues from energy arbitrage, critical flexibility service and non-critical flexibility service. The average revenue from the energy arbitrage service is £8,518.14, while the average revenues per month from critical and non-critical flexibility services are £28,217.93 and £27,838.21, respectively. Fig. 4-13 shows the total revenue and net profits over time.

Table 4-4 STATES OF SLBS AFTER 10-YEARS OPERATION

Number of dead SLBs because of low energy capacity	Number of dead SLBs because of low terminal voltage
1,439	3,246

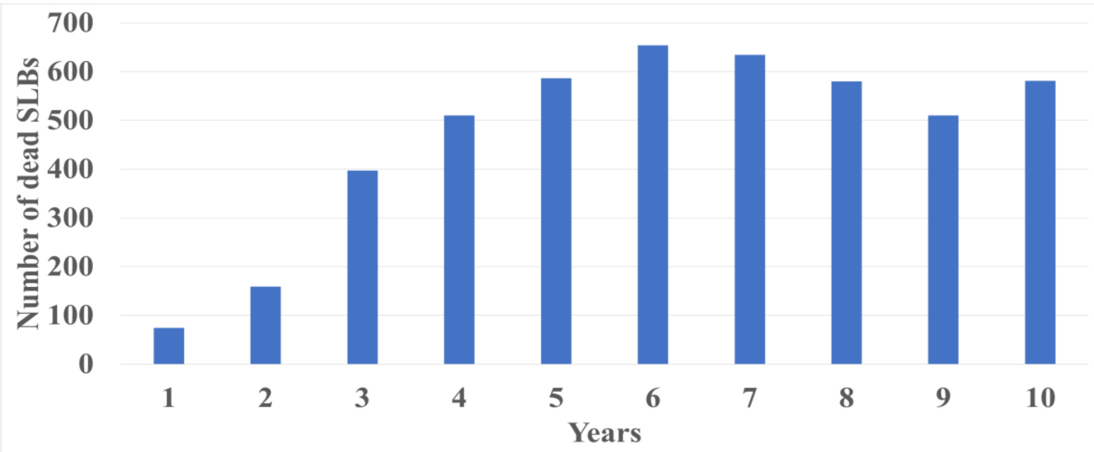

Fig. 4-10 The number of dying batteries each year in scenario 2.

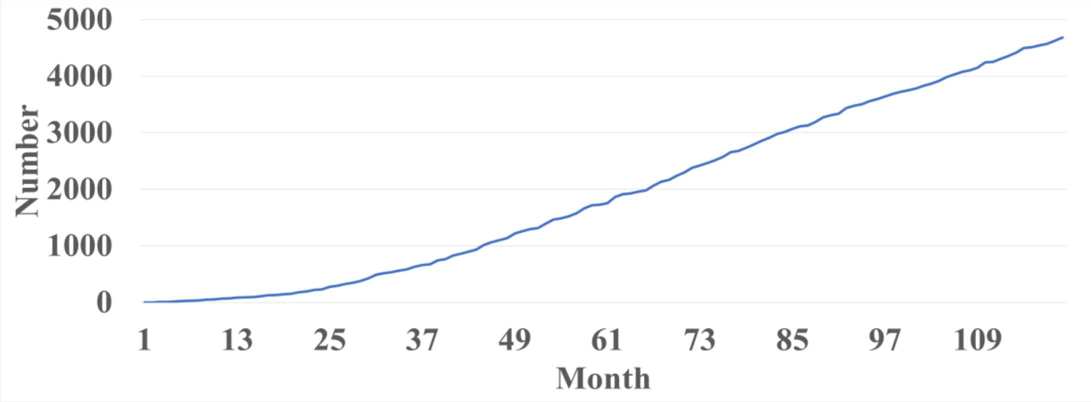

Fig. 4-11 The 'cumulative function' of the dying batteries

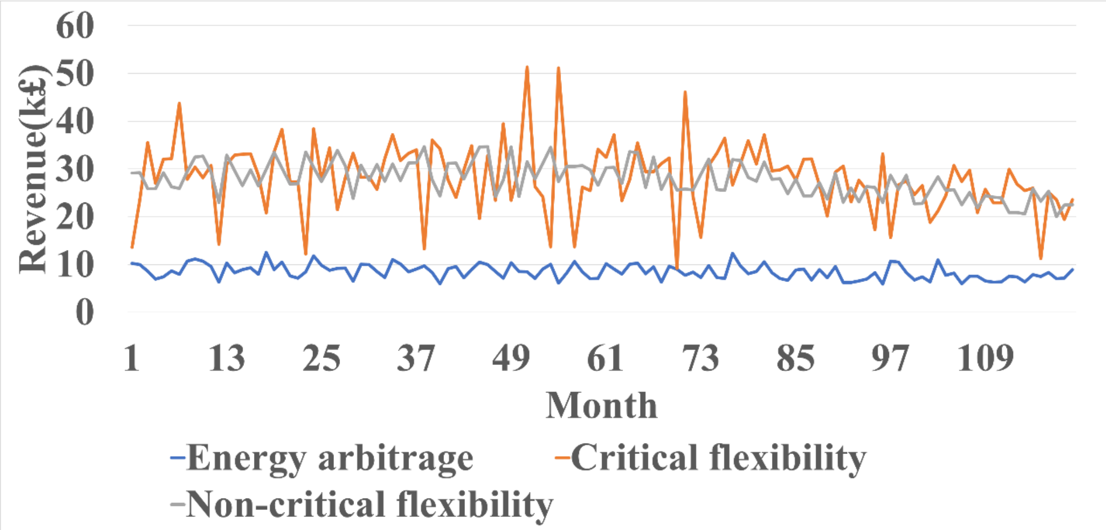

Fig. 4-12 The revenue of the battery matrix for the three services.

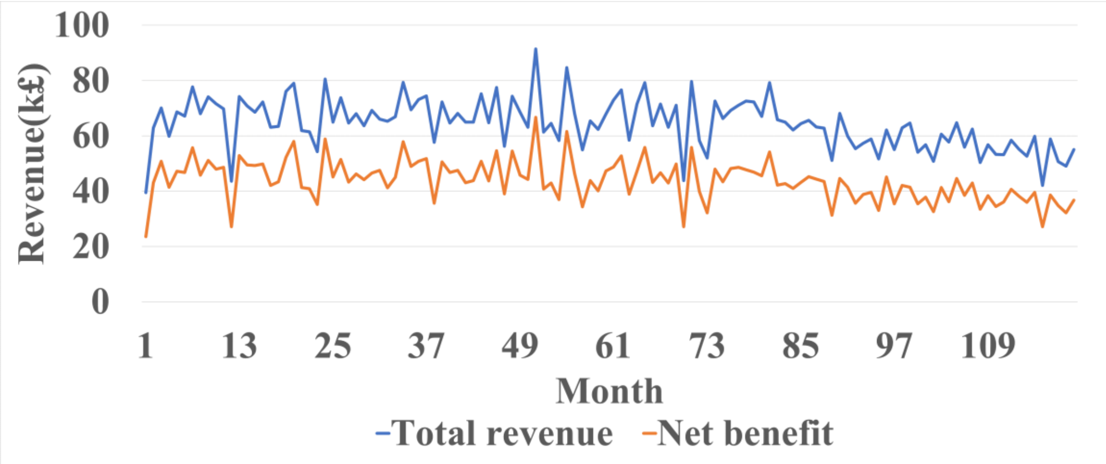

Fig. 4-13 The total revenue and the net benefit of the battery matrix.

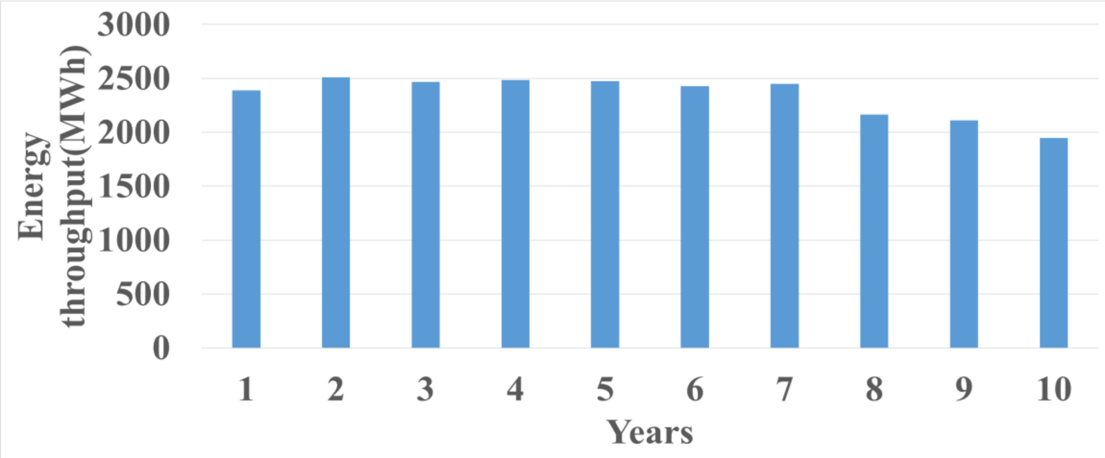

Fig. 4-14 The SLB energy throughput per year.

Table 4-5 FINAL PROFIT RESULTS OF SCENARIO 1) AND SCENARIO 2)

Scenario	1	2
Net profit (£)	5,423,465	7,735,270
Present value of profit (£)	2,648,782	3,433,247

In Scenario 1), the direct summation of the revenues over 10 years is £5,423,465, without being discounted to the present. On the other hand, given the 10% discount rate, the present value of the total revenue over 10 years is £2,648,782. Suppose the battery processer pays 20% of the total revenues to EV owners. The business would be profitable if the present value of the total cost over 10 years is less than £2,383,904, in which case it would correspond to a positive net present value (NPV). In Scenario 2), after the 10-year operation, the direct summation of the revenues over 10 years is £7,735,270. On the other hand, given the 10% discount rate, the present value of the total revenue over 10 years is £3,433,246. Suppose the battery processer pays 20% of the total revenues to EV owners. The business would be profitable if the present value of the total cost over 10 years is less than £3,089,922, in which case it would correspond to a positive net present value (NPV).

- **SLB degradation curve**

For both scenarios, the degradation curve of the energy capacity and the terminal voltage are shown in Fig. 4-15 and Fig. 4-16.

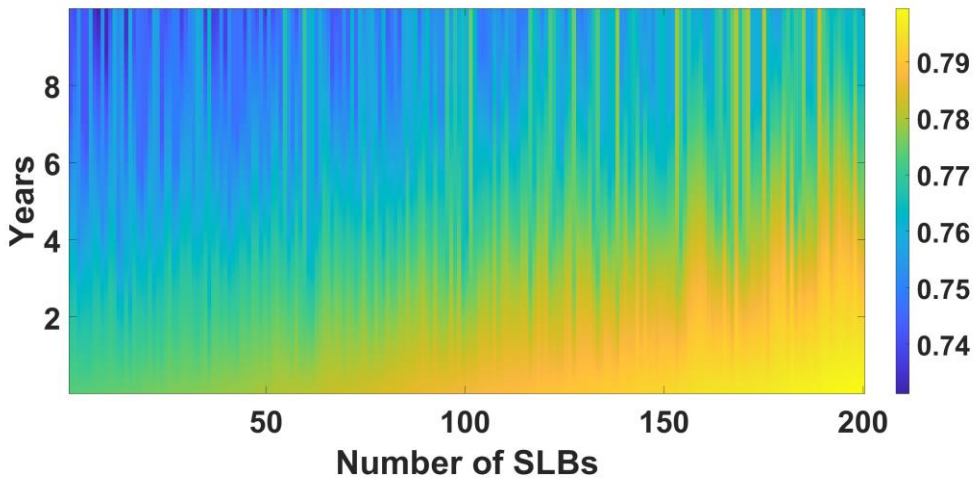

Fig. 4-15 The degradation curve of SLB energy capacity.

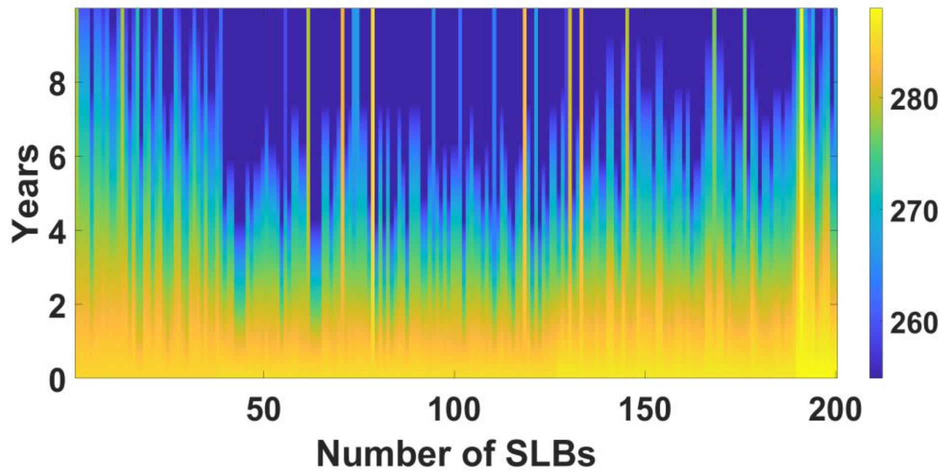

Fig. 4-16 The degradation curve of SLB terminal voltage.

The two figures choose 200 representative SLBs to demonstrate the degradation of energy capacity and terminal voltage. If one SLB is dead, its energy capacity and terminal voltage will keep the final value. In Fig. 4-15, the right vertical colour bar represents the per cent of the SLB energy capacity out of its nominal capacity. In Fig. 4-16, the colour bar represents the terminal voltage.

- **Profits for EV owners**

Lastly, the battery processer shares a percentage of the total revenues with EV owners as the profits. This percentage depends on a number of factors: market competition, regulation, etc. However, the SLB business model is in advance of commercialization. Therefore, these factors are unknown and are hard to predict. In this study, three scenarios with 5%, 10% and 15% sharing percentages are considered to present the profits for EV owners.

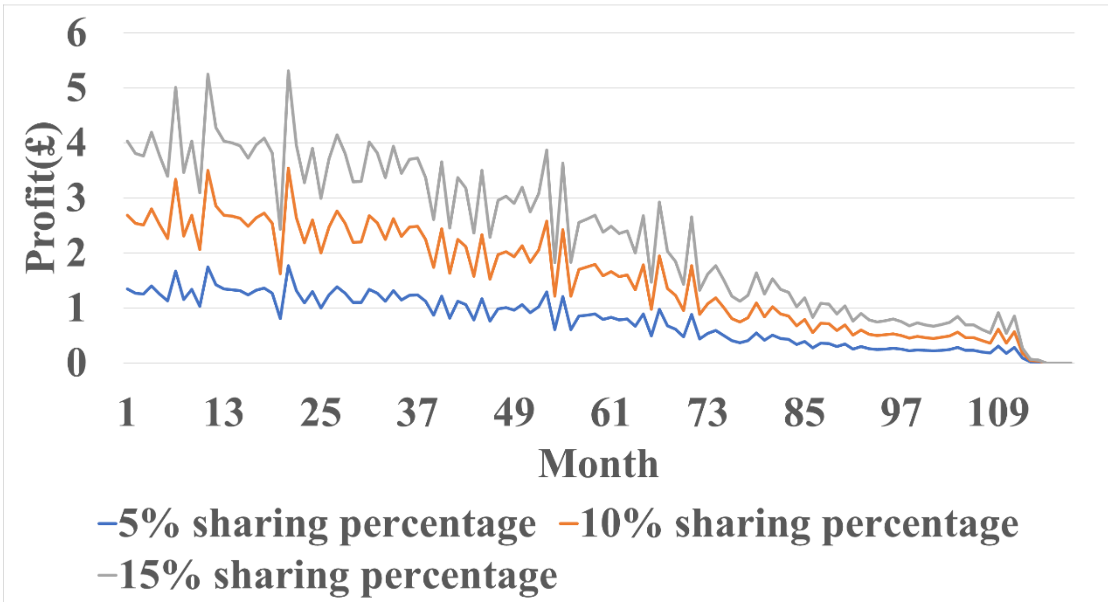

Fig. 4-17 The obtained profits for one example EV owner throughout the SLB's second-life.

Fig. 4-17 presents the obtained profits for one example EV owner throughout the second life of the retired battery. In Fig. 4-17, in the 21st month, the monthly profits achieve the maximum. However, after the 21st month, the monthly profits reduce by different levels. For example, for a 10% sharing percentage, the maximum monthly profits are approximately £3.54 in the 21st month, while the monthly profit reduces to zero in the 115th month. The total profits for the EV owner are approximately £90.67, £181.34 and £272.01, respectively, for scenarios with 5%, 10% and 15% sharing percentages throughout 10 years.

4.7. Discussion

The monthly-payment model essentially adopts a “wait and see” strategy. This model has advantages over the existing models where the battery processer offers one-off payments to buy back retired EV batteries: The one-off payment model requires SLB pricing at the beginning of its second life. Such pricing should reflect the true value of the SLB and it requires the forecast of the SLB lifetime and performance. This is a difficult task if considering the various types of SLBs and complicated field environment, posing serious difficulty to the SLB pricing. Although a number of references forecast battery lifetime and performance based on experiments and using data analytics [102] [57] [56], or advanced equipment [111], they are limited to specific battery types and are within controlled lab environments (including temperature, humidity, etc.). In reality, battery ageing occurs because of complex physical and/or chemical mechanisms, which depend on the battery type and environment. Therefore, if extrapolating the existing forecasting approaches to real scenarios where mixed types of batteries are deployed under different operating environments (which probably vary over time), the forecast accuracy is not guaranteed and significant errors may arise. What adds to the challenge is the replacement of dead SLBs with incoming new SLBs. In the worst case, the careless extrapolation of existing forecast approaches may lead to totally wrong and unusable forecast results. On the other hand, the monthly-payment model offers an advantage by completely bypassing the difficulty of forecasting.

In this paper, the battery processer is not a player large enough to directly enter the wholesale market for energy arbitrage. Rather, to save transaction costs, the battery processer enters into a Power Purchase Agreement (a bilateral contract) with the energy supplier, as is an ongoing practice for small-to-medium prosumers to sell energy in the UK [112]. This agreement stipulates the purchase and sale prices for electricity and the energy supplier effectively acts as an aggregator. Further, there is no flexibility market in the UK. Instead, there are bilateral contracts between network operators and flexibility suppliers. In this paper, the battery processer as a flexibility supplier enters into a bilateral contract with the DNO and this is detailed in Chapter 4.5.3. Both bilateral arrangements effectively reduce transaction costs and enable small-to-medium prosumers such as the battery processer to participate in the market.

In this chapter, the innovation of this research is to find a win-win business model for both the EV owners and the battery processers. In the monthly-payment business model, the total payment for the EV owners consists of two parts: the advance payment which will reflect the materials recycling prices and the monthly payment which reflects their SLBs' contribution to the less-demand applications. The month-payment business model will improve the energy and economic potential of the SLBs which cannot be directly adopted by the EV owners, and help the EV owners make profits to encourage them to send their retired batteries for possible second life applications. It is a relatively fair business model for both the EV owners and the battery processers.

It should be noted that the control strategy of the SLB matrix ensures that energy arbitrage does not add to grid congestion. When the distribution network operator calls for flexibility to relieve congestions, the SLB matrix control ensures no charging throughout the duration of the flexibility call but allows the SLB matrix to either discharge (thus helping the grid by meeting local demands with local generation) or idle, regardless of what the energy arbitrage prices are at that time. For example, Table. III shows the control strategy when a flexibility call comes. During this period, when the advance notice of a flexibility call comes at 20.50, the control system determines that the SLB matrix would provide the flexibility service and the SLB matrix is controlled to idle during the advance notice period. The SLB matrix then discharges during the actual flexibility service period. After the flexibility service ends at 21.40, the SLB matrix is then free to charge.

Another example is: when a flexibility call comes, the SLB matrix does not provide the full flexibility service because of insufficient energy stored in the SLB matrix. Table IV shows the SLB behaviour in this example: the SLB matrix is not allowed to charge during the advance notice period (starting from 20.30) of the flexibility call, thus not aggravating grid congestions. 2) the requested flexibility service time is from 21.00 to 21.30 when the SLB matrix is either discharged or idle. The SLB matrix only charges after the flexibility service ends at 21.30.

Accurate optimization solutions are difficult to obtain because of the combinatorial explosion [74]. A heuristic algorithm is a practical, easy-to-implement, cost-saving control solution in industrial applications. Adopting the heuristics is likely to be consistent with reality. If profit is achieved using realistic heuristics, the profit is also reasonable, not overly optimistic, and this would support the profitability of the business model. The control is performed under uncertain flexibility calls in terms of their uncertain time to occur. This further adds to the challenge of obtaining accurate optimization solutions. In this case, heuristics effectively tackle the uncertainties, whilst reducing complexity. In the area of optimal control, there is a “no free lunch” theory: no approach exists that is universally better than others in all cases. Consequently, there is no guarantee that more mathematically complex alternative approaches provide better results than heuristics.

The reasons for the SLB deaths are presented in Table 4-3 and Table 4-4. For both Scenarios 1 and 2, most SLBs reach the end of life because of the low terminal voltage. The result illustrates that for most SLBs, the terminal voltage determines its lifetime. However, for those SLBs whose initial energy capacity is near the lower threshold, they would be dead because of low energy capacity. In Scenario 2, the ratio of the two failures (low terminal voltage to low energy capacity) is lower than that in Scenario 1. This means that in Scenario 2, a greater percentage of SLBs reach the end of life because of low energy capacity, compared to that in Scenario 1.

To minimize the investment and operation costs for the SLB processers, in this paper, the existing car dealer launches and incorporates the SLB business into its existing car dealing business, using the same physical location and the same financial sheets. This business arrangement reduces the costs of SLB handling as well as the labour costs because existing members of staff and their expertise can be readily utilized. Further, it is a trend that car dealers are planning to deploy more rapid charging infrastructure at their sites. Therefore, there is the potential to integrate the rapid charging converters and the SLBs converters to further reduce investment costs.

4.8. Conclusions

This paper develops a novel business model for SLBs to make benefits for the battery processer and EV owners by providing flexibility services and energy arbitrage. The study validates the feasibility of the business model through two different scenarios: one scenario with incoming SLBs replacing the dead ones and the other scenario without incoming SLBs. Several key findings are obtained from the studies:

1) The monthly-payment business model can make economic benefits for both the battery processer and the EV owners. For the first scenario, after 10 years' operation, the benefit of the battery business model is £5,423,465. The present value of profit of the SLB business model is £2,648,782, which means that the business model is economically feasible. For the second scenario, the 10 years benefit is £7,735,270 and the present value of profit is £3,433,247. It means that the business model is also worth investing with the dead SLBs replaced.

2) For both scenarios, the profits mostly come from offering flexibility services rather than energy arbitrage. In the first scenario, the profits from the flexibility services account for approximately 87.87% of the total profits, while in the second scenario, the profits from the flexibility services account for approximately 86.81%.

3) Both scenarios can be adopted in reality based on the economic potential of the SLB business model. The advantage of Scenario 1) is that the SLB matrix can be replaced as a whole, without the complication of partially replacing the SLB matrix and making the day-to-day operation easy. A limitation of Scenario 1) is: the difficulty of processing the new arrivals of SLBs, which will be piled up to form a new SLB matrix for re-use. The merit of Scenario 2) is its advantage in processing incoming new SLBs, which replace the dead ones from the SLB matrix, respecting the metabolism nature of the business. A limitation of Scenario 2), however, is that the performance of the relatively "heathier" new SLBs are compromised by the "unhealthier" old ones.

4) Although the case studies prove the economic feasibility of the SLB business model, it is subject to a steady supply chain of SLBs from retired electric vehicles and a friendly regulatory framework. The limitation as well as the risks, however, are the uncertainties within the supply chain and future regulatory framework.

Chapter 5.

Energy management for an electric bus charging station with facilitated second-life batteries

Chapter contents:

5.1. Chapter overview 99
5.2. Abstract 102
5.3. Introduction 102
5.4. Overview of methodology 106
5.5. System model 107
5.6. Framework Formulation 111
5.7. Case studies 119
5.8. Conclusions 131

This chapter develops an EB charging station model with SLB energy storage system. In this system, the SLB energy system will support the EB charging and provide flexibility services for DNOs.

5.1. Chapter overview

The UK government has announced that the UK will meet the target of net-zero carbon emission by 2050. In this process, it is important to replace the petrol and diesel buses with electric buses (EBs). To make the penetration of EBs friendly to the network, it is necessary to optimally control their charging behaviours. At the same time, as mentioned in Chapter 4, the application of SLBs is becoming a highlight in the study of EV development. In this chapter, an EB charging station model with an SLB energy storage system is proposed and a customized day-ahead scheduling approach is designed to solve the optimisation problem.

In this EB charging model, the main objective is to reduce operational costs. The timetable of the EBs is known in advance and all the EBs should depart from the station with enough SoC on time. In this model, the arrival time and SoC of each EB are unknown and random. To address this problem, a sample average approximation (SAA) based stochastic programming is proposed to estimate the arrival time of SoC of each EB at any time stage and it is adopted based on the historical data. Besides, the model is necessary to satisfy several constraints, including the constraints of the capacity of the distribution transformer and the constraints of the continuous charging behaviour.

For the EB charging model, the SLB energy storage has several contributions: firstly, it can reduce the energy purchased cost for the EB charging station. Secondly, by reducing the charging demand during the peak time, it will help the DNO manage the peak load and reduce the network congestions. Finally, the SLB energy storage system will provide flexibility services for the DNO, which will reduce network loading and support the grid.

Case studies show a comparison of three different control strategies to validate the feasibility of the EB charging model. The results indicate that the day-ahead scheduling can reduce 10% of the operational cost compared with the heuristic control strategy; and significantly reduce the charging demand during the peak time. The connection of SLB energy storage will lead to another 10% reduction compared with the charging station without an SLB system. The results of the study will contribute to both the EB charging station and the DNOs.

The rest of the chapter is cited from the author’s submitted article in IEEE Transactions on Smart Grid. The structure of this chapter is organised in an alternative-based format, where the indices, equations, tables, figures and titles are numbered independently.

Statement of Authorship

This declaration concerns the article entitled:	
Energy Management for Electric Bus Charging Station with Facilitated Second-Life Batteries	
Publication status (tick one)	
Draft manuscript ☐ **Submitted** ☐ **In review** √ **Accepted** ☐ **Published** ☐	
Publication details (reference)	R. Wei, K. Ma, C. Gu, Z. Zhang" Energy Management for Electric Bus Charging Station with Facilitated Second-Life Batteries " in IEEE Transactions on Smart Grid
Copyright status (tick the appropriate statement)	
I hold the copyright for this material √	Copyright is retained by the publisher, but I have been given permission to replicate the material here ☐
Candidate's contribution to the paper (provide details, and also indicate as a percentage)	The candidate proposed the idea of the paper, he designed the methodology, and predominantly executed the coding to derive the experimental results. Other authors helped the candidate with the design of case studies, the format of the paper, and the improvement of academic writing. The percentage of the candidate did compare with the whole work is indicated as follows: Formulation of ideas: 80% Design of methodology: 100% Simulation work: 100% Presentation of data in journal format: 90%
Statement from Candidate	This paper reports on original research I conducted during the period of my Higher Degree by Research candidature.
Signed	Renjie Wei
Date	26/07/2022

5.2. Abstract

Electric buses (EBs) play an important role in transport electrification as a pathway toward net-zero carbon emissions. In this paper, an EB charging station model is developed with centralized control of EB charging. The control strategy is customized, based on day-ahead scheduling, to achieve the objective of minimizing total costs. The charging demand is estimated based on the bus timetable and related historical data. To improve the performance of the control strategy, a second-life battery (SLB) energy storage system is adopted. Further, the SLB system is controlled to provide peak demand reduction/generation services (or flexibility in short) for distribution network operators (DNOs) to relieve network congestions. Three different control algorithms are trailed in the case studies: heuristic control algorithm, 'day-ahead scheduling' without SLB energy storage and 'day-ahead scheduling' with SLB energy storage. Results show that compared to the heuristic algorithm, the 'day-ahead scheduling' can significantly reduce the operational cost and the charging demand during the peak time. The connection of SLB can not only reduce operational cost but also improve the fault tolerance of the 'day-ahead' scheduling and provide contracted flexibility services without affecting EB charging.

5.3. Introduction

The UK government has set the target to achieve net-zero carbon emissions by 2050 [2]. Transport electrification is necessary for achieving this target. Public transportation electrification plays an important role in this process. The UK government has announced more than £120 million in funding for electric buses (EBs) from 2021 [113]. EBs can cause overloads to the grid by consuming large power especially when the grid is already supplying peak demand. To make EB charging friendly to the grid and to facilitate EB integration, EB optimal control is needed to save costs while meeting EB's business needs and not overloading the grid. The EB optimal control is a challenge, considering various uncertainties including traffic conditions, time of journey and energy consumption uncertainties.

Existing research studied the EB charging strategies from multiple perspectives. References [114], [115] suggested that distributed control be applied to EB charging. However, references [116], [117] developed central control strategies for EB charging. References [118], [119] developed control strategies based on battery swapping. To solve the uncertainties in EB operation, various studies modelled the uncertainties within traffic conditions. References [120], [121] model uncertain traffic conditions and develop solutions that reduce the uncertainties. Reference [122] considers observable variables such as time of journal in the modelling of traffic conditions. Reference [123] uses historical traffic data to plan the EB routines through a K-shortest routes algorithm.

The above references mainly focus on addressing the traffic uncertainties in an EB setting without storage systems. Introducing an energy storage system is a possible solution that can reduce uncertainties. In this paper, considering the number of batteries retiring from electric vehicles in future, second-life batteries are regarded as the stationary energy storage for an EB charging station. An illustration of the EB charging station is shown in Fig. 5-1.

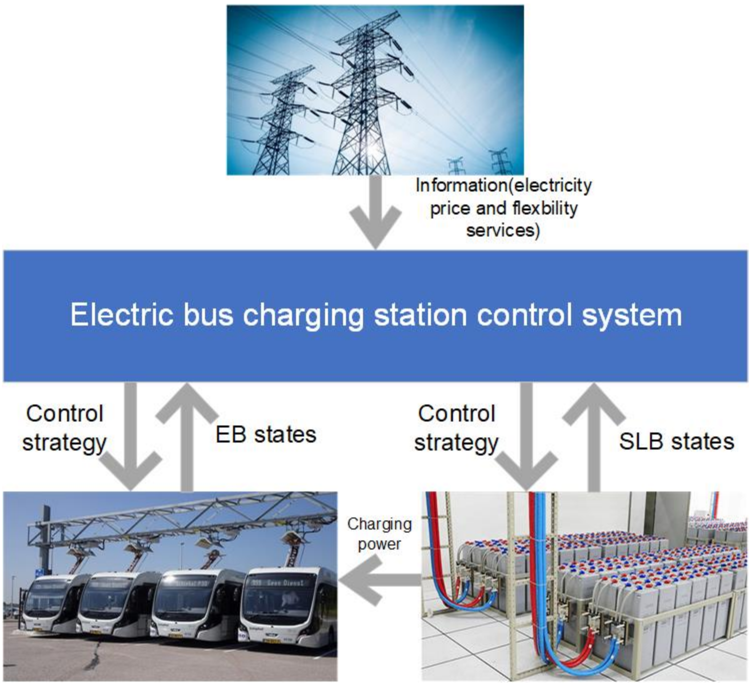

Fig. 5-1 The control system of the EB charging station with SLB energy storage.

The processing of retired EV batteries is gaining increasing research attention. According to UK laws, the battery suppliers are required to collect the retired batteries and repurpose them for second-life applications, e.g. serving as energy storage for power systems. In this paper, an EB operator deploys SLBs to support EB charging as well as providing grid services, thus reducing operation costs, relieving grid congestions and promoting more sustainable uses of batteries.

From the existing references, the adoption of SLB can help mitigate environmental impact, improve battery energy utilizations and promote life-cycle economics. Compared with batteries not having a second life, the SLB energy storage system might be a better choice considering its economic benefits [89]. A number of references explored the applications of SLBs. Reference [124] shows the SLB application in an electric/thermal hybrid energy storage system. Reference [125] focuses on the SLB application in microgrids. It is a major type of application for SLBs to provide ancillary services for the grid. These services include frequency regulation [91], spinning reserve [126], demand side response [94] and rural energy access [96].

A large-scale EV charging coordination requires sufficient computer power and information & control technologies (ICTs) to solve the optimal control problem in a timely manner with a satisfactory accuracy. For charging stations, it is necessary to model various constraints, process accumulated as well as continuously generated data, and obtain optimal charging strategies for real-time control. For the EB charging station, the bus schedule will be determined in advance and it is necessary to consider its stochastic working nature, including its uncertain arrival time as well as energy consumption that affect the state of charge (SoC). The requirement for efficient computation is much more demanding as compared to the charging stations for other types of EVs. To ensure computation efficiency, day-head scheduling is developed in this paper to guide the EB charging. A sample average approximation (SAA) method [127] is adopted to model the stochastic nature of this optimal control problem.

The contributions of this paper are summarized as follows:

This paper proposes a novel EB charging station with the connection of SLB energy storage system. The SLB energy storage system will help charge the EB during peak time and provide flexibility services to the network. Considering SLB energy storage as well as uncertainties, this paper develops a novel optimal control scheme for an EB charging station. Day-ahead scheduling with SAA stochastic programming is introduced to produce the day-ahead optimal control strategy. In real-time operations, control adjustments are made on EBs when the information unfolds with regard to EB arrival time and the overall economics of the model is assessed.

The rest of this paper is organized as follows: Chapter 5.4 shows the overview of the proposed EB charging station model; Chapter 5.5 presents the detailed model of the different parts of the EB charging station; Chapter 5.6 presents the optimization problem and its related control algorithm; Chapter 5.7 performs the case studies with the real-world data and Chapter 5.8 concludes the paper.

5.4. Overview of methodology

An overview of the EB charging station control methodology is presented in Fig. 5-2.

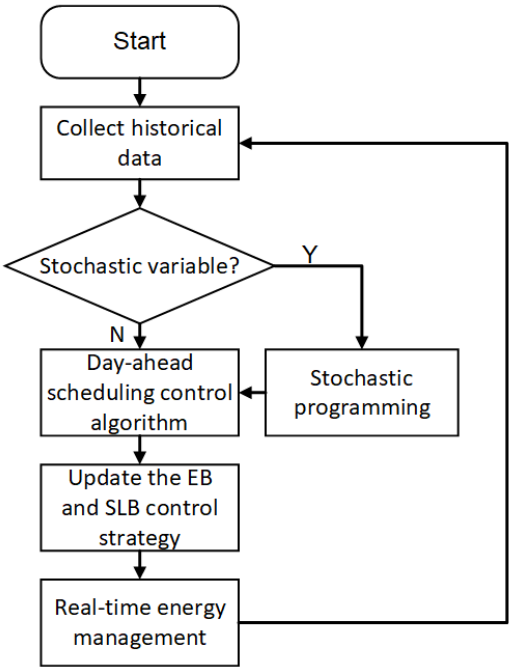

Fig. 5-2 The overview of the EB charging station control methodology.

For the control methodology, firstly, the historical data are collected and set as different inputs in the optimization problem. Among these different inputs, some of them can be directly adopted in the EB charging optimization, e.g. the electricity prices, base load consumptions, EB timetable and flexibility requirements. If the inputs belong to stochastic variables, such as the EB arrival time and the energy consumption for each travel, stochastic programming is utilized to reduce the effects of the uncertainties of these stochastic variables. With these inputs for the day-ahead scheduling, the model can make control planning on both the EB and SLB for the coming day. The output of the day-ahead scheduling, the real-time management system guides the EB and SLB for charging or discharging. Finally, after the real-time operation, the data of EB and SLB will be recorded and updated the historical data for the next scheduling.

5.5. System model

5.5.1. Electric bus model

It is assumed that the EB charging is centrally controlled by the EB station operator. There are *M* EBs in total for control every day. For EB *i*, its working schedule is settled in advance, including the number of travels *Nt* on the day and the departure time of each travel. However, the arrival time of each travel, the SoC upon arrival, the time and SoC required for serving a trip is uncertain. However, their probability distribution can be learned from historical data.

5.5.2. EB charging model

The charging mode of the charging station is chosen as fast charging at 220 kW If the SoC of the EB battery is far from its upper limit, the charging power is capped at its nominal value. When the SoC of the battery is near its upper limit, the charging power is reduced to ensure the battery will not be over-charged. This is expressed as:

$$SoC_{i,t} + P_{i,t}^{char} * \Delta t \leq SoC_{max} \tag{5-1}$$

where $SoC_{i,t}$ denotes the SoC of the EB *i* at time *t*, $P_{i,t}^{char}$ is the charging power for EB *i*, Δt is the charging interval and SoC_{max} is the upper limit of the SoC.

Apart from charging from the grid, EBs can also be charged by the SLBs. However, considering the SLB degradations, SLBs serve as a secondary charging source for the EB. There are two scenarios where an EB would be charged by the SLBs: 1) the EB arrives late at the station and charging to a sufficient level is urgently needed for the next travel; 2) the EB has to be charged during peak time, reflected by either the peak demand experienced by the DNO or the peak electricity price of the day. The SLBs themselves are charged from the grid, then discharge to EBs. The charging power for EB *i* at time *t* is given by:

$$P_{i,t}^{char} = P_{i,t}^{grid} + P_{i,t}^{SLB} \tag{5-2}$$

where $P_{i,t}^{grid}$ and $P_{i,t}^{SLB}$ represents the charging power from the grid and the SLB respectively.

5.5.3. SLB degradation model

The equivalent circuit of an SLB is shown in Fig. 5-3 [103].

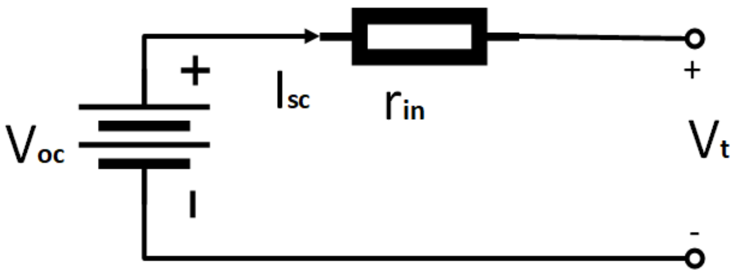

Fig. 5-3 The equivalent circuit of the SLB.

An SLB suffers from two degradations: the degradation of the energy capacity and the degradation of the open-circuit voltage. For the energy capacity degradation, it leads to decreasing energy capacity with the energy discharged. The process of capacity degradation can be approximated as:

$$\overline{EC_t} = \frac{EC_{SLB}^{nominal} - EC_{SLB}^{EoL}}{N_{Life} \cdot EC_{SLB}^{nominal} \cdot SoC_{SLB}^{max}(k + SoC_t^{SLB})} \tag{5-3}$$

where $EC_{SLB}^{nominal}$ is the nominal energy capacity of SLB, EC_{SLB}^{EoL} is the energy capacity when SLB reach its end of life, N_{Life} denotes the life cycles, SoC_{SLB}^{max} and SoC_t^{SLB} represent the maximum SoC and the current SoC at the time stage *t* of SLB. k is a constant variable that is determined by the battery type.

From Fig. 5-3, the degradation of the open-circuit voltage is caused by the increase of the internal resistance. The increase in internal resistance, $r_{SLB,t}^{in}$, is shown in (5-4):

$$\overline{\Delta r_{SLB,t}^{in}} = \frac{V_{SLB}^{nominal} - V_{SLB}^{EoL}}{I_{SLB}^{nominal} \cdot N_{Life} \cdot EC_{SLB}^{nominal} \cdot SoC_{SLB}^{max}(k_r + SoC_t^{SLB})} \tag{5-4}$$

where $I_{SLB}^{nominal}$ denotes the nominal discharge current of SLB, $V_{SLB}^{nominal}$ denotes the nominal open-circuit voltage, V_{SLB}^{EoL} denotes the open-circuit voltage when SLB reaches its end of life. k_r is the constant variable of the internal resistance and it is related to the battery type. N_{Life}, $EC_{SLB}^{nominal}$, SoC_{SLB}^{max} and SoC_t^{SLB} are defined in (5-3).

Besides the two degradations mentioned above, there is also calendar ageing, which is caused by the self-chemistry reaction with the time going on. In this paper, considering the short timeframe of the simulation, the effect of the ageing degradation is not considered.

5.5.4. Base load power consumption

Besides the charging for EBs and SLB energy storage, the base load consumption will also occupy the power capacity of the distribution transformer. The base load demand includes the electricity demands of the charging station, such as the infrastructure, air conditioners, heaters and so on. In this paper, the base load power consumption is collected from historical data.

5.5.5. Flexibility services for the network

In this paper, the SLB is encouraged to provide flexibility services for the distribution grid. According to published documents from Western Power Distribution (WPD), a UK distribution network operator (DNO), there are three different flexibility services that WPD requires: the secure service, the dynamic service and the restore service [109]. The secure service aims to reduce the peak demand and achieve the phase balance. It occurs frequently and the DNO declares the service demand in advance. The dynamic service is to support the grid when specific faults occur, such as the reinforcement work during summer. The restore service means to provide power when the network suffers from severe faults and the power system needs restoration. In this paper, the SLB is controlled to provide secure services. This is because the secure service is more frequent than the other two services and the power demand of this service is also more flexible. Additionally, the secure service is predictable and the requirements are announced to providers one week in advance. Both the dynamic service and the restore service are only declared 15 minutes in advance, too short for the EB charging station to schedule.

In this paper, it is assumed that every time a secure flexibility service is provided, the EB charging station delivers constant power for the required duration. The flexibility service for each day is given by:

$$S_i^{flex} = \left(T_i^{flex}, P_i^{flex}, t_{i,start}^{flex}, t_{i,end}^{flex}\right) \tag{5-5}$$

where T_i^{flex} denotes the scheduled time interval of the flexibility service, $t_{i,start}^{flex}$ and $t_{i,end}^{flex}$ denote the start time and the end time of the flexibility service, P_i^{flex} shows the delivered power of the flexibility service.

Although the SLBs can be adopted to provide flexibility service, their priority is to ensure EBs depart with sufficient energy, i.e. sufficient SoC levels. Therefore, it is possible that the SLBs cannot satisfy the demand for a secure flexibility service. A performance factor, PF, is defined to measure the performance of the SLBs. The performance factor is shown as:

$$PF = g\left(\frac{T_i^{real}}{T_i^{flex}}\right) = \begin{cases} 1 & \text{if } T_i^{real}/T_i^{flex} \geq 0.9 \\ 0.8 & \text{if } 0.8 \leq T_i^{real}/T_i^{flex} < 0.9 \\ 0.7 & \text{if } 0.7 \leq T_i^{real}/T_i^{flex} < 0.8 \\ 0.6 & \text{if } 0.6 \leq T_i^{real}/T_i^{flex} < 0.7 \\ 0 & \text{if } T_i^{real}/T_i^{flex} < 0.6 \end{cases} \tag{5-6}$$

where T_{real} represents the real-time duration of the SLB providing flexibility service and T_i^{flex} is shown in (5-5). With the insufficient performance factor, the revenue from flexibility service will be reduced.

5.6. Framework Formulation

This paper proposes day-ahead scheduling for the EB charging. The day-ahead scheduling produces an optimal control strategy that minimizes the expected cost, including the energy purchase cost and the SLB degradation cost. Stochastic programming is adopted to account for uncertainties in the bus arriving time and the arriving SoC of EBs. In the process of day-ahead scheduling, the SLBs help to reduce the charging demand during the peak time and provide the secure flexibility service for the DNO. During off-peak time and when not providing services for the DNO, the SLBs serve as backup power for the EBs if the EB arrives late or with less SoC than predicted by the day-ahead scheduling.

5.6.1. Day-ahead scheduling

In the day-ahead scheduling, the control variables of the EB $u_{j,t}$ are determined. The objective of the day-ahead scheduling is to minimize the total operation cost of the EB charging station. The objective function of the scheduling is shown in (5-7):

$$minf_1 = \sum_{t=1}^{T}(C_t^{EBgrid} + C_t^{SLBgrid} + C_t^{SLBdeg} - B_t^{flex}) \tag{5-7}$$

where f_1 means the total operational cost for the EB charging station, C_t^{EBgrid} denotes the energy cost of EBs purchased from the grid at time slot *t*, $C_t^{SLBgrid}$ denotes the energy cost of SLB charging at time slot *t*, C_t^{SLBdeg} denotes the SLB degradation cost at time slot *t* and B_t^{flex} denotes the benefits of providing flexibility service.

The EB energy cost for the EB and SLB charging at time slot *t* is given by:

$$C_t^{EBgrid} = \sum_{j=1}^{N}(P_{j,t}^{grid} * EP_t^{grid} * \Delta t) \tag{5-8}$$

$$C_t^{SLBgrid} = P_{SLB,t}^{grid} * EP_t^{grid} * \Delta t \tag{5-9}$$

where N is the total number of charging EBs at stage *t*, EP_t^{grid} denotes the electricity price at time slot *t*, $P_{SLB,t}^{grid}$ denotes the SLB charging power at time slot *t*, Δt is the duration of each time slot. $P_{j,t}^{grid}$ is given in (5-2).

The SLB degradation cost of SLB at stage *t* is given by:

$$C_t^{SLBdeg} = f(SoC_t^{SLB}, E_t^{SLB}, LC_t^{SLB}) \tag{5-10}$$

where E_t^{SLB} denotes the SLB discharged power at time slot *t*, LC_t^{SLB} denotes, at time *t*, the remaining life cycles until its end-of-life. $SoC_t^{SLB}$is given in (5-3). The function f is a function for the battery degradation cost and the detailed function is given in [22].

The profit from providing flexibility services is given by:

$$B_t^{flex} = PF * P_t^{flex} * \Delta t * EP_t^{flex} \tag{5-11}$$

where P_t^{flex} denotes the delivered power for the flexibility service, EP_t^{flex} shows the price of the flexibility power. PF is defined in (5-6) and Δt is given in (5-8).

To protect the power system and satisfy the business demand, there are several constraints that the charging station should meet:

- **The constraints of the distribution transformer**

The capacity of the distribution transformer of the EB charging station limits the total EB charging power from the grid at all time slots *t*. The base load consumption of the charging station should be satisfied as a priority. The constraint of the distribution transformer is shown as:

$$\sum_{j=1}^{N} P_{j,t}^{grid} + P_{SLB,t}^{grid} + P_{t}^{flex} \leq (1 - A_t) * S_T * \eta \tag{5-12}$$

where A_j denotes the percentage of the power of the base load consumption for the distribution transformer at time slot *t*, S_T denotes the total capacity of the distribution transformer, η is the efficiency of the transformer. $P_{j,t}^{grid}$ and $P_{SLB,t}^{grid}$ is given in (5-2) and P_{t}^{flex} is given in (5-11).

- **The constraints of the chargers**

In the EB charging station, to save the infrastructure investment cost, the number of chargers is less than the number of EBs. The constraint of the number of chargers is given by:

$$\sum_{j=1}^{N} u_{j,t} \leq N_{pot} \tag{5-13}$$

where $u_{j,t}$ denotes the control variable for EB *j* at time slot *t*. If $u_{j,t} = 1$, it means that EB *j* is charging at time slot *t*. If $u_{j,t} = 0$, it means that EB *j* is under an ‘idle’ state or does not park in the charging station at time slot *t*. N_{pot} is the total number of chargers in the EB charging station.

- **The constraints of the continuous charging behaviour**

To protect the EB batteries and SLB, if an EB starts the charging process, the charging behaviour should be kept until the EB battery reaches its target SoC or charging time. To express the 'continuous charging' constraints, two intermediate variables are introduced:

$$a_{j,t} \geq u_{j,t} - u_{j,t-1} \quad a_{j,t} \epsilon \{0,1\} \tag{5-14}$$

$$b_{j,t} \geq u_{j,t} - u_{j,t+1} \quad b_{j,t} \epsilon \{0,1\} \tag{5-15}$$

where *t* in these two equations for EB *j* is the time slot when EB *j* is parking in the charging station, $u_{j,t}$ is given in (5-13). In (5-13), only if the EB j starts charging at time stage *t*, the value of $a_{j,t}$ will be 1. Similarly, in (5-14), only if the EB *j* finishes charging at time $t + 1$, the value of $a_{j,t}$ will be 1.

With the two variables $a_{j,t}$ and $b_{j,t}$, the constraints are given by:

$$\sum_{t=T_{arrive}}^{T_{departure}} a_{j,t} = \sum_{t=T_{arrive}}^{T_{departure}} b_{j,t} \leq n \tag{5-16}$$

In this equation, for EB *j*, *t* is the time slot during its waiting time at the charging station. T_{arrive} is its arrival time and $T_{departure}$ is its scheduled departure time. This equation represents that for EB *j* during its parking time, it can be charged for *n* times.

- **The constraints of working**

The EB cannot be charged during its working time. The constraints are given by:

$$\boldsymbol{u_{j,t} = 0} \qquad \boldsymbol{t} \in \left(\boldsymbol{T_m^{departure}}, \boldsymbol{T_m^{arrive}}\right) \qquad m = 1, 2, \dots M \tag{5-17}$$

where m denotes the m*th* travel for EB *j*, $T_m^{departure}$ denotes the scheduled departure time and T_m^{arrive} denotes the expected arrival time. *M* is the number of travels that EB *j* should take on a certain day.

- **The constraints of SoC**

There are two types of constraints for the SoC of EB and SLB. To avoid overcharging or discharging and protect the batteries, the SoC of both the EB and SLB is limited to a certain range, which is given by:

$$\boldsymbol{SoC_{min}^{EB} \leq SoC_{j,t}^{EB} \leq SoC_{max}^{EB}} \tag{5-18}$$

$$\boldsymbol{SoC_{min}^{SLB} \leq SoC_{t}^{SLB} \leq SoC_{max}^{SLB}} \tag{5-19}$$

where $SoC_{j,t}^{EB}$ denotes the SoC of EB *j* at time slot *t*, SoC_{min}^{EB} denotes the minimum value of the EB and SoC_{max}^{EB} denotes its maximum value. SoC_{min}^{SLB} is the lower threshold of the SLB and SoC_{t}^{SLB} and SoC_{max}^{SLB} are given in (5-3).

To ensure the constraints of the SoC range and the demand of travelling, the EB should satisfy SoC constraints when reaching the departure time. The SoC constraints of EB battery is described as:

$$\boldsymbol{SoC_{j,t}^{EB} \geq SoC_{min}^{EB} + \Delta SoC_{exp,t}^{EB} \quad if\ t = T_m^{departure}} \tag{5-20}$$

$$m = 1, 2, \dots M$$

where $\Delta SoC_{exp,t}^{EB}$ denotes the expected SoC reduction for a trip at time *t*. The SoC reduction is a stochastic variable and the stochastic programming will be shown in Chapter 5.6.2 in detail.

- **SLB power constraints**

In the EB charging station, the SLBs serve as both the stationary energy storage and the flexibility service provider. The total output power is limited by:

$$\sum_{j=1}^{N} P_{j,t}^{SLB} + P_t^{flex} \leq P_{dischar,max}^{SLB} \tag{5-21}$$

where $P_{dischar,max}^{SLB}$ denotes the maximum discharging power of the SLB. $P_{j,t}^{SLB}$, P_t^{flex} and N are given in (5-2), (5-11).

Similarly, the charging power of SLB is limited by:

$$P_{SLB,t}^{grid} < P_{char,max}^{SLB} \tag{5-22}$$

where $P_{char,max}^{SLB}$ denotes the maximum charging power of SLB and $P_{SLB,t}^{grid}$ is given in (5-2).

- **Energy balance constraints**

In this system, the total charging power of one day should be balanced with the total energy consumption, including both the EBs and the SLB. It is given by:

$$\sum_{t=1}^{T}\sum_{j=1}^{N}\left(P_{j,t}^{grid} * \Delta t\right) + \sum_{t=1}^{T}\left(P_{SLB,t}^{grid} * \Delta t\right) = \sum_{t=1}^{T}\sum_{j=1}^{N}\left(P_{j,t}^{SLB} * \Delta t\right) + \sum_{t=1}^{T}\left(P_{t}^{flex} * \Delta t\right) + \sum_{t=1}^{T}\sum_{j=1}^{N}\left(P_{j,t}^{travel} * \Delta t\right) \tag{5-23}$$

where $P_{j,t}^{travel}$ denotes the energy consumption per hour for EB *j* at time slot *t*. $P_{j,t}^{grid}$, $P_{SLB,t}^{grid}$, $P_{j,t}^{SLB}$, P_{t}^{flex}, and $P_{j,t}^{travel}$ are given by (5-2), (5-11).

- **EB charging power constraints**

For the EBs, although the SLB storage system can help increase the charging power at some special time, the total charging power from the grid and the SLB energy storage cannot be more than its maximum charging power. It is given by:

$$P_{j,t}^{grid} + P_{j,t}^{SLB} < P_{j}^{max} \tag{5-24}$$

where P_{j}^{max} denotes the maximum charging power for EB *j*, $P_{j,t}^{grid}$ $P_{j,t}^{SLB}$ are given by (5-2)

5.6.2. Sample average approximation based stochastic programming

In this model, for the stochastic variables including the time for each travel and the reduction of SoC after each travel, a stochastic programming is introduced to find the solutions with the distribution of historical data. However, with a large number of EB fleets and different travel routes, it is difficult to calculate all the possible scenarios. In this paper, the SAA based stochastic programming is adopted to reduce the scenarios.

For the variables, the time interval of each travel T_{travel} and the consumption of SoC SoC_{travel}, firstly, the 24 hours of one day are divided into three different types: the peak time, the off-peak time and the midnight. It is according to the historical EB energy data and traffic data. The time interval of one day is shown in Fig. 5-4.

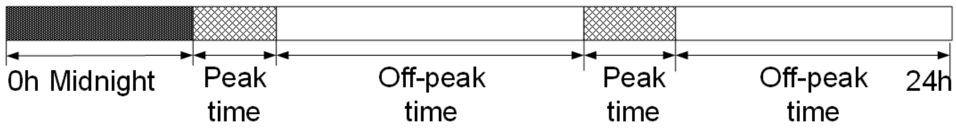

Fig. 5-4 The different time intervals of one day.

To further reduce the complexity, during the different time intervals, the distribution of the time and energy consumption, $\psi_{j,t}^{time}$ and $\psi_{j,t}^{SoC}$ are obtained from the historical data. In this paper, Monte Carlo Sampling is utilized to obtain the samples for SAA. In each sample scenario, the stochastic variables, T_{travel} and SoC_{travel}, are calculated based on their distributions $\psi_{j,t}^{time}$ and $\psi_{j,t}^{SoC}$, respectively.

5.7. Case studies

In this chapter, the performance of the EB charging station with SLB and the customized control strategy is evaluated with the practical data. The calculation algorithm in this model is designed based on a mixed-integer linear programming. The control optimization problem is modelled in Matlab 2021a and solved by the IBM ILOG CPLEX Optimizer.

The case studies are based on a medium-sized bus charging station in the UK. This station serves two different bus routes: the first one is a 24-hour bus service and the other bus service starts from 7 am and ends at 7.45 pm on weekdays. The first bus service is called U1 and the second bus service is 22 in Bath, the UK. The detailed information, including the bus timetable, the historical data of the bus is obtained from the bus aggregator, First Bus company. Considering that for each day, 20 U1 buses and 8 22 buses are controlled to work. The type of the bus is all BYD K9 [128] and the battery capacity of each bus is 324 kWh. The average power consumption for the bus is 1.3 kWh/km. The upper and lower threshold of SoC for the EB batteries is set as 0.8 and 0.2 respectively. In the bus charging station, the base load consumption is shown in Fig. 5-5 and the capacity of the distribution transformer is assumed as 4000 KVA. The number of chargers in the charging station is 8 and its nominal power output is 200 kW, following the fast-charging mode. The tariff of the electricity is a three-level tariff system and it is shown in Fig. 5-6. From the historical data, for a certain day, the midnight is from 0 am to 7 am, the peak time is from 7 am to 10am and 5.30 pm to 7.30 pm, and the off-peak time is from 10 am to 5.30 pm and from 7.30pm to the end of the day. The duration of each time slot is set as 5 minutes.

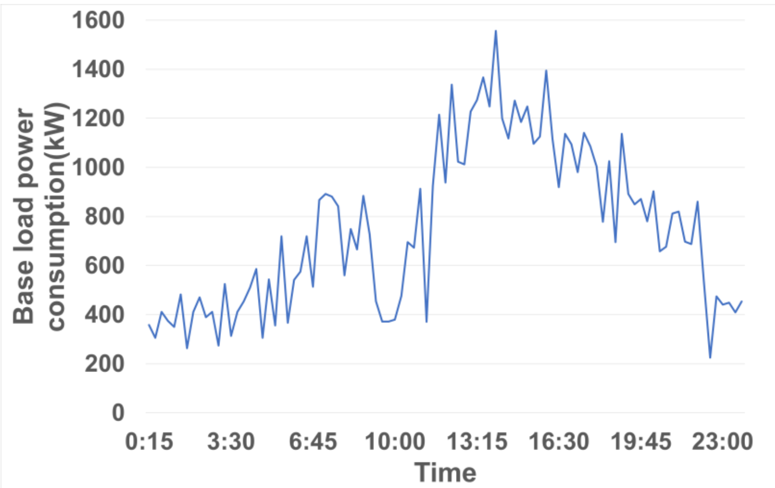

Fig. 5-5 The base load power consumption of the charging station.

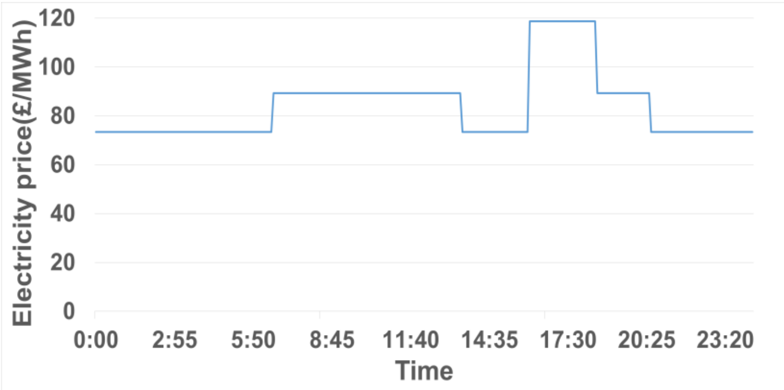

Fig. 5-6. The electricity price in one day.

For the SLB energy storage in this system, the capacity of the SLB storage is assumed as 1000 kWh. The maximum input power and output power is assumed as 200 kW and 220 kW. To protect the SLB from deep charging or discharging, the maximum SoC is assumed as 0.8 and the minimum SoC is assumed as 0.2. The efficiency of the battery charging and discharging to the grid is 0.9. The efficiency of the power from SLB to the EBs is assumed as 0.85. From the WPD flexibility service introduction [103], the fixed price of the secure flexibility service is £300/MWh. The requirements of the flexibility service for the coming day include: the required time duration is from 7.10 pm to 8.05 pm, the required delivered power is 110 kW.

To validate the feasibility of the proposed EB charging model, a comparison is taken between three different scenarios. In the first scenario, the EB charging station is operated based on a 'greedy charging' mode. The 'greedy charging' is to charge the EB as soon as its SoC does not reach the upper threshold. In this mode, the EB charging station is not equipped with SLB energy storage and the other limits of the EB and the charging station should also be satisfied.

In the second scenario, the EB charging station is not equipped with SLB storage. But the charging strategy will still follow the day-ahead scheduling model. The objective function of the optimization and the constraints are all the same as given before. The third scenario is the EB charging station with an SLB storage system.

To better compared with the three scenarios, for the three scenarios, the EBs of route 22 should be fully charged after finishing the whole day's work. For the U1 EBs, those who do not work at midnight should be charged to satisfy the next day's work. In Scenario 3, the SLB should be fully charged at the end of the day.

5.7.1. Scenario 1): the 'greedy charging' strategy for the EB charging station

As mentioned above, in Scenario 1, a 'greedy charging' charging algorithm is adopted for the EB charging. The simulation is taken on a weekday.

In this scenario, all of the charging power is from the grid supply. The power output for EB charging is shown in Fig. 5-7 and the number of charging EBs at each time slot is shown in Fig. 5-8.

From Fig. 5-7, the average power output at the midnight is 100.91 kW, the average power output of the first peak time is 522.27 kW and for the second peak time, it is 838.267 kW. For two off-peak times, the average power output is 777.32 kW and 649.19 kW respectively. From Fig. 5-8, with the 8 chargers for the EB charging station, there are 6 time slots when all the chargers are charging EBs, 3 in the peak time and 3 in the off-peak time.

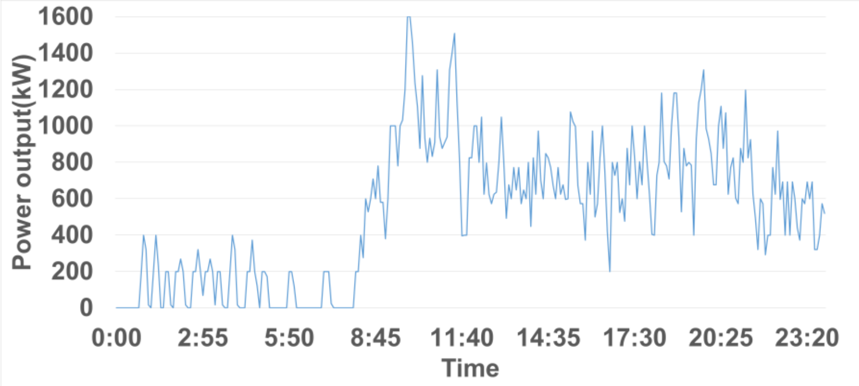

Fig. 5-7 The power of the EB charging station for charging services under 'greedy charging' algorithm.

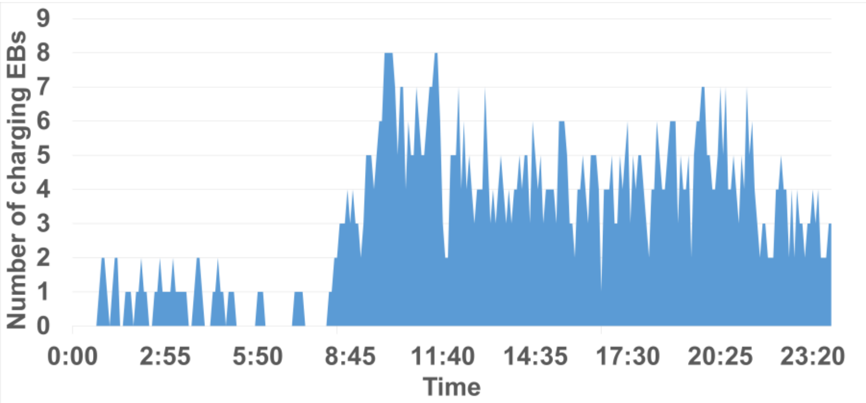

Fig. 5-8. The number of charging EBs on the day with 'greedy charging' algorithm.

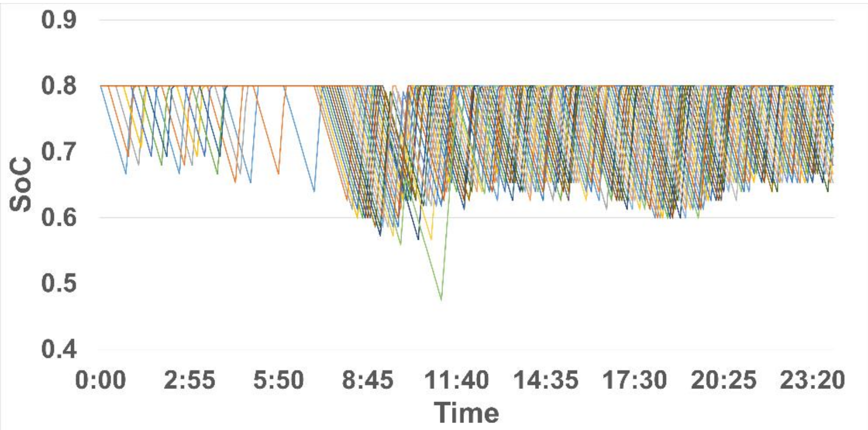

Fig. 5-9 The SoC of the EBs on the day under 'greedy charging' algorithm.

In Fig. 5-9, the SoC of the EBs under the ‘greedy charging’ algorithm is shown. The minimum SoC during the day is 0.47, which is much higher than the SoC lower limit. The trend of the SoC directly reflects the bus timetable at different time intervals. At the end of the day, except for the EBs which is in the travel, almost every EB is fully charged.

5.7.2. Scenario 2): the optimal control strategy for the EB charging station without SLB storage

For scenario 2, the control strategy is partly adopted the day-ahead scheduling. The difference is that there is no SLB energy storage. The chosen weekday is the same as that in scenario 1. The simulation results are shown below:

Fig. 5-10 and Fig. 5-11 show the power for EB charging and the number of charging EBs on the chosen day. In Fig. 5-10, the average charging power at the two peak time is 131.43 kW and 91.43 kW, while the average charging power at the two off-peak time is 677.65 kW and 1437.74 kW. From Fig. 5-11, the average number of charging EBs at the peak time is 0.5 and at the off-peak time, the average number is 5.3. There are 73 stages when there are 8 EBs are being charged. All of them is at the peak time and 30 of them is at the first peak time and 43 is during the second peak time.

Fig. 5-12. demonstrates the SoC of the EBs under the day-ahead scheduling without SLB energy storage. It shows that the SoC of the EB ranges from 0.21 to 0.8, which is more than that under the ‘greedy charging’ strategy. Furthermore, except for the beginning and the end of the day, the EBs is possible to be fully charged only during the first off-peak time, from 2.55 pm to 4.10 pm. Different from the EB SoC under ‘greedy charging’ in Fig. 5-9, the trend of the EB SoC reflects the different levels of the electricity price.

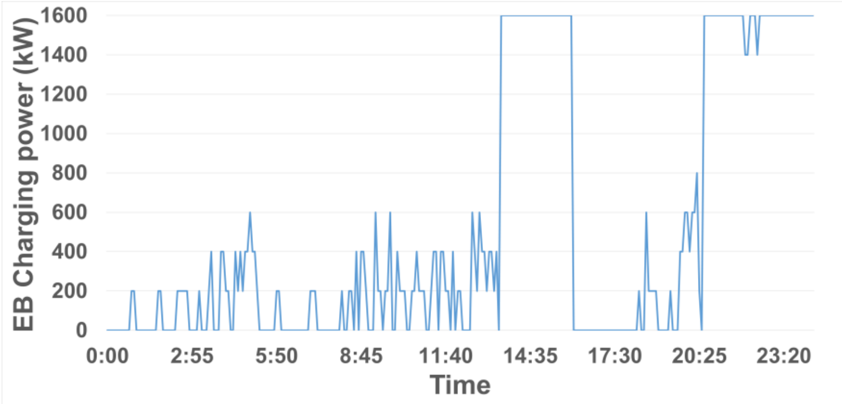

Fig. 5-10. The EB charging power under 'day-ahead scheduling' without SLB energy storage

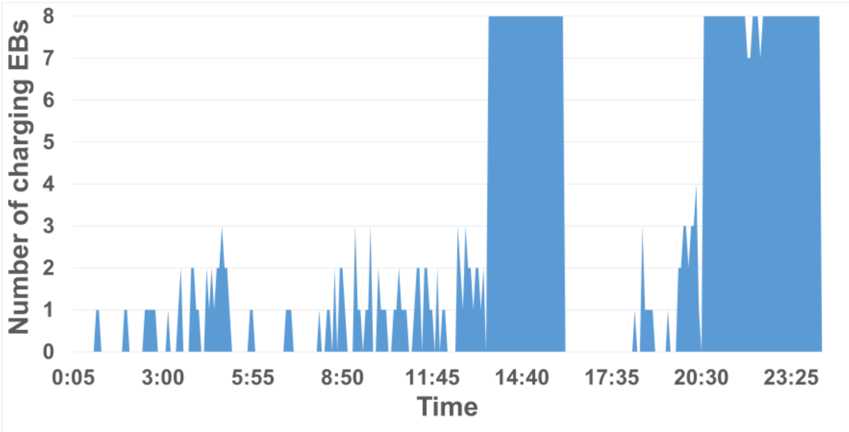

Fig. 5-11 The number of charging EBs under day-ahead scheduling without SLB energy storage.

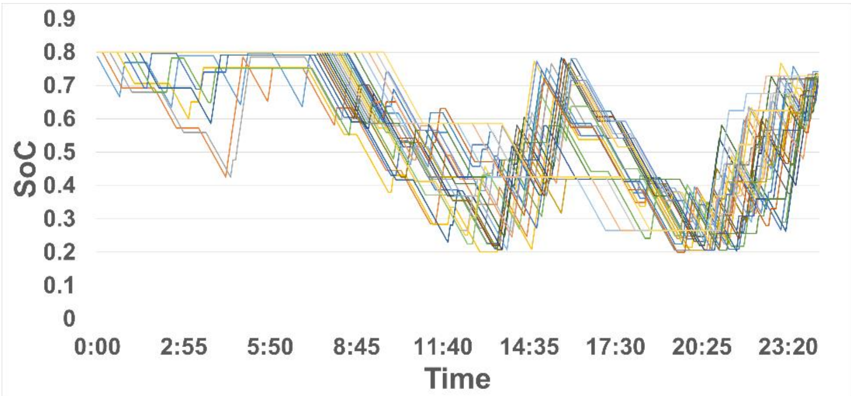

Fig. 5-12 The SoC of the EBs under day-ahead scheduling without SLB energy storage

5.7.3. Scenario 3): the optimal control strategy for the EB charging station with an SLB storage system

In the third scenario, the EB charging station adopts the ‘day-ahead’ scheduling and it is equipped with SLB energy storage. It is simulated on the same day as scenario 1 and scenario 2. The simulation results are shown as follows:

Fig. 5-13 and Fig. 5-14 show the charging power from the grid and the number of charging EBs at each time slot. Fig. 15 illustrates the change in EBs’ SoC. In Fig. 5-13, the average charging power from the grid is 172.22 kW, 654.76 kW, 126.32 kW and 1090.57 kW at the two peak-time intervals and the two off-peak time intervals respectively. The number of charging EBs at the four different time intervals are 0.9, 3.3, 0.5 and 5.6. However, in this scenario, the EB can also be charged from the SLB energy storage. The charging power from the energy storage is shown in Fig. 5-16. The figure shows that the SLB energy storage provides power for the EBs mostly between 9.35 am and 11.30 am. Additionally, from 5.50 pm to 7.30 pm, considering the high energy consumption during the peak time, the SLB provide energy for EBs but just satisfy their energy demand for the next travel. When it comes to the night, when the electricity price is low and the bus scheduling is not as frequent as the peak time, the EBs would rather purchase energy from the grid.

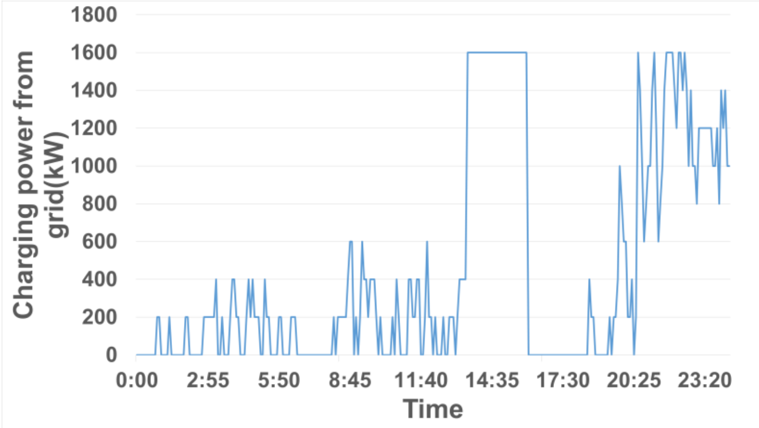

Fig. 5-13 The EB charging power from the network under ‘day-ahead scheduling’ with SLB energy storage.

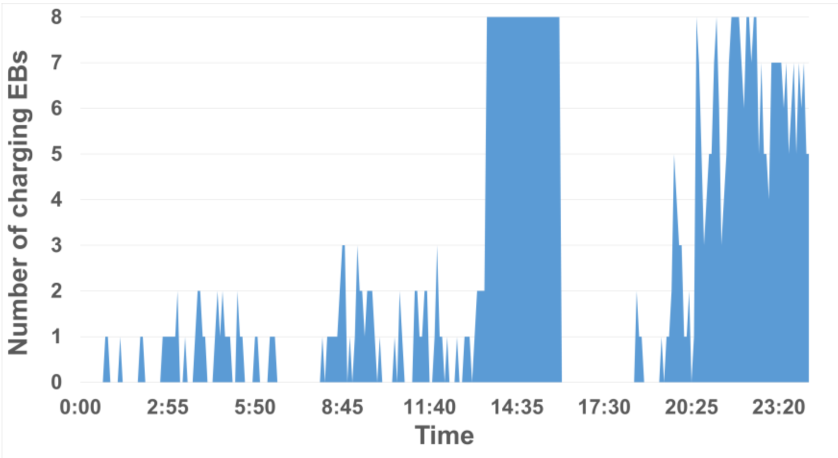

Fig. 5-14. The number of charging EBs under day-ahead scheduling with SLB energy storage.

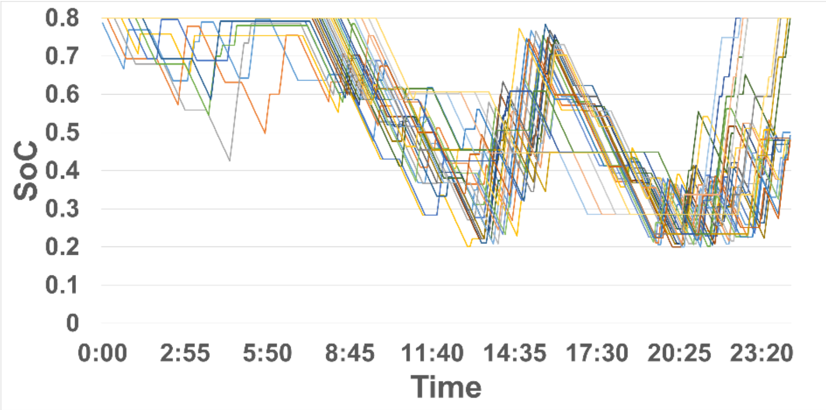

Fig. 5-15. The SoC of the EBs under day-ahead scheduling with SLB energy storage.

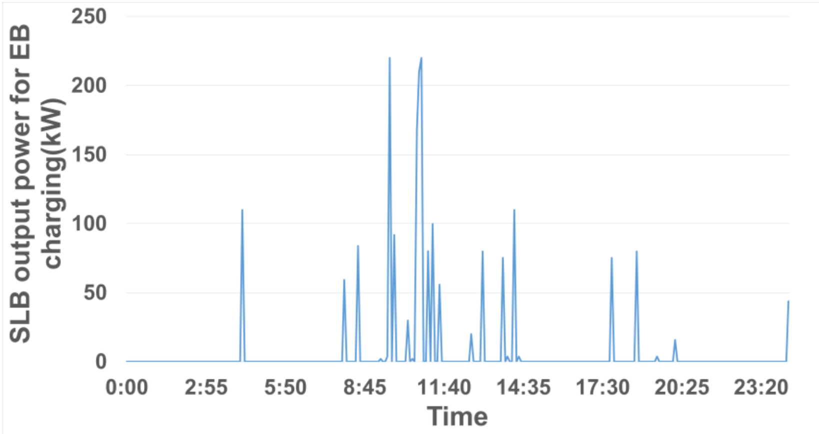

Fig. 5-16. The EB charging power from the SLB energy storage under 'day-ahead scheduling'.

5.7.4. The comparison of the energy cost of the three control algorithms

As mentioned above, the target of the EB charging optimization is minimizing the operational cost, including the energy purchase cost and the battery degradation cost. For the first two scenarios, the operational cost is the energy cost. The cost comparison is taken on 5 continuous working days. The simulation results of the cost are shown in Fig. 5-17.

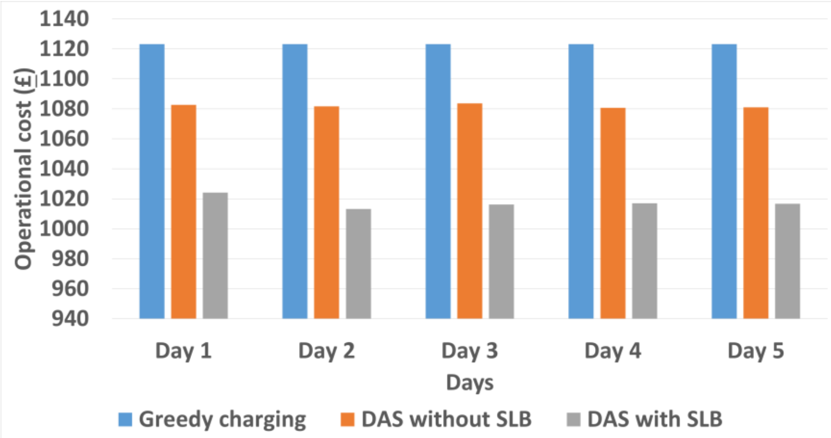

Fig. 5-17. The comparison of the operational cost in the three scenarios of 5 continuous days.

In Fig. 5-17, the operational cost of the EB charging station under the ‘greedy charging’ algorithm is £1123.13. The same operational cost is because, under the ‘greedy charging’ strategy, the EB will be charged if there are free chargers in the station, without considering the electricity price. The SoC of EBs keeps in the range of 0.4 to 0.8. Thus, when it reaches night, the EBs does not work as frequently as in the daytime and there is sufficient time for the EBs to be fully charged, except for those under business demands.

For scenario 2, the operational cost of the five days is £1082.67, £1081.67, £1083.34, £1080.43 and £1081.01 respectively. The cost reduction of scenario 2 compared with scenario 1 is on average £41.18. For scenario 3, the operational cost of the five days is £1024.10, £1013.27, £1016.16, £1017.06 and £1016.76. The cost reduction of this scenario is £64.48 compared with scenario 2 and £105.65 compared with scenario 1 on average. From the comparison of the three scenarios, the day-ahead scheduling with SLB energy storage can save more than 11% on the operational cost of the EB charging station.

5.7.5. Numerical results analysis

To validate the feasibility of adopting the ‘day-ahead scheduling’ with SLB energy storage to the EB charging station, the simulation results of the three scenarios under different control strategies are shown above. The discussion of the numerical results is given as follows:

The main difference between the ‘greedy charging’ algorithm and the ‘day-ahead scheduling’ is that the charging load of the former control algorithm is mainly at the two peak-time intervals of the day, which increases the difference in the load demand for the networks. While the ‘day-ahead scheduling’ controls the EBs to concentrate the charging demand on the off-peak time with the consideration of the capacity of the distribution transformer, it leads to high power demand during the two off-peak time.

The SoC of EBs in the first scenario varies from 0.4 to 0.8, while in the second and the third scenario, the SoC of EBs varies from 0.21 to 0.8. The difference in the SoC of EBs in the three scenarios is because: in the first scenario, the EB will be charged without considering the electricity price. The EBs can be charged at any time stage only if there are free chargers. In scenario 2 and scenario 3, the EBs will be charged with the consideration of different electricity prices at different time stages. Thus, with the ‘greedy charging’ control strategy, the EB battery suffers from a ‘shallow charging cycle’ mode and with the ‘day-ahead’ control strategy, the EB battery is under ‘deep charging cycle’ mode.
With the comparison of Fig. 5-6, Fig. 5-9 and Fig. 5-12, it is shown that all the chargers are adopted during the off-peak time under the ‘day-ahead scheduling’ strategy. This not only achieves the target of reducing operational cost but also achieve the peak shaving for the DNOs. The ‘day-ahead scheduling’ increases the energy efficiency and transfer

the energy benefit to economic benefits. With the ‘greedy charging’ control strategy, the working time of the charging machine is related to the EB timetable.

This paper proposes a ‘day-ahead’ control strategy for the EB charging station to guide its operation of the EB charging station. In real-time operation, the EB station will follow the given strategy. If an EB arrives late or its SoC is lower than the scheduled SoC, the SLB can be worked as a backup power to increase the charging rate and ensure that the EB will depart for the next travel with the scheduled SoC on time. For the control strategy without SLB storage, when the EB does not follow the scheduled model, it should report the difference to the bus operator and the operator will be determined whether the departure time will delay. The detailed steps of the real-time adjustment are not discussed in this paper.

With the comparison mentioned above, the ‘day-ahead scheduling’ strategy can significantly reduce the operational cost and achieve peak shaving by charging EBs mostly at the off-peak time. Furthermore, with the connection of SLB, the EB charging station can further avoid charging EB at the peak time by charging EBs with SLB energy storage and providing flexibility services for DNOs to enhance the grid.

5.8. Conclusions

This paper develops an optimal EB charging methodology for an EB charging station equipped with SLB energy storage. With the target of reducing the operational cost, a customized ‘day-ahead scheduling’ strategy is proposed to achieve the optimal charging control of the EB charging station, by controlling the charging power and the EB charging time. In this process, the SLB energy storage takes three roles: 1) the SLB can be charged during the off-peak time and support the charging of the EBs to reduce the charging demand during peak time; 2) the SLB is controlled to provide flexibility services for a DNO to relieve network congestions; 3) the SLB is regarded as a secondary source to increase the charging power for the EBs. The case study is performed, where three different control strategies are compared. Conclusions are presented as follows:

1) The 'day-ahead scheduling' control strategy can effectively reduce the operational cost by 11% for the EB charging station compared with the 'greedy charging' strategy, considering the constraints of the distribution transformer capacity and the bus timetable.

2) Through the day-ahead scheduling control strategy, the charging demand at the peak time is significantly reduced compared with the 'greedy charging'. It is very remarkable for the DNOs to reduce the load demand during the peak time and balance the network system.

3) The connection of the SLB energy storage system brings benefits to both the EB charging station and the distribution network. For the EB charging station, the energy purchased cost is further reduced by SLB providing charging power during the peak time, and the SLBs can directly make profits by providing flexibility services for DNOs. For the distribution network, with the SLB energy storage system, the charging demand will be reduced more during the peak time. In addition, the SLBs can participate in the flexibility services, which will support the network and reduce network congestion.

Chapter 6.
Conclusion

This chapter concludes the thesis by listing the contributions and findings from the studies.

With the target of zero carbon emission in the future, the development of EVs plays an important role in transportation electrification. However, there are a massive number of challenges that need to be addressed in this process, for example, the over-penetration of EVs to the network and the recycling of their retired batteries. The over-penetration of EVs to the grid is due to the uncontrolled EV charging behaviour and it will lead to network overloads, the reduction of power quality, an increase in network phase imbalance, and the increasing reinforcement investment for the DNOs. With the increase of EVs, they will bring a huge number of retired batteries eventually. However, directly splitting the battery module and recycling the materials is discarding the batteries' energy potential and reducing their economic efficiency. Nowadays, adopting retired batteries for a second life application is a better choice compared with traditional recycling. But some problems still exist in the application of SLB: how to set the pricing of SLBs which reflects their true value, which second life services they will take and the benefits of the SLB applications for their potential consumers.

This thesis makes intensive efforts to solve the two problems. For the EV penetration problems, the current studies mainly focus on the optimal control for domestic EVs, and the environment is always the parking lots. Few of them study the industrial/commercial EV control optimization. This thesis chooses the ASEVs as the research objects and proposes a dynamic model for the ASEVs. To optimally control the ASEVs and address the problems brought by the uncertainties, a customized near-optimal approach is proposed for the ASEV dynamics model.

For the SLBs, this thesis for the first time proposes a business model which is designed based on a monthly-payment model. Unlike the traditional business model, it is not necessary to pay more attention to the prediction of the SOH and the remaining life of the SLBs. The payment of each battery in this model will reflect the true value of each SLB based on its performance in the second life applications. Further, in this model, the

SLB is used to provide flexibility service for DNOs and perform energy arbitrage, which can make profits for the battery processers.

Finally, this thesis for the first time proposes that it is possible to adopt the SLB energy storage in the EV optimal control, which addresses the two problems in one scenario. This thesis develops an EB charging station control strategy with the participant with SLB energy storage. With the connection of the SLB energy storage, the EB charging station can not only further reduce the operational cost for the bus aggregators and the charging demand during the peak time but also provide flexibility services for the DNOs to support the networks.

The detailed conclusions of the thesis are summarised as follows:

- **The optimal control of ASEVs for reducing operational costs and matching the renewable generation in the airport.**

In this thesis, a novel dynamic model is proposed for ASEVs. To achieve the control optimisation of the ASEV model, a customized near-optimal approach, the rollout approach is designed to guide the management of the ASEVs. The dynamic model considers the uncertainties in the operation environment, including the arrival time and the departure time of flights, the load of the ground transport. To solve the problems, the rollout approach is designed based on two different heuristic algorithms which represent the underlying control strategies. To validate the feasibility of the dynamic ASEV model and the rollout algorithm, two case studies compare the rollout approach with a benchmark algorithm (‘greedy charging’ in this case study) in a winter month and a summer month. The differences between the two seasons include the different flight information and the different PV generation. The key findings from the comparison of the two scenarios are shown as follows:

- In both the winter month and the summer month, the performance of the rollout approach is better than that of the greedy charging approach. In the two scenarios, with the rollout approach, the total operational cost can be reduced by more than 10% compared with the ‘greedy charging’ strategy.
- Among all the types of cost, the rollout algorithm mainly focuses on the reduction of the energy cost, which will reduce 50% of the cost compared with the ‘greedy charging’ algorithm. Unlike the energy cost, the battery degradation of the ASEVs with the ‘greedy charging’ algorithm is approximately 11% lower than that with the rollout approach. With the development of EV batteries, battery degradation costs can be reduced in the future.
- The research outcome helps develop the transportation electrification for the airports. With the ASEV model and the customized rollout control algorithm, the total operational cost of the ASEVs will be reduced and the renewable generation will be efficiently adopted. Further, reducing the charging demand during the peak time will make the EV charging friendly to the network.

- **SLB monthly-payment business model**

This thesis develops an SLB business model based on the monthly-payment model. The business model aims to make benefits for both the battery processer and the battery providers (EV owners in this research). The business model does not predict the accurate remaining life and SOH of the SLBs for their potential second-life applications. The battery processer will share the profits monthly with the EV owners based on their contributions. In this model, the SLBs are controlled to provide flexibility services for the DNOs and perform energy arbitrage. The flexibility services consist of two different types: the critical flexibility service, including the dynamic service and the restore service, and the non-critical flexibility service, including the secure service. To validate the feasibility of the business model, a 10-year simulation is taken to check the degradation of the

SLBs, the performance of the SLBs on energy arbitrage and flexibility services, and the profits of the model. There are two different scenarios for the case studies: In the first scenario, the SLBs will not be replaced individually until the SLB matrix can not work. In the second one, the SLBs will be replaced individually as soon as the SOH drops to the threshold. Several key findings from the studies are summarised as follows:

- With the business model, the SLB can make profits in the two scenarios. In the first scenario, the profits in 10 years are £2,648,782, while in the second scenario the profits are £3,433,247. The profits are from the energy arbitrage service and the flexibility services. For both two scenarios, the profits from the flexibility services account more compared with performing energy arbitrage. The profits from the flexibility services account for over 85% in the two scenarios.
- The two scenarios represent two different battery replacement modes. For the first scenario, the advantage of it is that with the battery matrix replaced as a whole, the computational complexity is reduced without partially replacing the SLBs. For the second scenario, the advantage is that the incoming SLBs will replace those reaching their end-of-life directly. It respects the metabolism nature of the business.
- The case studies have proved the economic potential of the SLB business model. With the SLB business model, those retired EV batteries with enough energy potential can be adopted to perform energy arbitrage and provide flexibility services for DNOs. In general, the SLB business model improves the energy and economic efficiency of the SLBs.

- **Optimal control of EB charging station cooperated with SLB energy storage system**

This paper develops an EB charging station model with the SLB energy storage system participating. In this model, a 'day-ahead scheduling' algorithm is adopted to manage the

EB charging station. The 'day-ahead scheduling' algorithm is designed based on historical and statistical data. To address the uncertainties, e.g. the EB arriving time and the arriving SoC, an SAA stochastic programming is applied in the management system. To validate the feasibility of the system, case studies show the comparison between three different scenarios with different control strategies. The key findings are summarised as follows:

- Compared with the 'greedy charging' strategy, the 'day-ahead scheduling' will reduce the charging demand during the peak time, which can relieve the gird congestions for DNOs. For the EB aggregators, the 'day-ahead scheduling' will efficiently reduce the operational cost considering the transformer capacity and ensuring that all the EB departures are on time.
- For the EB charging station, with the SLB being connected to the EB charging station, the operational cost will be reduced more compared with that without the SLB storage system. Furthermore, the EB charging station will provide flexibility services for the DNOs to support the network.
- In these case studies, the SLBs can be directly from the retired batteries. This significantly reduces the difficulties in the process of SLB collection. Meanwhile, the EB retired batteries can be adopted in an appropriate second-life application, which increases the energy and economic efficiency of the batteries.

In general, this thesis firstly helps control the ASEV charging with a novel dynamic model and a customized rollout approach. Secondly, a proposed business model for SLBs will guide the battery processers to develop the energy and economic potential of the SLBs and make profits through suitable applications, like performing energy arbitrage and providing flexibility services. Thirdly, the thesis proposes to utilize the SLB energy storage system in the EB charging station. The EB control strategy is further developed with the connection of SLB energy storage. Relatively, the energy and economic potential of the

SLBs are improved by participating in the EB optimal control process. With the study outcomes, the problems of EB optimal charging and the application of retired batteries would be solved in one scenario.

Chapter 7.

Future work

This chapter presents future works that can be done to further improve the EV control optimisation and the application of SLBs.

In this thesis, to help the development of EVs, previous chapters have reviewed the existing studies and proposed feasible solutions for ASEV dynamic control and SLB business model; and developed an EB charging station model to utilize the SLB energy storage for EB charging strategies. This chapter focuses on the potential future work on the optimal control of EV charging and the application of SLBs, which are not discussed in this thesis but have the potential to improve transportation electrification.

- **The control strategy of EV charging with the consideration of renewable energy generation**

Nowadays, renewable generation is widely connected to networks and provide clean energy to reduce carbon emission. In the UK, wind power and PV generation are the two most popular renewable energy resources for DNOs. In the future smart grid, for EV charging, renewable generation will become an important power supplier. However, the connection of PV generation or wind power generation will bring several challenges:

- The output power of renewable energy is uncertain and difficult to make an accurate prediction. Such power will be significantly affected by the environment, such as the sunshine intensity, the temperature, and the humidity. It leads to huge uncertainties in the process of EV charging management.
- With the renewable energy system, it is necessary for the system to be equipped with an energy storage system. Thus, the initial investment will increase and it requires that the energy and economic efficiency of the energy management system (EMS) should be higher.
- For the energy storage system, the batteries are the most popular storage in the smart grid. The battery degradation is supposed to be considered when making the control strategy for EV charging.

To address these challenges, future work should firstly propose stochastic programming for renewable energy. Then the battery degradation model needs to be developed based on the existing studies. Furthermore, the control strategy should help both the planning and the real-time operation. The objective of the control strategy should include reducing the operational cost, improving the energy efficiency of renewable energy, and enhancing the lifetime of the batteries.

- **Proposing a control strategy for SLB applications considering the battery longevity**

With the proposed business model and potential second life applications, retired batteries will improve their economy and energy efficiency. However, like the new batteries, the battery ageing should be mitigated, and a relative control strategy needs to be proposed. In the process, there are several challenges and constraints which should be considered:

- As mentioned in Chapter. 4, the degradation of the battery can be sorted into two different types: calendar ageing and cycling ageing. The two degradation models are different and both of them should be considered in the SLB model.
- With the two different degradation types, there are many factors that will affect the lifetime of the SLBs. It is necessary to consider all of these factors and make reasonable assumptions.
- The objective function of the problem contains at least two different parts: Firstly, the SLB should make benefits the potential consumers. Secondly, the control strategy should extend the lifespan of the SLBs compared with some existing methods without affecting the performance of the second-life applications.

To address these challenges, firstly, future work needs to propose a battery degradation model, which can directly reflect the calendar ageing and the cycling ageing for the SLBs. Secondly, although there are several different factors that will influence battery degradation, the number of optimization variables should be limited to no more than three. Thus, sensitivity analysis should be made to determine which factors can be set as the optimization variables. Finally, the control algorithm should be designed to solve the multi-objective optimisation problem with several variables.

- **Applying V2G service for the industrial/commercial EVs**

In Chapter. 3 and Chapter. 5, the control optimisation of ASEV and EB charging will help relieve the network congestion for the DNOs by reducing the charging load during the peak time. In Chapter. 4 and Chapter. 5, the SLB system is designed to provide flexibility services for DNOs to support the distribution network. Nowadays, the V2G service is another important grid service for the power system. Compared with domestic EVs, commercial/industrial EVs are equipped with large-capacity batteries, which means that commercial/industrial EVs can provide more energy capacity. Also, these EVs are mostly controlled based on centralized control strategies. It leads to more optimisation space for the operators. However, it is necessary to address some challenges from V2G services:

- For the commercial/industrial EVs, it is prior to satisfying the business demands they need to take. They can only provide V2G service during the parking time at the charging station. Thus, it is necessary to balance the time for V2G services and EV charging.
- For the V2G service, one of the major concerns is that it will reduce the lifespan of EV batteries by increasing the charging-discharging cycles. For commercial/industrial EVs, the cost of their batteries is higher than the domestic EV

batteries. In the energy management system, it is essential to consider the EV battery degradation in the optimisation model.

- Chapter. 3 mentioned that uncertainties exist in the ASEV model and they will deeply affect the EV state control. Similarly, these uncertainties will also significantly affect the performance of the V2G service. In the control strategy, stochastic programming or a suitable prediction method should be adopted to address these uncertainties.

To overcome these challenges, future work should contain an EV model which describes the state control, an EV battery model which can demonstrate the battery degradation caused by the V2G service, a V2G service model, and a customized control strategy. The control strategy is required to make the optimal decisions with the updated information of constraints in real-time operation. The objective of the optimisation problem should consider not only the economic benefits for the EV owners or the favour to the network but also developing a protective strategy for the EV batteries.

Reference

[1] European Environment Agency, "Electric Vehicles and the Energy Sector - Impacts on Europe's Future Emissions," 2021. [Online].

[2] Climate Change Committee, "Reaching Net Zero in the UK," 2021, [Online].

[3] European Environment Agency, "New Registrations of Electric Vehicles in Europe," 2021, [Online]. Available: https://www.eea.europa.eu/ims/new-registrations-of-electric-vehicles

[4] European Commission, "European Green Deal: Commission Proposes Transformation of EU Economy and Society to Meet Climate Ambitions," 2021.

[5] UK Government, "Transport and Environment Statistics 2021 Annual Report," 2021.

[6] House of Commons Library, "Electric Vehicles and Infrastructure," 2021.

[7] HM Government, "Transitioning to Zero Emission Cars and Vans: 2035 Delivery Plan. " 2021.

[8] HM Government, "Net Zero Strategy: Build Back Greener. " 2021.

[9] Climate Change Committee, "2021 Progress Report to Parliament," 2021.

[10] M. J. David Stringer. "Where 3 Million Electric Vehicle Batteries Will Go When They Retire," 2021, [Online].Available: https://www.bloombergquint.com/technology/where-3-million-electric-vehicle-batteries-will-go-when-they-retire.

[11] G. Harper, et al., "Recycling Lithium-ion Batteries from Electric Vehicles," Nature, vol. 575, no. 7781, pp. 75-86, 2019/11/01 2019, doi: 10.1038/s41586-019-1682-5.

[12] Energy Saving Trust. "Smart Charging for Electric Vehicles," 2021, [Online]. Available: https://energysavingtrust.org.uk/advice/smart-charging-electric-vehicles/.

[13] Y. U. Fumiko Koyanagi, "A Strategy of Load Leveling by Charging and

Discharging Time Control of Electric ehicles " IEEE Transactions on Power Systems.

[14] A. Ghavami, K. Kar, and A. Gupta, "Decentralized Charging of Plug-in Electric Vehicles With Distribution Feeder Overload Control," IEEE Transactions on Automatic Control, vol. 61, no. 11, pp. 3527-3532, 2016, doi: 10.1109/TAC.2016.2516240.

[15] N. I. Nimalsiri, C. P. Mediwaththe, E. L. Ratnam, M. Shaw, D. B. Smith, and S. K. Halgamuge, "A Survey of Algorithms for Distributed Charging Control of Electric Vehicles in Smart Grid," IEEE Transactions on Intelligent Transportation Systems, vol. 21, no. 11, pp. 4497-4515, 2020, doi: 10.1109/TITS.2019.2943620.

[16] R. Shi, S. Semsar, and P. W. Lehn, "Constant Current Fast Charging of Electric Vehicles via a DC Grid Using a Dual-Inverter Drive," IEEE Transactions on Industrial Electronics, vol. 64, no. 9, pp. 6940-6949, 2017, doi: 10.1109/tie.2017.2686362.

[17] D. B. Wickramasinghe Abeywardana, P. Acuna, B. Hredzak, R. P. Aguilera, and V. G. Agelidis, "Single-Phase Boost Inverter-Based Electric Vehicle Charger With Integrated Vehicle to Grid Reactive Power Compensation," IEEE Transactions on Power Electronics, vol. 33, no. 4, pp. 3462-3471, 2018, doi: 10.1109/tpel.2017.2700944.

[18] S. Muthusamy, N. Senthilnathan, A. M. Monnisha, V. KamaleshKumar, K. Srinivasan, and P. Sundari, "Measurement and Analysis of Power Quality Issues Due to Electric Vehicle Charger," IOP Conference Series: Materials Science and Engineering, vol. 1055, p. 012131, 02/01 2021, doi: 10.1088/1757-899X/1055/1/012131.

[19] G. Sharma and V. Sood, "Power Quality Problems in Grid-Connected Electric Vehicle (EV) Fast Charging Stations," 2021, pp. 11-27.

[20] T. Zhang, H. Pota, C.-C. Chu, and R. Gadh, "Real-time Renewable Energy Incentive System for Electric Vehicles Using Prioritization and Cryptocurrency," Applied Energy, vol. 226, pp.

[21] J. Zheng, X. Wang, K. Men, C. Zhu, and S. Zhu, "Aggregation Model-Based Optimization for Electric Vehicle Charging Strategy," IEEE Transactions on Smart Grid, vol. 4, no. 2, pp. 1058-1066, 2013, doi: 10.1109/TSG.2013.2242207.

[22] P. Aliasghari, B. Mohammadi-Ivatloo, M. Alipour, M. Abapour, and K. Zare,

"Optimal Scheduling of Plug-in Electric Vehicles and Renewable Micro-grid in Energy and Reserve Markets Considering Demand Response Program," Journal of Cleaner Production, vol. 186, pp.

[23] L. Jian, Y. Zheng, X. Xiao, and C. C. Chan, "Optimal Scheduling for Vehicle-to-grid Operation with Stochastic Connection of Plug-in Electric Vehicles to Smart Grid," Applied Energy, vol. 146, pp.

[24] D. Wu, H. Zeng, C. Lu, and B. Boulet, "Two-Stage Energy Management for Office Buildings With Workplace EV Charging and Renewable Energy," IEEE Transactions on Transportation Electrification, vol. 3, no. 1, pp. 225-237, 2017, doi: 10.1109/tte.2017.2659626.

[25] A. Y. S. Lam, Y. W. Leung, and X. Chu, "Electric Vehicle Charging Station Placement: Formulation, Complexity, and Solutions," IEEE Transactions on Smart Grid, vol. 5, no. 6, pp. 2846-2856, 2014, doi: 10.1109/TSG.2014.2344684.

[26] F. Pan, R. Bent, A. Berscheid, and D. Izraelevitz, "Locating PHEV Exchange Stations in V2G," in 2010 First IEEE International Conference on Smart Grid Communications, 4-6 Oct. 2010 2010, pp. 173-178, doi: 10.1109/SMARTGRID.2010.5622037.

[27] B. Han, S. Lu, F. Xue, L. Jiang, and H. Zhu, "A Two-stage Electric Vehicles Scheduling Strategy to Address Economic Inconsistency Issues of Stakeholders," in 2017 IEEE Intelligent Vehicles Symposium (IV), 11-14 June 2017 2017, pp. 1904-1909, doi: 10.1109/IVS.2017.7995983.

[28] Z. Hu, K. Zhan, H. Zhang, and Y. Song, "Pricing Mechanisms Design for Guiding Electric Vehicle Charging to Fill Load Valley," Applied Energy, vol. 178, pp.

[29] Z. Ma, D. S. Callaway, and I. A. Hiskens, "Decentralized Charging Control of Large Populations of Plug-in Electric Vehicles," IEEE Transactions on Control Systems Technology, vol. 21, no. 1, pp. 67-78, 2013, doi: 10.1109/TCST.2011.2174059.

[30] M. Pilát, "Controlling the Charging of Electric Vehicles with Neural Networks," in 2018 International Joint Conference on Neural Networks (IJCNN), 8-13 July 2018 2018, pp. 1-8, doi: 10.1109/IJCNN.2018.8489027.

[31] E. B. Iversen, J. M. Morales, and H. Madsen, "Optimal Charging of An Electric Vehicle Using a Markov Decision Process," Applied Energy, vol. 123, pp.

[32] L. Gan, U. Topcu, and S. H. Low, "Optimal Decentralized Protocol for Electric Vehicle Charging," IEEE Transactions on Power Systems, vol. 28, no. 2, pp. 940-951, 2013, doi: 10.1109/TPWRS.2012.2210288.

[33] A. Ghavami, K. Kar, S. Bhattacharya, and A. Gupta, "Price-driven Charging of Plug-in Electric Vehicles: Nash Equilibrium, Social Optimality and Best-response Convergence," in 2013 47th Annual Conference on Information Sciences and Systems (CISS), 20-22 March 2013 2013, pp. 1-6, doi: 10.1109/CISS.2013.6552326.

[34] Z. Ma, S. Zou, and X. Liu, "A Distributed Charging Coordination for Large-Scale Plug-In Electric Vehicles Considering Battery Degradation Cost," IEEE Transactions on Control Systems Technology, vol. 23, no. 5, pp. 2044-2052, 2015, doi: 10.1109/TCST.2015.2394319.

[35] P. Richardson, D. Flynn, and A. Keane, "Local Versus Centralized Charging Strategies for Electric Vehicles in Low Voltage Distribution Systems," IEEE Transactions on Smart Grid, vol. 3, no. 2, pp. 1020-1028, 2012, doi: 10.1109/TSG.2012.2185523.

[36] N. G. Paterakis, O. Erdinc, I. N. Pappi, A. G. Bakirtzis, and J. P. S. Catalao, "Coordinated Operation of a Neighborhood of Smart Households Comprising Electric Vehicles, Energy Storage and Distributed Generation," IEEE Transactions on Smart Grid, vol. 7, no. 6, pp. 2736-2747, 2016, doi: 10.1109/tsg.2015.2512501.

[37] O. Erdinc, N. G. Paterakis, T. D. P. Mendes, A. G. Bakirtzis, and J. P. S. Catalao, "Smart Household Operation Considering Bi-Directional EV and ESS Utilization by Real-Time Pricing-Based DR," IEEE Transactions on Smart Grid, vol. 6, no. 3, pp. 1281-1291, 2015, doi: 10.1109/tsg.2014.2352650.

[38] "Guide to EV charging," 2019, [Online]. Available: https://www.zap-map.com/charge-points/.

[39] A. Ito, A. Kawashima, T. Suzuki, S. Inagaki, T. Yamaguchi, and Z. Zhou, "Model Predictive Charging Control of In-Vehicle Batteries for Home Energy Management Based on Vehicle State Prediction," IEEE Transactions on Control Systems Technology, vol. 26, no. 1, pp. 51-64, 2018, doi: 10.1109/TCST.2017.2664727.

[40] N. Rahbari-Asr and M. Chow, "Cooperative Distributed Demand Management for Community Charging of PHEV/PEVs Based on KKT Conditions and Consensus

Networks," IEEE Transactions on Industrial Informatics, vol. 10, no. 3, pp. 1907-1916, 2014, doi: 10.1109/TII.2014.2304412.

[41] L. Zhang and Y. Li, "Optimal Management for Parking-Lot Electric Vehicle Charging by Two-Stage Approximate Dynamic Programming," IEEE Transactions on Smart Grid, vol. 8, no. 4, pp. 1722-1730, 2017, doi: 10.1109/TSG.2015.2505298.

[42] M. Rastegar, M. Fotuhi-Firuzabad, H. Zareipour, and M. Moeini-Aghtaieh, "A Probabilistic Energy Management Scheme for Renewable-Based Residential Energy Hubs," IEEE Transactions on Smart Grid, vol. 8, no. 5, pp. 2217-2227, 2017, doi: 10.1109/TSG.2016.2518920.

[43] C. Yang, W. Lou, J. Yao, and S. Xie, "On Charging Scheduling Optimization for a Wirelessly Charged Electric Bus System," IEEE Transactions on Intelligent Transportation Systems, vol. 19, no. 6, pp. 1814-1826, 2018, doi: 10.1109/TITS.2017.2740329.

[44] S. S. G. Perumal, T. Dollevoet, D. Huisman, R. M. Lusby, J. Larsen, and M. Riis, "Solution Approaches for Integrated Vehicle and Crew Scheduling with Electric Buses," Computers & Operations Research, vol. 132, p.

[45] T. Liu and A. Ceder, "Battery-electric Transit Vehicle Scheduling with Optimal Number of Stationary Chargers," Transportation Research Part C: Emerging Technologies, vol. 114, pp.

[46] E. Yao, T. Liu, T. Lu, and Y. Yang, "Optimization of Electric Vehicle Scheduling with Multiple Vehicle Types in Public Transport," Sustainable Cities and Society, vol. 52, p.

[47] L. Cilio and O. Babacan, "Allocation Optimisation of Rapid Charging Stations in Large Urban Areas to Support Fully Electric Taxi Fleets," Applied Energy, vol. 295, p. 117072, 08/01 2021, doi: 10.1016/j.apenergy.2021.117072.

[48] Y. Wang, W. Ding, L. Huang, Z. Wei, H. Liu, and J. A. Stankovic, "Toward Urban Electric Taxi Systems in Smart Cities: The Battery Swapping Challenge," IEEE Transactions on Vehicular Technology, vol. 67, no. 3, pp. 1946-1960, 2018, doi: 10.1109/tvt.2017.2774447.

[49] H. Song, M. Cai, J. Cen, C. Xu, and Q. Zeng, "Research on Energy Saving Optimization Method of Electric Refrigerated Truck Based on Genetic Algorithm," International Journal of Refrigeration, 2022/02/05/ 2022, doi:

[50] M. H. S. M. Haram, J. W. Lee, G. Ramasamy, E. E. Ngu, S. P. Thiagarajah, and Y. H. Lee, "Feasibility of Utilising Second Life EV Batteries: Applications, Lifespan, Economics, Environmental Impact, Assessment, and Challenges," Alexandria Engineering Journal, vol. 60, no. 5, pp.

[51] I. Mathews, B. Xu, W. He, V. Barreto, T. Buonassisi, and I. M. Peters, "Technoeconomic Model of Second-life Batteries for Utility-scale Solar Considering Calendar and Cycle Aging," Applied Energy, vol. 269, p.

[52] H. Rallo, G. Benveniste, I. Gestoso, and B. Amante, "Economic Analysis of the Disassembling Activities to the Reuse of Electric Vehicles Li-ion Batteries," Resources, Conservation and Recycling, vol. 159, p.

[53] B. Sanghai, D. Sharma, K. Baidya, and M. Raja, "Refurbished and Repower: Second Life of Batteries from Electric Vehicles for Stationary Application," SAE Technical Paper, 0148-7191, 2019.

[54] G. Dong, Z. Chen, J. Wei, and Q. Ling, "Battery Health Prognosis Using Brownian Motion Modeling and Particle Filtering," IEEE Transactions on Industrial Electronics, vol. 65, no. 11, pp. 8646-8655, 2018, doi: 10.1109/TIE.2018.2813964.

[55] H. Li, D. Pan, and C. L. P. Chen, "Intelligent Prognostics for Battery Health Monitoring Using the Mean Entropy and Relevance Vector Machine," IEEE Transactions on Systems, Man, and Cybernetics: Systems, vol. 44, no. 7, pp. 851-862, 2014, doi: 10.1109/TSMC.2013.2296276.

[56] Y. Ma, L. Wu, Y. Guan, and Z. Peng, "The Capacity Estimation and Cycle Life Prediction of Lithium-ion Batteries Using a New Broad Extreme Learning Machine Approach," Journal of Power Sources, vol. 476, p.

[57] J. Hong, D. Lee, E.-R. Jeong, and Y. Yi, "Towards the Swift Prediction of the Remaining Useful Life of Lithium-ion Batteries with End-to-end Deep Learning," Applied Energy, vol. 278, p.

[58] W. C. Lih, J. H. Yen, F. H. Shieh, and Y. M. Liao, "Second Use of Retired Lithium-ion Battery Packs from Electric Vehicles: Technological Challenges, Cost Analysis and Optimal Business Model," in 2012 International Symposium on Computer, Consumer and Control, 4-6 June 2012 2012, pp. 381-384, doi: 10.1109/IS3C.2012.103.

[59] N. Jiao and S. Evans, "Business Models for Repurposing a Second-Life for Retired Electric Vehicle Batteries," in Behaviour of Lithium-Ion Batteries in

Electric Vehicles: Battery Health, Performance, Safety, and Cost, G. Pistoia and B. Liaw Eds. Cham: Springer International Publishing, 2018, pp. 323-344.

[60] Indira. M S, "Optimised Business Model for Effective Charging of Batteries in Electric Vehicles, " 2021.

[61] House of Parliament, "Electric Vehicles", 2010, [Online].

[62] C. Lin, D. Deng, C. Kuo, and Y. Liang, "Optimal Charging Control of Energy Storage and Electric Vehicle of an Individual in the Internet of Energy With Energy Trading," IEEE Transactions on Industrial Informatics, vol. 14, no. 6, pp. 2570-2578, 2018, doi: 10.1109/TII.2017.2782845.

[63] X. Wu, X. Hu, X. Yin, and S. J. Moura, "Stochastic Optimal Energy Management of Smart Home With PEV Energy Storage," IEEE Transactions on Smart Grid, vol. 9, no. 3, pp. 2065-2075, 2018, doi: 10.1109/TSG.2016.2606442.

[64] M. Shafie-khah et al., "Optimal Behavior of Electric Vehicle Parking Lots as Demand Response Aggregation Agents," IEEE Transactions on Smart Grid, vol. 7, no. 6, pp. 2654-2665, 2016, doi: 10.1109/TSG.2015.2496796.

[65] M. Maigha and M. L. Crow, "A Transactive Operating Model for Smart Airport Parking Lots," IEEE Power and Energy Technology Systems Journal, vol. 5, no. 4, pp. 157-166, 2018, doi: 10.1109/JPETS.2018.2876453.

[66] M. Muratori et al., "Technology Solutions to Mitigate Electricity Cost for Electric Vehicle DC Fast Charging," Applied Energy, vol. 242, pp.

[67] K. Seddig, P. Jochem, and W. Fichtner, "Two-stage Stochastic Optimization for Cost-minimal Charging of Electric Vehicles at Public Charging Stations with Photovoltaics," Applied Energy, vol. 242, pp.

[68] S. K. Moon and J. O. Kim, "Balanced Charging Strategies for Electric Vehicles on Power Systems," Applied Energy, vol. 189, pp.

[69] M. Weiszer, J. Chen, and G. Locatelli, "An Integrated Optimisation Approach to Airport Ground Operations to Foster Sustainability in the Aviation Sector," Applied Energy, vol. 157, pp.

[70] X. Li, O. Omotere, L. Qian, and E. R. Dougherty, "Review of Stochastic Hybrid Systems with Applications in Biological Systems Modeling and Analysis," EURASIP journal on bioinformatics & systems biology, vol. 2017, no. 1, pp. 8-8,

2017, doi: 10.1186/s13637-017-0061-5.

[71] "Bradshaw Electric Vehicles," 2021, [Online]. Available: https://www.airport-suppliers.com/supplier/bradshaw-electric-vehicles/ .

[72] "Smith Electric Vehicles," 2020, [Online]. Available: https://www.airport-technology.com/contractors/groundequipment/smith-electric/ .

[73] "Alke Electric Vehicles," 2020, [Online]. Available: https://www.alke.com/doc/alke-atx-electric-vehicles-catalog-eng.pdf .

[74] D. P. Bertsekas, Dynamic Programming and Optimal Control, 4th ed. Athena Scientific, 2017.

[75] R. S. Sutton and A. G. Barto, Reinforcement Learning An Introduction, 2nd ed. The MIT Press, 2017.

[76] J. Burkardt, "The Truncated Normal Distribution," Florida State University, , 2014. [Online].

[77] C. Bordin, H. O. Anuta, A. Crossland, I. L. Gutierrez, C. J. Dent, and D. Vigo, "A Linear Programming Approach For Battery Degradation Analysis and Optimization In Offgrid Power Systems with Solar Energy Integration," Renewable Energy, vol. 101, pp.

[78] "Bristol Airport Arrivals and Departures," 2019, [Online]. Available: https://www.bristolairport.co.uk/arrivals-and-departures/arrivals.

[79] "Weather & Local Environment," 2020, [Online]. Available: http://www.uq.edu.au/solarenergy/pv-array/weather.

[80] "Live Monitoring of the UK Electricity National Grid," 2019, [Online]. Available: http://gridwatch.co.uk/.

[81] "Understanding Electric Car Charging," 2020, [Online]. Available: https://www.spiritenergy.co.uk/kb-ev-understanding-electric-car-charging.

[82] X. Zhang, Y. Yuan, L. Hua, Y. Cao, and K. Qian, "On Generation Schedule Tracking of Wind Farms With Battery Energy Storage Systems," IEEE Transactions on Sustainable Energy, vol. 8, no. 1, pp. 341-353, 2017, doi: 10.1109/TSTE.2016.2598823.

[83] "Electric Car Boom in Europe Starts This Year," 2020, [Online]. Available: https://pushevs.com/2019/01/28/electric-car-boom-in-europe-starts-this-year/ .

[84] "UK Battery Storage Startup Connected Energy Secures £1.2M," 2021, [Online]. Available: https://www.uktech.news/news/uk-battery-storage-startup-connected-energy-funding-20210112.

[85] "Sustainability Assessment of Second Life Application of Automotive Batteries (SASLAB)," 2018, [Online].

[86] European Commission, "Green Deal: Sustainable Batteries for a Circular and Climate Neutral Economy," 2020.

[87] "Lithium-ion Batteries: Changes to the EU Batteries Directive," 2020, [Online]. Available: https://roskill.com/news/lithium-ion-batteries-changes-to-the-eu-batteries-directive/.

[88] H. Rallo, L. Canals Casals, D. Torre, R. Reinhardt, C. Marchante, and B. Amante, "Lithium-ion Battery 2nd Life Used as a Stationary Energy Storage System: Ageing and Economic Analysis in Two Real Cases," Journal of Cleaner Production, vol. 272, p. 122584, 07/01 2020, doi: 10.1016/j.jclepro.2020.122584.

[89] T. Steckel, A. Kendall, and H. Ambrose, "Applying Levelized Cost of Storage Methodology to Utility-scale Second-life Lithium-ion Battery Energy Storage Systems," Applied Energy, vol. 300, p.

[90] Y. Deng, Y. Zhang, and F. Luo, "Operational Planning of Centralized Charging Stations Using Second-Life Battery Energy Storage Systems," IEEE Transactions on Sustainable Energy, vol. PP, pp. 1-1, 06/09 2020, doi: 10.1109/TSTE.2020.3001015.

[91] C. White, B. Thompson, and L. Swan, "Repurposed Electric Vehicle Battery Performance in Second-life Electricity Grid Frequency Regulation Service," Journal of Energy Storage, vol. 28, p. 101278, 04/01 2020, doi: 10.1016/j.est.2020.101278.

[92] D. Strickland, L. Chittock, D. Stone, M. Foster, and B. Price, "Estimation of Transportation Battery Second Life for Use in Electricity Grid Systems," Sustainable Energy, IEEE Transactions on, vol. 5, pp. 795-803, 07/01 2014, doi: 10.1109/TSTE.2014.2303572.

[93] A. Saez-de-Ibarra, E. Martinez-Laserna, C. Koch-Ciobotaru, P. Rodriguez, D.

Stroe, and M. Swierczynski, "Second Life Battery Energy Storage System for Residential Demand Response Service," in 2015 IEEE International Conference on Industrial Technology (ICIT), 17-19 March 2015 2015, pp. 2941-2948, doi: 10.1109/ICIT.2015.7125532.

[94] A. Assunção, P. Moura, and A. de Almeida, "Technical and Economic Assessment of the Secondary Use of Repurposed Electric Vehicle Batteries in the Residential Sector to Support Solar Energy," Applied Energy, vol. 181, pp. 120-131, 11/01 2016, doi: 10.1016/j.apenergy.2016.08.056.

[95] C. Heymans, S. B. Walker, S. B. Young, and M. Fowler, "Economic Analysis of Second Use Electric Vehicle Batteries for Residential Energy Storage and Load-levelling," Energy Policy, vol. 71, pp. 22-30, 2014, doi: 10.1016/j.enpol.2014.04.016.

[96] H. Ambrose, D. Gershenson, A. Gershenson, and D. Kammen, "Driving Rural Energy Access: a Second-life Application for Electric-vehicle Batteries," Environmental Research Letters, vol. 9, p. 094004, 09/23 2014, doi: 10.1088/1748-9326/9/9/094004.

[97] S. Rohr et al., "Quantifying Uncertainties in Reusing Lithium-Ion Batteries from Electric Vehicles," Procedia Manufacturing, vol. 8, pp. 603-610, 12/31 2017, doi: 10.1016/j.promfg.2017.02.077.

[98] U. Debnath, I. Ahmad, and D. Habibi, "Gridable Vehicles and Second Life Batteries for Generation Side Asset Management in the Smart Grid," International Journal of Electrical Power & Energy Systems, vol. 82, pp. 114-123, 11/01 2016, doi: 10.1016/j.ijepes.2016.03.006.

[99] A. Saez-de-Ibarra, E. Martinez-Laserna, D. Stroe, M. Swierczynski, and P. Rodriguez, "Sizing Study of Second Life Li-ion Batteries for Enhancing Renewable Energy Grid Integration," IEEE Transactions on Industry Applications, vol. 52, no. 6, pp. 4999-5008, 2016, doi: 10.1109/TIA.2016.2593425.

[100] S. Tong, T. Fung, M. P. Klein, D. A. Weisbach, and J. W. Park, "Demonstration of Reusing Electric Vehicle Battery for Solar Energy Storage and Demand Side Management," Journal of Energy Storage, vol. 11, pp. 200-210, 2017, doi: 10.1016/j.est.2017.03.003.

[101] Sandia National Laboratories, Office of Scientific, Technical Information, "Technical and Economic Feasibility of Applying Used EV Batteries in Stationary Applications". United States. Department of Energy, 2003.

[102] L. Chang et al., "A Novel Fast Capacity Estimation Method Based on Current Curves of Parallel-connected Cells for Retired Lithium-ion Batteries in Second-use Applications," Journal of Power Sources, vol. 459, p. 227901, 05/01 2020, doi: 10.1016/j.jpowsour.2020.227901.

[103] H. Hongwen, R. Xiong, and F. Jinxin, "Evaluation of Lithium-Ion Battery Equivalent Circuit Models for State of Charge Estimation by an Experimental Approach," Energies, vol. 4, 12/01 2011, doi: 10.3390/en4040582.

[104] E. Hossain, D. Murtaugh, J. Mody, H. M. R. Faruque, M. S. Haque Sunny, and N. Mohammad, "A Comprehensive Review on Second-Life Batteries: Current State, Manufacturing Considerations, Applications, Impacts, Barriers & Potential Solutions, Business Strategies, and Policies," IEEE Access, vol. 7, pp. 73215-73252, 2019, doi: 10.1109/access.2019.2917859.

[105] E. Martinez-Laserna et al., "Technical Viability of Battery Second Life: A Study From the Ageing Perspective," IEEE Transactions on Industry Applications, vol. 54, no. 3, pp. 2703-2713, 2018, doi: 10.1109/TIA.2018.2801262.

[106] "Charging Lithium-ion," Batteryuniversity, 2019, [Online]. Available: https://batteryuniversity.com/learn/article/charging_lithium_ion_batteries.

[107] UK Power Networks, "Flexibility Services Invitation to Tender - 2018/19," December 2018.

[108] "The Poisson and Exponential Distributions", [Online].

[109] Western Power Distribution, "Flexible Power By Western Power Distribution." [Online].

[110] Western Power Distribution, "Industrial & Business Customers." [Online].

[111] Y. Chen, Y. He, Z. Li, L. Chen, and C. Zhang, "Remaining Useful Life Prediction and State of Health Diagnosis of Lithium-Ion Battery Based on Second-Order Central Difference Particle Filter," IEEE Access, vol. 8, pp. 37305-37313, 2020, doi: 10.1109/ACCESS.2020.2974401.

[112] Wholesale Markets & Commercial, "Annual Report on the Operation of the Capacity Market in 2019/20," 2020. [Online].

[113] Smart Transport, "Electric Buses Receive £120m Extra Funding." [Online]. Available: https://www.smarttransport.org.uk/news/latest-news/electric-buses-

receive-120m-extra-funding.

[114] W. Dafang, N. Jinrui, and S. Fengchun, "The Application of CAN Communication in Distributed Control System of Electric City Bus," 09/01 2008, doi: 10.1109/VPPC.2008.4677533.

[115] Z. Gong et al., "Distributed Control of Active Cell Balancing and Low-Voltage Bus Regulation in Electric Vehicles Using Hierarchical Model-Predictive Control," IEEE Transactions on Industrial Electronics, vol. 67, no. 12, pp. 10464-10473, 2020, doi: 10.1109/TIE.2019.2956396.

[116] L. A. L. Zaneti, N. B. Arias, M. C. de Almeida, and M. J. Rider, "Sustainable Charging Schedule of Electric Buses in a University Campus: A Rolling Horizon Approach," Renewable and Sustainable Energy Reviews, vol. 161, p.

[117] J. Lee, H. Shon, I. Papakonstantinou, and S. Son, "Optimal Fleet, Battery, and Charging Infrastructure Planning for Reliable Electric Bus Operations," Transportation Research Part D: Transport and Environment, vol. 100, p.

[118] K. An, W. Jing, and I. Kim, "Battery-swapping Facility Planning for Electric Buses with Local Charging Systems," International Journal of Sustainable Transportation, vol. 14, no. 7, pp.

[119] W. Jing, I. Kim, and K. An, "The Uncapacitated Battery Swapping Facility Location Problem with Localized Charging System Serving Electric Bus Fleet," Transportation Research Procedia, vol. 34, pp.

[120] P. Li, Y. Zhang, Y. Zhang, K. Zhang, and M. Jiang, "The Effects of Dynamic Traffic Conditions, Route Characteristics and Environmental Conditions on Trip-based Electricity consumption prediction of electric bus," Energy, vol. 218, p.

[121] X. Tang, X. Lin, and F. He, "Robust Scheduling Strategies of Electric Buses Under Stochastic Traffic Conditions," Transportation Research Part C: Emerging Technologies, vol. 105, pp.

[122] Y. Wu, H. Tan, J. Peng, H. Zhang, and H. He, "Deep Reinforcement Learning of Energy Management with Continuous Control Strategy and Traffic Information for a Series-parallel Plug-in Hybrid Electric Bus," Applied Energy, vol. 247, pp.

[123] M. Huang and J. Q. Li, "The Shortest Path Problems in Battery-Electric Vehicle Dispatching with Battery Renewal," Sustainability, vol. 8, p. 607, 06/28 2016, doi: 10.3390/su8070607.

[124] M. Guo, Y. Mu, H. Jia, Y. Deng, X. Xu, and X. Yu, "Electric/Thermal Hybrid Energy Storage Planning for Park-level Integrated Energy Systems with Second-life Battery Utilization," Advances in Applied Energy, vol. 4, p.

[125] J. Lacap, J. W. Park, and L. Beslow, "Development and Demonstration of Microgrid System Utilizing Second-Life Electric Vehicle Batteries," Journal of Energy Storage, vol. 41, p.

[126] D. Strickland, L. Chittock, D. A. Stone, M. P. Foster, and B. Price, "Estimation of Transportation Battery Second Life for Use in Electricity Grid Systems," IEEE Transactions on Sustainable Energy, vol. 5, no. 3, pp. 795-803, 2014, doi: 10.1109/TSTE.2014.2303572.

[127] S. Kim, R. Pasupathy, and S. G. Henderson, "A Guide to Sample Average Approximation," Handbook of simulation optimization, pp. 207-243, 2015.

[128] "The BYD K9", BYD, 2019.